Analysis of Horizontally Curved Pseudo Slab Type Bridge Deck Continuous Over Discrete Pier Supports

by

Medhat Kamal Abdullah

A Thesis Presented to the

FACULTY OF THE COLLEGE OF GRADUATE STUDIES

KING FAHD UNIVERSITY OF PETROLEUM & MINERALS

DHAHRAN, SAUDI ARABIA

In Partial Fulfillment of the
Requirements for the Degree of

MASTER OF SCIENCE

In

CIVIL ENGINEERING

June, 1988

INFORMATION TO USERS

This manuscript has been reproduced from the microfilm master. UMI films the text directly from the original or copy submitted. Thus, some thesis and dissertation copies are in typewriter face, while others may be from any type of computer printer.

The quality of this reproduction is dependent upon the quality of the copy submitted. Broken or indistinct print, colored or poor quality illustrations and photographs, print bleedthrough, substandard margins, and improper alignment can adversely affect reproduction.

In the unlikely event that the author did not send UMI a complete manuscript and there are missing pages, these will be noted. Also, if unauthorized copyright material had to be removed, a note will indicate the deletion.

Oversize materials (e.g., maps, drawings, charts) are reproduced by sectioning the original, beginning at the upper left-hand corner and continuing from left to right in equal sections with small overlaps. Each original is also photographed in one exposure and is included in reduced form at the back of the book.

Photographs included in the original manuscript have been reproduced xerographically in this copy. Higher quality 6" x 9" black and white photographic prints are available for any photographs or illustrations appearing in this copy for an additional charge. Contact UMI directly to order.

UMI

A Bell & Howell Information Company
300 North Zeeb Road, Ann Arbor MI 48106-1346 USA
313/761-4700 800/521-0600

ANALYSIS OF HORIZONTALLY CURVED PSEUDO SLAB TYPE BRIDGE DECK CONTINUOUS OVER DISCRETE PIER SUPPORTS

BY

MEDHAT KAMAL ABDULLAH

A Thesis Presented to the

FACULTY OF THE COLLEGE OF GRADUATE STUDIES

KING FAHD UNIVERSITY OF PETROLEUM & MINERALS

DHAHRAN, SAUDI ARABIA

In Partial Fulfillment of the

Requirements for the Degree of

MASTER OF SCIENCE

In

CIVIL ENGINEERING

JUNE 1988

بسم الله الرحمن الرحيم

وقل ربّ زدني علما

صدق الله العظيم

KING FAHD UNIVERSITY OF PETROLEUM AND MINERALS
DHAHRAN, SAUDI ARABIA

COLLEGE OF GRADUATE STUDIES

This thesis, written by

MEDHAT KAMAL ABDULLAH

under the direction of his Thesis Committee, and approved by all the members, has been presented to and accepted by the Dean, College of Graduate Studies, in partial fulfillment of the requirements for the degree of

MASTER OF SCIENCE IN CIVIL ENGINEERING

THESIS COMMITTEE

Chairman (Dr. A. K. Azad)

Member (Dr. M. H. Baluch)

Member (Dr. Alfarabi Sharif)

Chairman,
Civil Engineering

Dr. Abdullah S. Al-Zakri,
Dean, College of Graduate Studies

Date: August 2, 1988

I dedicate this work to my beloved parents.

ACKNOWLEDGEMENT

Praise and thanks be to Almighty ALLAH with whose gracious help this work was accomplished.

This work was carried out at King Fahd University of Petroleum and Minerals under the supervision of Dr A.k. Azad to whom I would like to express my great debt of gratitude for suggesting the problem, helping and guiding me. I would also like to thank deeply Dr M.H. Baluche and Dr Al-Faraby for their valuable help.
Thanks also are due to Dr Al-Khatheian for his sincere advice and intelligent suggestions, and to Mr Mumtaz for his great efforts in typing this thesis.

Lastly, but not the last I would like to express my deep appreciation to King Fahd University of Petroleum and Minerals for the great efforts which have been done to make it as convenient as possible for me to achieve this work.

TABLE OF CONTENTS

Appendices

LIST OF TABLES

LIST OF FIGURES

THESIS ABSTRACT

FULL NAME OF STUDENT: Medhat Kamal Abdullah

TITLE OF STUDY: ANALYSIS OF HORIZONTALLY CURVED PSEUDO SLAB TYPE BRIDGE DECK CONTINUOUS OVER DISCRETE PIER SUPPORT

MAJOR FIELD: CIVIL ENGINEERING (STRUCTURES)

DATE OF DEGREE: June, 1988.

A computer aided method of analysis has been developed for a curved slab type bridge deck with a variable thickness along the radial direction incorporating one dimensional finite difference method in conjunction with the method of consistent deformation. The deck is simply supported along the radial edges and may be continuous over arbitrarily located interior pier supports and is subjected to any arbitrary loading due to line load, patch load, uniformly distributed load and point load. A generalized computer program, FSTCBA, in FORTRAN-77 is developed to readily apply the proposed method. The accuracy of the proposed method has been verified using some available solutions. The method appears to be accurate and the computer program is shown to be easy to use and economical with respect to C.P.U. time and storage required. Several examples are analyzed using the proposed method to study the effect of various parameters on deck behavior and distribution of internal forces. The proposed method is also used to verify the accuracy of the simplified method of analysis.

MASTER OF SCIENCE DEGREE

KING FAHD UNIVERSITY OF PETROLEUM AND MINERALS
Dhahran, Saudi Arabia

June, 1988.

خلاصة الرسالة

اسم الطالب : مدحت كمال عبد الله

عنوان الدراسة : تحليل أسطح الكباري المنحنية أفقيا والتي من نوع البلاطات المستمرة داخليا فوق ركائز عمودية .

التخصص : الهندسة المدنية (انشاءات)

تاريخ الشهادة : يونيو ١٩٨٨م

لقد أقترحت طريقة لتحليل أسطح الكباري المنحنية أفقيا والتي على هيئة بلاطات ذات سمك متغير على امتداد الاتجاه القطري باستخدام طريقة " الفرق المحدد في بعد واحد " مع طريقة " التشكل المتوافق " . ويكون مسطح الكوبري مدعم بدعامات بسيطة عند الحواف القطرية بينما يكون مستمر داخليا فوق دعامات عمودية عشوائية التوزيع . وبالنسبة للأحمال فقد تكون حمل خطي أو حمل موزع على مساحة محدودة من سطح الكوبري أو حمل موزع على سطح الكوبري بالكامل أو حمل مركز عشوائي الموقع . وقد تم برمجة هذه الطريقة في برنامج عام بلغة الفورتران – ٧٧ بحيث يمكن استخدامها بسهولة . وتم التحقق من دقة هذه الطريقة باستخدام بعض الأمثلة المحلولة . ولقد تبين أن هذه الطريقة دقيقة وأن البرنامج سهل التشغيل واقتصادي من حيث وقت التشغيل أو السعة المطلوبة . ولقد تم تحليل العديد من الامثلة باستخدام الطريقة المقترحة لدراسة تأثير بعض المتغيرات على تصرف أسطح هذه الكباري وعلى توزيع القوى الداخلية , كذلك استخدمت هذه الطريقة للتأكد من دقة الطريقة المبسطة لتحليل هذا النوع من الكباري .

درجة الماجستير في العلوم

جامعة الملك فهد للبترول والمعادن
الظهران – المملكة العربية السعودية

يونيو ١٩٨٨م

NOMENCLATURE

D_r	Bending rigidity/unit length in the radial direction
D_1	Bending rigidity due to coupling of the curvatures in the orthogonal directions due to Poisson's ratio
D_θ	Bending rigidity/unit length in the angular direction
$D_{r\theta}$	Torsional rigidity/unit length
E	Young's modulus of elasticity of material of the bridge deck
G	Shear modulus of material
H	$D_1 + D_{r\theta}$
h	Spacing between nodes
M_r	Bending moment/unit length in the radial direction
M_θ	Bending moment/unit length in the angular direction
$M_{r\theta}$	Twisting moment/unit length
n	Harmonic number
N_1	$n\pi/\varphi_o$
Q_r	Shearing force unit length with outward drawn normal in the radial direction
Q_θ	Shearing force unit length with outward drawn normal in the angular direction
R	Radius of curvature to the centerline of the deck
r_i	Radius of curvature of ith node
t	Thickness of plate

U	D_1/D_r
V	D_1/D_θ
V_r	Kirchoff's edge reaction/unit length with outward drawn normal in the radial direction.
V_θ	Kirchoff's edge reaction/unit length with outward drawn normal in the angular direction.
W	Vertical displacement funciton (function of r only)
w	Deflection of the middle surface ofthe plate (positive downward).
θ	Polar coordinate in the angular direction
φ_o	Bridge deck angle subtended at the center
ν	Poisson's ratio

Chapter 1

INTRODUCTION

1.1 General

In recent years, horizontally curved bridges are increasingly used due mainly to their aesthetics and to comply with the need of such bridge geometrics in roadway intersections and interchanges. This has generated interest in the development of a computer aided analysis which can routinely be applied in practice.

A common form of horizontally curved bridges is the slab type or pseudo slab type bridge deck which is continuous over a number of discrete columns or pier supports as shown in Fig. 1.1. These piers provide basically vertical supports to the deck with virtually no rotational restraint. Typical sections of such bridge decks are shown in Fig.1.1.b

Both classical and numerical methods have been employed to solve a curved plate problem. While the application of classical methods is limited in scope, the numerical methods , which includes finite element, finite strip and finite difference methods , have been attempted more rigorously.

The proposed method of analysis employs a numerical method of finite difference to solve the governing differential equation of a hor-

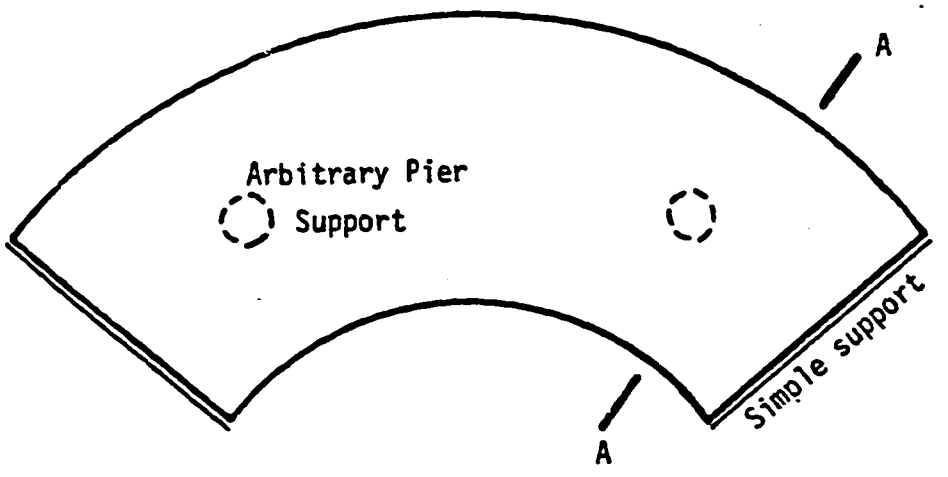

(a) Plan

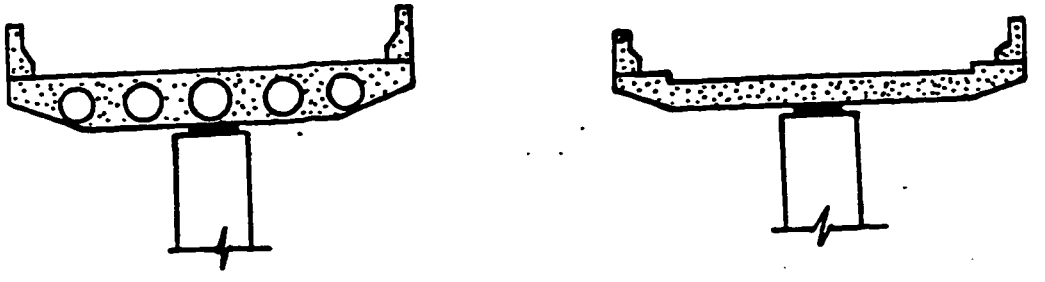

(b) Cross-section A-A

Fig. 1.1 Horizontally curved bridge deck with intermediate pier supports

izontally curved orthotropic plate. The equilibrium equations are generated only along the central radial line of the curved slab employing a Levy type series solution (1). The developmental work includes both uniform deck slab thickness as well as deck slabs of variable thickness.

For the continuous bridge deck over a number of intermediate pier supports, the method of consistent deformation has been employed for analysis. By removing these supports, the primary structure is solved first with all applied loads. Using the method of consistent deformation, the redundant pier reactions are determined and then, the entire structure is solved.

Sinosoidal affinity between load and deformation permits the generation of equilibrium differential equations along the central radial line only, obviating the need of large computational molecules. The repetitive nature of the computational tasks is an advantage for easy adaptation on a computer.

1.2 Literature Review

The use of curved plates and curved bridges have persuaded researchers to conduct researches in developing accurate methods of analysis. In general, most of the methods used in the analysis of curved bridge deck are based on the classical theory of thin plates(2,3), and they can be divided into two groups: analytical

methods (4,5) and numerical methods (6-16). The analytical methods are applicable to a few limited cases only such as plates with uniform thickness and simple loading, due to mathematical complexities. For numerical methods of analysis of curved slabs, all three popular methods, namely, the finite element method (6-9),the finite strip method (10-14) and the finite difference method (1,15,16) have been used.

The finite element method, in which the actual continuous structure is idealized into an assembly of discrete elements for which force-displacement relations and stress distribution are determined, has been used extensively for solving this type of problem. The most suitable element is the triangular element. However, to reduce the errors due to approximation of the curved boundaries with a series of straight lines would require a fine mesh and hence, a large number of elements(1). Olson and Lundberg (7) have derived the plate bending element in polar coordinates and deduced the stiffness matrix of circular and annular sector elements, hence they have provided close fit to the curved boundaries eliminating the boundary line approximation errors. Sawko and Merriman(8) have developed a higher order element in polar coordinates. Singh and Ramaswamy (9) have provided close solutions by developing another higher order element in polar coordinates. Despite being the most powerful and perhaps most popular method in dealing with all types of plates, finite element sometimes is not the best method to use regarding the time and cost involved in preparing the data and solving a large number

of equations.

The finite strip method (10, 11) has been used in the analysis of orthotropic curved deck slabs reducing the algebraic equations encountered in finite element method. This method was first published by Cheung, Y. K., in 1968 and it was known as an excellent method of analysis for simply supported bridge deck structures in terms of accuracy and efficiency. In 1969, Cheung (10) applied this method to the analysis of simple-curve slab and box bridges. Issam (11) has presented a computer oriented exact method of solution for the analysis of horizontally curved and orthotropic bridge decks using the finite strip procedure.

The finite difference method can be conveniently used for a variety of plates. The conventional finite difference solution in plates is obtained by using nodal points spaced all over the surface of the plate. The differential equation for displacements of these nodes are solved numerically and the number of simultaneous equations required is generally only about one third of that number required in finite element method(27). Heins and Hails (15) have analyzed a curved stiffened plate as an equivalent orthotropic plate applying the finite difference method to solve the equilibrium equation of thin plates and neglecting the Poisson's ratio to simplify the problem. Otter (16) has pioneered another technique of finite difference known as dynamic relaxation, which is basically an iterative approach. In this technique, the structure is assumed to vibrate freely in a viscous fluid,

this yields a governing equation of motion in dynamic form and the solution is obtained by an iterative procedure until the steady-state solution is achieved and the static solution is obtained. Although the finite difference method was checked for accuracy and found to be satisfactory and more economical than finite element method, it requires a very large number of nodal points to get an acceptable solution and it is very tedious as it requires a large number of computational molecules to include the boundary conditions.

In 1980 Dey and Samuel (1) proposed the use of the One-Directional finite difference in the analysis of curved orthotropic plates simply supported at the radial edges. This method appears to be an attractive numerical method for the solution of a horizontally curved bridge deck problem due to its relative simplicity involving solution of a smaller number of equilibrium equations, (Fig. 1.2 shows a comparison between the three numerical methods mentioned above with respect to the number of nodes required for each method).

This method has been used (19,20) to analyze a curved girder-slab bridge deck idealizing the deck as a curved isotropic plate supported by curved girders whose rotational and vertical flexibilities are taken into account in finite difference equations. Using this method, the influence of torsional stiffness of steel I-girders and the radius of curvature of the deck has been demonstrated in refs. (19-21).

The proposed method of analysis introduced here is to utilize a

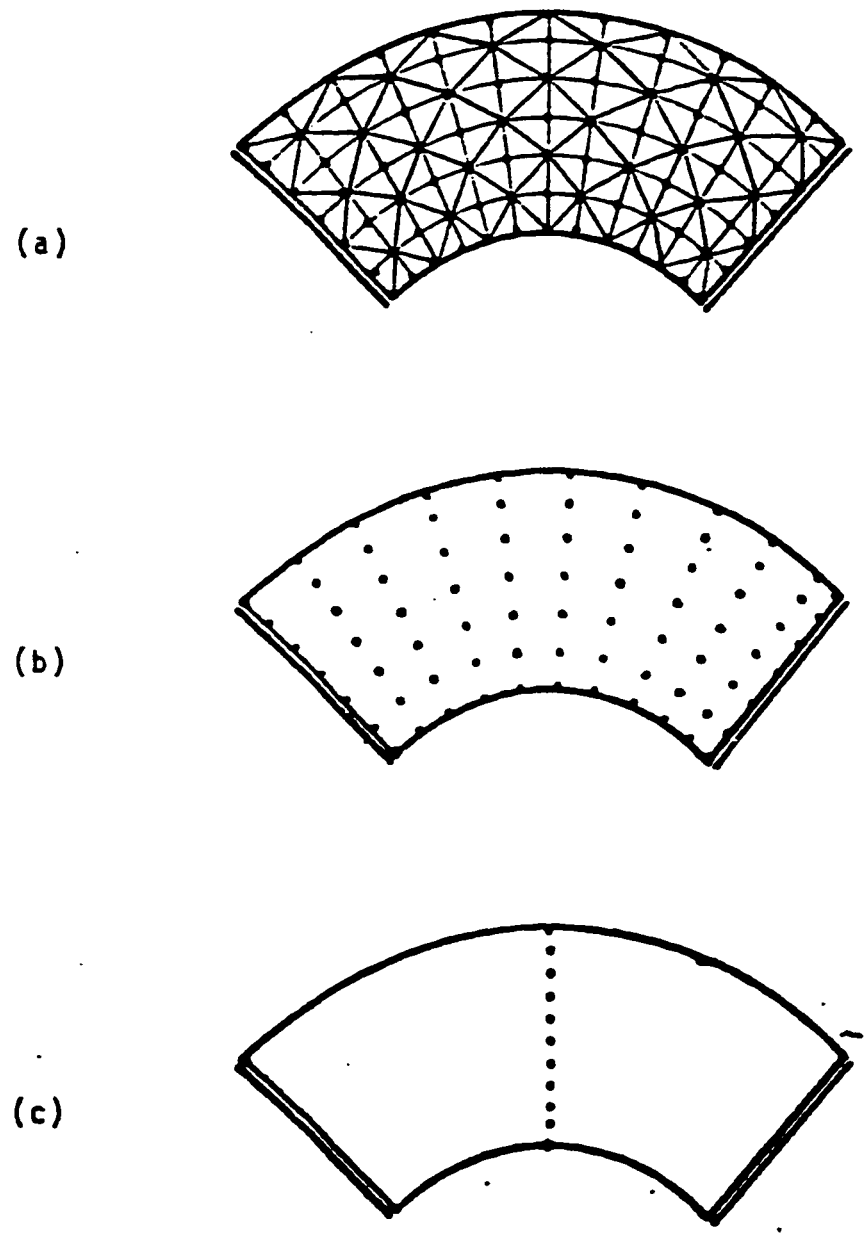

Fig. 1.2 Nodes required for different methods of analysis: (a) finite element method, (b) 2-dimension finite difference, (c) 1-dimension finite difference

combination of the method of one-directional finite difference and the method of consistent deformation in the analysis of an orthotropic curved pseudo-slab type bridge deck continuous over discrete pier supports which is a common form of horizontally curved bridges. The method appears to be accurate but yet relatively simpler than other methods for easy adaptation on a computer and it can account for any bridge loading and arbitrary locations of pier supports. The developmental work includes also the case of variable slab thickness (Fig.1.1.b) to demonstrate the influence of thinner overhangs normally used in bridge decks.

1.3 Scope and Objectives

Of the two suitable numerical methods which can be used to reliably analyze a curved slab type bridge deck, namely, finite element and finite difference, the former tends to be time and storage demanding for a computer. To develop a simplified, yet accurate method of analysis, one-dimensional finite difference method has been adopted in the work.

The primary objectives of this work are as follows:

1) Develop the finite difference formulation of the governing fourth order partial differential equations of an orthotropic curved plate with variable plate rigidities due to the variation of plate thickness. Also, the appropriate finite differ-

ence equations for moments, shear and torsion will be developed.

2) Develop a generalized computer program for the analysis of a horizontally curved deck being continuous over discrete pier supports and subjected to arbitrary loading. Finite difference method as developed in item (1) will be followed in conjunction with the method of consistent deformation.
3) Verify the accuracy of the proposed method of analysis by comparing the results with those available from other methods.
4) Study the influence of various parameters on the behavior of this type of bridge deck.
5) Verify the accuracy of the simplified method of analysis (22) by comparing results with those obtained from the proposed method.

The proposed method of analysis is general and can be applied to any number of spans continuous over arbitrarily located discrete piers. This method is envisaged to be the most simplified computerized method which can readily be used to analyze accurately a curved bridge deck of the geometry shown in Fig.1.1 and which can also be used to compare the results obtained from other existing methods and experimental investigations.

Chapter 2

BASIC EQUATIONS OF A CURVED PLATE

2.1 Orthotropic Curved plates of Uniform Thickness

2.1.1 Equilibrium Equations

For a curved orthotropic plate element shown in Fig. 2.1, subjected to an arbitrary load P (r, 0), the three equilibrium equations in polar coordinates (r, 0) are (2):

$$Q_r = \frac{M_r}{r} + \frac{\partial M_r}{\partial r} + \frac{1}{r}\frac{\partial M_{r0}}{\partial 0} - \frac{M_0}{r} \tag{2.1}$$

$$Q_\theta = \frac{1}{r}\frac{\partial M_\theta}{\partial \theta} + \frac{2M_{r0}}{r} + \frac{\partial M_{r0}}{\partial r} \tag{2.2}$$

$$\frac{Q_r}{r} + \frac{\partial Q_r}{\partial r} + \frac{1}{r}\frac{\partial Q_\theta}{\partial 0} + P = 0 \tag{2.3}$$

Substitution of Q_r and Q_θ (Eqns. 2.1 and 2.2) into Eq. 2.3 leads to the governing equilibrium equation:

$$\frac{2}{r}\frac{\partial M_r}{\partial r} + \frac{\partial^2 M_r}{\partial r^2} + \frac{2}{r}\frac{\partial^2 M_{r0}}{\partial r \partial 0} - \frac{1}{r}\frac{\partial M_0}{\partial r}$$

$$+ \frac{2}{r^2}\frac{\partial M_{r0}}{\partial 0} + \frac{1}{r^2}\frac{\partial^2 M_0}{\partial 0^2} = -P(r,0) \tag{2.4}$$

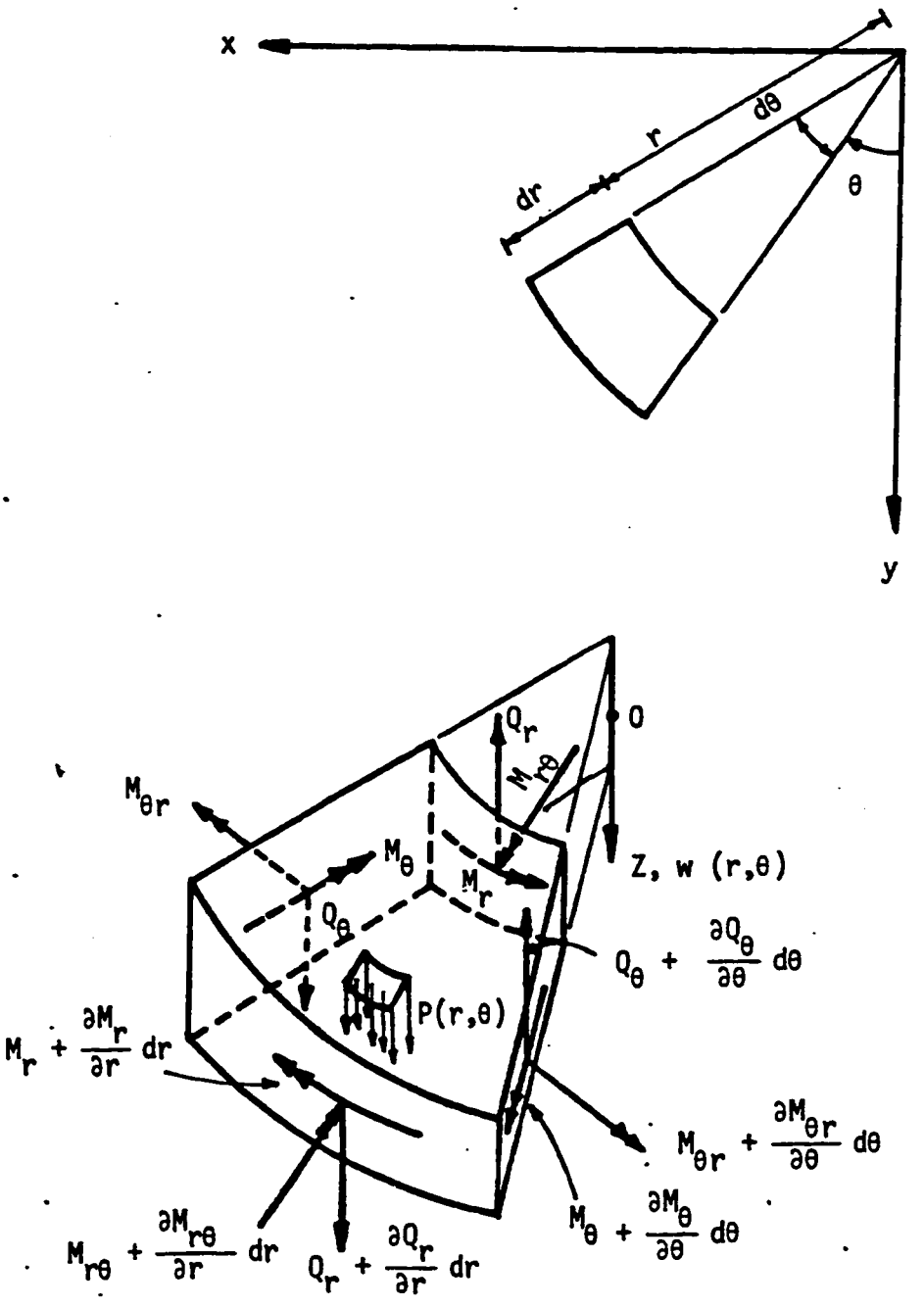

Fig. 2.1 Forces on a curved plate element in polar coordinates

2.1.2 Force-Displacement Relationships

Force-displacement relationships can be expressed in terms of the vertical displacement w as (2, 3):

$$M_r = - D_r \left[\frac{\partial^2 w}{\partial r^2} + \upsilon_\theta \left(\frac{1}{r}\frac{\partial w}{\partial r} + \frac{1}{r^2}\frac{\partial^2 w}{\partial \theta^2}\right)\right] \tag{2.5}$$

$$M_\theta = - D_\theta \left[\upsilon_r \frac{\partial^2 w}{\partial r^2} + \frac{1}{r}\frac{\partial w}{\partial r} + \frac{1}{r^2}\frac{\partial^2 w}{\partial \theta^2}\right] \tag{2.6}$$

$$M_{r\theta} = - 2D_{r\theta} \left[\frac{1}{r}\frac{\partial^2 w}{\partial r \partial \theta} - \frac{1}{r^2}\frac{\partial w}{\partial \theta}\right] \tag{2.7}$$

$$Q_r = - \left[D_r \left(\frac{\partial^3 w}{\partial r^3} + \frac{1}{r}\frac{\partial^2 w}{\partial r^2}\right) + H\left(\frac{1}{r^2}\frac{\partial^3 w}{\partial r \partial \theta^2} - \frac{1}{r^3}\frac{\partial^2 w}{\partial r^2}\right)\right.$$

$$\left. - D_\theta \left(\frac{1}{r^2}\frac{\partial w}{\partial r} + \frac{1}{r^3}\frac{\partial^2 w}{\partial \theta^2}\right)\right] \tag{2.8}$$

$$Q_\theta = - \left[\frac{H}{r}\frac{\partial^3 w}{\partial r^2 \partial \theta} + D_\theta \left(\frac{1}{r^2}\frac{\partial^2 w}{\partial r \partial \theta} + \frac{1}{r^3}\frac{\partial^3 w}{\partial \theta^3}\right)\right] \tag{2.9}$$

The Kirchhoff edge reactions are:

$$V_r = \left[Q_r + \frac{1}{r}\frac{\partial M_{r\theta}}{\partial \theta}\right]$$

$$= -\left[D_r\left(\frac{\partial^3 w}{\partial r^3} + \frac{1}{r}\frac{\partial^2 w}{\partial r^2}\right) + (H + 2D_{r\theta})\left(\frac{1}{r^2}\frac{\partial^3 w}{\partial r \partial \theta^2}\right.\right.$$

$$\left.\left. - \frac{1}{r^3}\frac{\partial^2 w}{\partial \theta^2}\right) - D_\theta\left(\frac{1}{r^2}\frac{\partial w}{\partial r} + \frac{1}{r^3}\frac{\partial^2 w}{\partial \theta^2}\right)\right] \qquad (2.10)$$

$$V_\theta = \left[Q_\theta + \frac{\partial M_{r\theta}}{\partial r}\right]$$

$$= -\left[D_\theta\left(\frac{1}{r^2}\frac{\partial^2 w}{\partial r \partial \theta} + \frac{1}{r^3}\frac{\partial^3 w}{\partial \theta^3}\right) + (H + 2D_{r\theta})\left(\frac{1}{r}\frac{\partial^3 w}{\partial r^2 \partial \theta}\right)\right.$$

$$\left. + 4D_{r\theta}\left(\frac{1}{r^2}\frac{\partial w}{\partial \theta} - \frac{1}{r^2}\frac{\partial^2 w}{\partial r \partial \theta}\right)\right] \qquad (2.11)$$

Where

$$D_r = \frac{E_r t^3}{12(1 - \upsilon_r \upsilon_\theta)} \qquad (2.12.a)$$

$$D_\theta = \frac{E_\theta t^3}{12(1 - \upsilon_r \upsilon_\theta)} \qquad (2.12.b)$$

$$D_{r\theta} = \frac{G_{r\theta} t^3}{12} \qquad (2.12.c)$$

$$H = D_1 + 2D_{r\theta} \qquad (2.12.d)$$

$$D_1 = \upsilon_r D_\theta = \upsilon_\theta D_r \qquad (2.12.e)$$

t = thickness of plate

r = radius of curvature

Substitution of M_r, M_θ, $M_{r\theta}$ from Eqns. 2.5 - 2.7 into Eq. 2.4 leads to the governing differential equation of a curved orthotropic plate of uniform thickness in terms of the displacement w as:

$$D_r \frac{\partial^4 w}{\partial r^4} + 2\frac{H}{r^2} \frac{\partial^4 w}{\partial r^2 \partial \theta^2} + \frac{D_\theta}{r^4} \frac{\partial^4 w}{\partial \theta^4} + \frac{2D_r}{r} \frac{\partial^3 w}{\partial r^3} - 2\frac{H}{r^3} \frac{\partial^3 w}{\partial r \partial \theta^2}$$

$$- \frac{D_\theta}{r^2} \frac{\partial^2 w}{\partial r^2} + \frac{2(D_\theta + H)}{r^4} \frac{\partial^2 w}{\partial \theta^2} + \frac{D_\theta}{r^3} \frac{\partial w}{\partial r} = P(r, \theta) \qquad (2.13)$$

For an isotropic plate $H = D_r = D_\theta = D = \frac{Et^3}{12(1-\upsilon^2)}$ and Eq. 2.13 reduced to:

$$\frac{\partial^4 w}{\partial r^4} + \frac{2}{r^2} \frac{\partial^4 w}{\partial r^2 \partial \theta^2} + \frac{1}{r^4} \frac{\partial^4 w}{\partial \theta^4} + \frac{2}{r} \frac{\partial^3 w}{\partial r^3} - \frac{2}{r^3} \frac{\partial^3 w}{\partial r \partial \theta^2}$$

$$- \frac{1}{r^2} \frac{\partial^2 w}{\partial r^2} + \frac{4}{r^4} \frac{\partial^2 w}{\partial \theta^2} + \frac{1}{r^3} \frac{\partial w}{\partial r} = \frac{P(r,\theta)}{D} \qquad (2.14)$$

2.2 Levy-Type Series Solution for Simply Supported Curved Plates

For a curved plate where two radial edges are simply supported and two other edges are arbitrarily supported, as shown in Fig. 2.2, a Levy-type solution can be postulated by expressing both the applied load P(r, θ) and the resulting vertical displacement w in terms of sine series. The sinusoidal displacement simplifies the problem

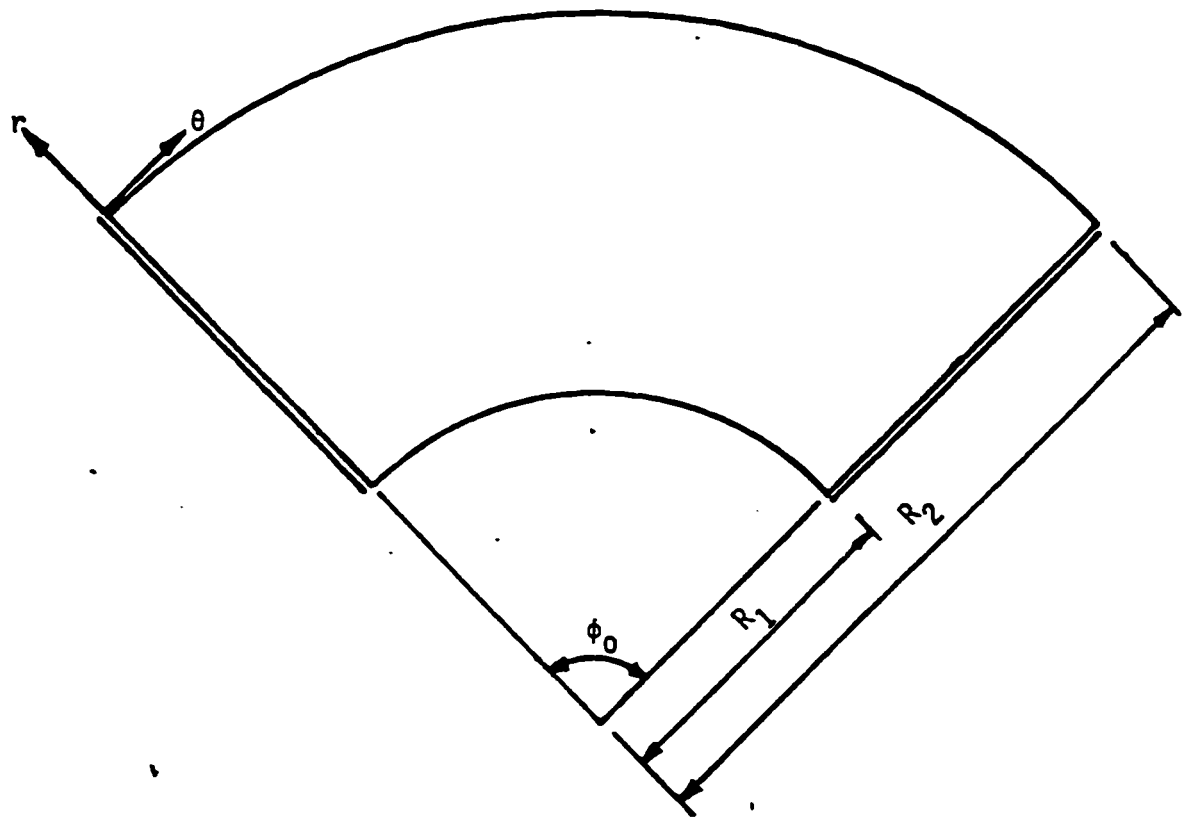

Fig. 2.2 Simply supported curved plate

considerably and it also enables to express the internal forces in the plate in series. The governing partial differential equation (Eqn. 2.13) can be transformed into ordinary fourth order differential equation by taking w as:

$$w(r, \theta) = \sum_{n=1}^{\infty} W_n (r) \sin N\theta \qquad (2.15)$$

where $N = \frac{n\pi}{\varphi_o}$ and W_n is a function in r only, and the loading P can be taken as:

$$P(r, \theta) = \sum_{n=1}^{\infty} P_n \sin N\theta \qquad (2.16)$$

P_n being the Fourier load coefficient for the nth cycle.

The Fourier coefficient, P_n, for the cases shown in Fig. 2.3 is as follows:

(a) A Concentrated Load P (force):

$$P_n = \frac{2P}{\varphi_o r_k} \sin N\theta_k \qquad (2.17)$$

(b) A Uniformly Distributed Line Load P_1 (force/length):

$$P_n = \frac{4P_1}{n\pi} \sin^2 (\frac{n\pi}{2}) \qquad (2.18)$$

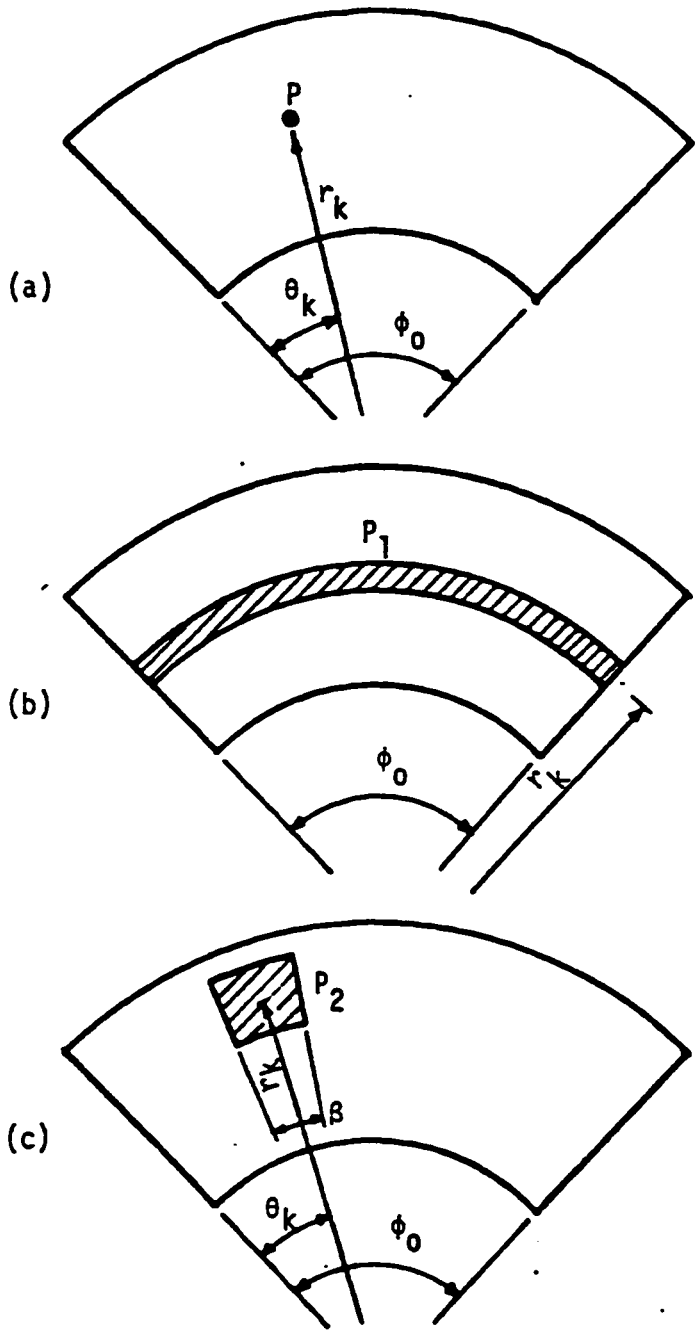

Fig. 2.3 Different loading on a curved plate (a) point load, (b) line load and (c) patch load

(c) A Uniformly Distributed Patch Load P_2 (force/unit area):

$$P_n = \frac{4P_2}{n\pi} \sin N\theta_k \cdot \sin \frac{N\beta}{2} \tag{2.19}$$

Substitution of Eqs. (2.15) and (2.16) into Eqn. (2.13) yields the equilibrium equation for the nth cycle as (1):

$$D_r \left[\frac{d^4W}{dr^4} + \frac{2}{r}\frac{d^3W}{dr^3} - \frac{\lambda}{r^2}\frac{d^2W}{dr^2} + \frac{\lambda}{r^3}\frac{dW}{dr} + \frac{\mu}{r^4}W\right] = P_n \tag{2.20}$$

where:

$$\mu = N^4\beta - 2(\alpha + \beta)N^2 \tag{2.20.a}$$

$$\lambda = 2\alpha N^2 + \beta \tag{2.20.b}$$

$$\alpha = H/D_r \tag{2.20.c}$$

$$\beta = D_\theta/D_r \tag{2.20.d}$$

$$N = n\pi/\varphi_o \tag{2.20.e}$$

Thus the fourth order ordinary differential equation (Eqn. 2.20) prescribes the displacement amplitude W for a horizontally curved orthotropic plate with two radial edges simply supported for the nth harmonic load component.

Substitution of Eqn. 2.15 in Eqns. 2.5 - 2.11 yields:

$$M_r = -\sum_{n=1}^{\infty} \left[D_r \frac{d^2W}{dr^2} + \frac{D_1}{r}\frac{dW}{dr} - \frac{D_1N^2}{r^2}W\right] \sin N\theta \tag{2.21}$$

$$M_\theta = - \sum_{n=1}^{\infty} [D_1 \frac{d^2W}{dr^2} + \frac{D_\theta}{r} \frac{dW}{dr} - D_0 \frac{N^2}{r^2} W \mid \sin N0 \qquad (2.22)$$

$$M_{r\theta} = - \sum_{n=1}^{\infty} \mid 2D_{r\theta} (\frac{1}{r} \frac{dW}{dr} - \frac{1}{r^2} W) N \mid \cos N0 \qquad (2.23)$$

$$Q_r = - \sum_{n=1}^{\infty} \mid D_r \frac{dW^3}{dr^3} + \frac{D_r}{r} \frac{d^2W}{dr^2} - (H + D_0) \frac{1}{r^2} \frac{dW}{dr}$$

$$+ (H + D_0) \frac{N^2}{r^3} W \mid \sin N\theta \qquad (2.24)$$

$$Q_\theta = - \sum_{n=1}^{\infty} \mid \frac{H}{r} \frac{d^2W}{dr^2} + \frac{D_\theta}{r^2} \frac{dW}{dr} - D_0 . \frac{N^2}{r^3} W \mid N . \cos N0 \qquad (2.25)$$

$$V_r = - \sum_{n=1}^{\infty} \mid D_r \frac{d^3W}{dr^3} + \frac{D_r}{r} \frac{d^2W}{dr^2} - (HN^2 + 2D_{r0} . N^2 + D_0)$$

$$\frac{1}{r^2} \frac{dW}{dr} + (HN^2 + 2D_{r0}N^2 + D_0) \frac{W}{r^3} \mid \sin N0 \qquad (2.26)$$

$$V_\theta = - \sum_{n=1}^{\infty} \mid (H + 2D_{r0}) \frac{1}{r} \frac{d^2W}{dr^2} - (4D_{r0} - D_0) \frac{1}{r^2} \frac{dW}{dr}$$

$$- (D_0 N^2 - 4D_{r0}) \frac{W}{r^3} \mid N . \cos N0 \qquad (2.27)$$

2.3 Orthotropic Curved Plates of Non-Uniform Thickness

Bridges are frequently designed with tapered overhangs for an economical proportioning. A typical cross-section of such bridges will have non-uniform deck thickness at the outer widths of the deck

as shown in Fig. (1.1). Since the taper is only in the radial direction, the variation in the rigidities, D_r, D_0, and D_{r0} due to the change in slab thickness must be accounted for in the analysis for refinement and to improve accuracy.

In this section, the necessary differential equations are rewritten for a curved orthotropic plate of variable thickness.

2.3.1 Force-Displacement Relationships

The moment-displacement relationships for an orthotropic curved plate of uniform thickness can be applied to the case of a non-uniform plate thickness by treating the plate rigidities D_r, D_0 and D_{r0} as variables along the width of the plate. Thus, the expressions for M_r, M_0 and M_{r0} are same as Eqns. 2.5-2.7 for uniform plate thickness. However, the shear equations are different due to the variation of the rigidities and they are as follows:

$$Q_r = -\left[D_r \frac{d^3w}{dr^3} + \left(\frac{D_r}{r} + \frac{dD_r}{dr}\right) \frac{\partial^2 w}{\partial r^2} + \left(\frac{dD_1}{rdr} - \frac{D_0}{r^2}\right)\frac{\partial w}{\partial r} + \right.$$

$$\left. (D_1 + 2D_{r\theta})\frac{1}{r^2} \frac{\partial^3 w}{\partial r \partial 0^2} + \left(r \frac{dD_1}{dr} - D_0 - 2D_{r0}\right) \frac{1}{r^3} \frac{\partial^2 w}{\partial 0^2}\right] \qquad (2.28)$$

$$Q_\theta = -\left[(D_1 + 2D_{r0}) \frac{1}{r} \frac{\partial^3 w}{\partial r^2 \partial 0} + \left(D_0 + 2r \frac{dD_{r0}}{dr}\right) \frac{1}{r^2} \frac{\partial^2 w}{\partial r \partial 0}\right.$$

$$- \left(\frac{2}{r^2} \frac{dD_{r\theta}}{dr}\right) \frac{\partial w}{\partial \theta} + \frac{D_\theta}{r^3} \frac{\partial^3 w}{\partial \theta^3} \Big] \qquad (2.29)$$

$$V_r = - \Big[D_r \frac{\partial^3 w}{\partial r^3} + \left(\frac{D_r}{r} + \frac{dD_r}{dr} \right) \frac{\partial^2 w}{\partial r^2} + \left(r \frac{dD_1}{dr} - D_\theta\right) \frac{1}{r^2} \frac{\partial w}{\partial r} +$$

$$(D_1 + 4D_{r\theta}) \frac{1}{r^2} \frac{\partial^3 w}{\partial r \partial \theta^2} + \left(r \frac{dD_1}{dr} - D_\theta - 4D_{r\theta}\right) \frac{1}{r^3} \frac{\partial^2 w}{\partial \theta^2} \Big] \qquad (2.30)$$

$$V_\theta = - \Big[(D_1 + 4D_{r\theta}) \frac{1}{r} \frac{\partial^3 w}{\partial r^2 \partial \theta} + \left(D_\theta + 4r \frac{dD_{r\theta}}{dr} - 4D_{r\theta}\right) \frac{1}{r^2} \frac{\partial^2 w}{\partial r \partial \theta}$$

$$+ \left(D_{r\theta} - r \frac{dD_{r\theta}}{dr}\right) \frac{4}{r^3} \frac{\partial w}{\partial \theta} + \frac{D_\theta}{r^3} \frac{\partial^3 w}{\partial \theta^3} \Big] \qquad (2.31)$$

2.3.2 Governing Differential Equation for Orthotropic Curved Plates of Variable Thickness

The differential equation for a curved plate of variable flexural rigidities in terms of the displacement w is obtained by substituting the expressions of moments (Eqns. 2.5-2.7) into the equilibrium equation (Eqn. 2.4). As the rigidities are now functions of r only, due to the taper in the r-direction, the governing differential equation becomes:

$$D_r \frac{\partial^4 w}{\partial r^4} + \left(\frac{2}{r} D_r + 2 \frac{dD_r}{dr}\right) \frac{\partial^3 w}{\partial r^3} + \left(\frac{2}{r} \frac{dD_r}{dr} + \frac{d^2 D_r}{dr^2}\right.$$

$$\left. + \frac{1}{r} \frac{dD_1}{dr} - \frac{D_\theta}{r^2}\right) \frac{\partial^2 w}{\partial r^2} + \left(\frac{1}{r} \frac{d^2 D_1}{dr^2} - \frac{1}{r^2} \frac{dD_\theta}{dr} + \frac{D_\theta}{r^3}\right) \frac{\partial w}{\partial r}$$

$$+ 2\frac{H}{r^2}\frac{\partial^4 w}{\partial r^2 \partial \theta^2} - (2\frac{H}{r^3} - \frac{2}{r^2}\frac{dD_1}{dr} - \frac{4}{r^2}\frac{dD_{r\theta}}{dr})\frac{\partial^3 w}{\partial r \partial \theta^2}$$

$$- (\frac{2}{r^3}\frac{dD_1}{dr} - \frac{1}{r^2}\frac{d^2D_1}{dr^2} + \frac{4}{r^3}\frac{dD_{r\theta}}{dr} + \frac{1}{r^3}\frac{dD_0}{dr} - \frac{2H}{r^4}$$

$$- 2\frac{D_\theta}{r^4})\frac{\partial^2 w}{\partial \theta^2} + \frac{D_\theta}{r^4}\frac{\partial^4 w}{\partial \theta^4} = P(r, 0) \qquad (2.32)$$

substitution of Eqns. 2.15 and 2.16 in Eqn. 2.32 leads to the Levy-type formulation of the governing differential equation of a curved plate of non-uniform thickness.

$$D_r\frac{d^4W}{dr^4} + (2D_r + \frac{2dD_r}{dr})\frac{d^3W}{dr^3} + (\frac{2}{r}\frac{dD_r}{dr} + \frac{d^2D_r}{dr^2}$$

$$+ \frac{1}{r}\frac{dD_1}{dr} - \frac{D_\theta}{r^2} - \frac{2N^2H}{r^2})\frac{d^2W}{dr^2} + (\frac{1}{r}\frac{d^2D_1}{dr^2}$$

$$- \frac{1}{r^2}\frac{dD_\theta}{dr} + \frac{D_\theta}{r^3} + \frac{2N^2H}{r^3} - \frac{2N^2}{r^2}\frac{dD_1}{dr} - \frac{4N^2}{r^2}\frac{dD_{r\theta}}{dr})\frac{dW}{dr}$$

$$+ (\frac{2}{r^3}\frac{dD_1}{dr} - \frac{1}{r^2}\frac{d^2D_1}{dr^2} + \frac{4}{r^3}\frac{dD_{r\theta}}{dr} + \frac{1}{r^3}\frac{dD_0}{dr}$$

$$- \frac{2H}{r^4} - \frac{2D_\theta}{r^4} + N^2\frac{D_0}{r^4})N^2W = P_n \qquad (2.33)$$

Eqn. 2.33 reduces to that of uniform plate thickness (Eqn. 2.20) by setting the variation in rigidities as zero.

The shear forces are:

$$Q_r = -\sum_{n=1}^{\infty} [\, D_r \frac{d^3W}{dr^3} + (\frac{dD_r}{dr} + \frac{D_r}{r}) \frac{d^2W}{dr^2} + (\frac{1}{r}\frac{dD_1}{dr} - \frac{D_\theta}{r^2} - \frac{HN^2}{r^2})\frac{dW}{dr} + (H + D_\theta - \frac{rdD_1}{dr}) \frac{N^2}{r^3} W \,|\, \sin N\theta \qquad (2.34)$$

$$Q_\theta = -\sum_{n=1}^{\infty} [\, \frac{H}{r}\frac{d^2W}{dr^2} + (\frac{D_\theta}{r^2} + \frac{2}{r}\frac{dD_{r\theta}}{dr})\frac{dW}{dr} - (\frac{2}{r^2}\frac{dD_{r\theta}}{dr} + \frac{D_\theta N^2}{r^3})W \,|\, N.\cos N\theta \qquad (2.35)$$

$$V_r = -\sum_{n=1}^{\infty} [D_r \frac{d^3W}{dr^3} + (\frac{dD_r}{dr} + \frac{D_r}{r}) \frac{d^2W}{dr^2} - (HN^2 + 2D_{r0}N^2 + D_\theta - \frac{rdD_1}{dr})\frac{1}{r^2}\frac{dW}{dr} + (H + D_0 - r\frac{dD_1}{dr} + 2D_{r0}) \frac{N^2}{r^3} W| \sin N\theta \qquad (2.36)$$

$$V_\theta = -\sum_{n=1}^{\infty} [\, (H + 2D_{r0}) \frac{1}{r}\frac{d^2W}{dr^2} + (\frac{D_0}{r^2} + \frac{4}{r}\frac{dD_{r0}}{dr} - \frac{4D_{r0}}{r^2})\frac{dW}{dr} + (\frac{4D_{r\theta}}{r^3} - \frac{4}{r^2}\frac{dD_{r\theta}}{dr} - \frac{D_\theta N^2}{r^3}) W| \, N.\cos N\theta \qquad (2.37)$$

Chapter 3

FINITE DIFFERENCE FORMULATION

3.1 Introduction to Finite Difference

3.1.1 General

Most of the methods used in structural analysis are based on the solution of the basic differential equations of equilibrium and compatibility. Analytical solutions of these differential equations are limited in scope. But, fortunately, for complex problems, numerical treatment of these equations can yield approximate but yet, very accurate results which are acceptable for most practical purposes.

Among the numerical methods presently available, the finite difference method has been used in applications to achieve results with sufficient accuracy.

Finite difference method is mainly based on replacing the derivatives of a function by difference expressions of this function at some selected points on the structure referred to as nodes or pivotal points, or simply as points of division(27). These points are located at the joints of a linear, rectangular, triangular, or other reference network called finite difference mesh. The differential equation then, is applied in difference form at each node, relating the values of the function at the given node and nodes in its vicinity to the external

applied load at this node. Eventually, a sufficient number of simultaneous equations for these values is obtained. For nodes on the boundary or close to it, the coefficients of the equations should account for the boundary conditions, so, they have to be modified compared with the coefficients used at the interior nodes.

3.1.2 One-Dimensional Finite Difference

In this work, we are only concerned with one-dimensional finite difference in which nodes are distributed along a line (Fig. 3.1).

Depending on the order of formulation of derivative expressions, four methods are available:

(i) forward difference

(ii) backward difference

(iii) central difference

(iv) combined difference

It has been proved, (3), that the central difference type is the most accurate among these different methods. Because of this higher accuracy, it has been used in this work.

In the central difference method, the equations for derivatives are as follows, (3)

$$\left(\frac{dy}{dx}\right)_m = \frac{1}{2\Delta x}\left(y_{m+1} - y_{m-1}\right) \qquad (3.1)$$

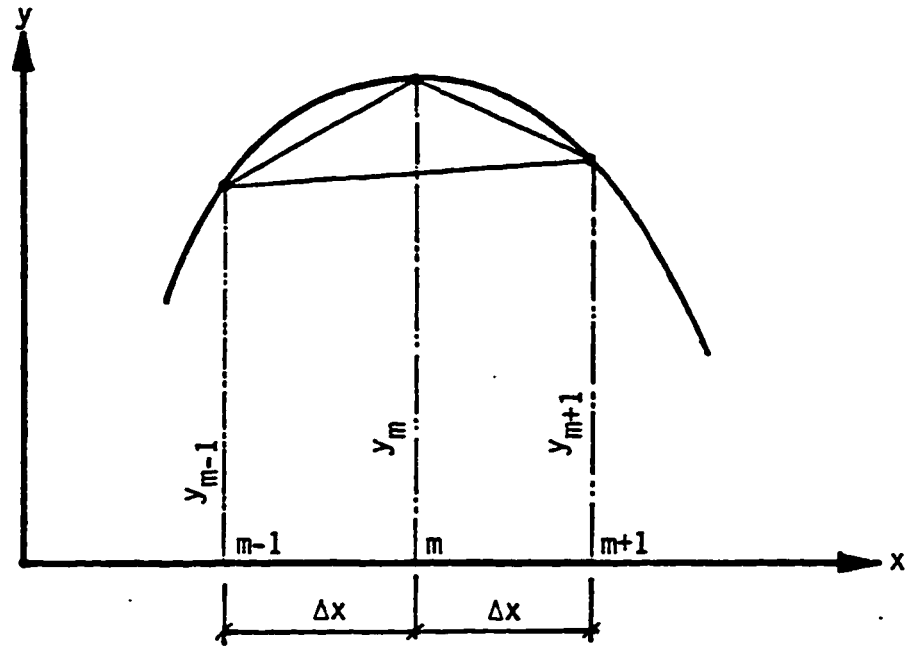

Fig. 3.1 One-dimensional finite-difference mesh

$$\left(\frac{d^2y}{dx^2}\right)_m = \frac{1}{(\Delta x)^2}\left(y_{m+1} - 2y_m + y_{m-1}\right) \tag{3.2}$$

$$\left(\frac{d^3y}{dx^3}\right)_m = \frac{1}{2(\Delta x)^3}\left(y_{m+2} - 2y_{m+1} + 2y_{m-1} - y_{m\ 2}\right) \tag{3.3}$$

$$\left(\frac{d^4y}{dx^4}\right)_m = \frac{1}{(\Delta x)^4}\left(y_{m+2} - 4y_{m+1} + 6y_m - 4y_{m\ 1} + y_{m-2}\right) \tag{3.4}$$

Table 3.1 represents these methods schematically.

3.2 Finite Difference Equations for A Curved Deck

The governing differential equations (Eqs. 2.20, 2.33) which are expressed in terms of the amplitude of sinusoidal deflection, W, can be transformed into finite difference form. The sinusoidal affinity between the displacement and load series (Eqs. 2.15, 2.16) allows one to write the difference equilibrium equations at the central radial line only, (Fig. 3.2), in terms of the amplitude of the deflection W of the slab for each Fourier load component and subsequently solve for W. Thus, the central radial line is divided into m number of closely spaced discrete nodes with a uniform spacing of h.

3.2.1 Curved Plate of Uniform Thickness

3.2.1.1 Governing Differential Equation: Applying the stencil equations, shown in Table 3.1, on the different derivatives of Eq. (2.20)

Table 3.1.a

TYPE	$y_m^{(k)}$	COEFFICIENTS
Forward	y'_m	$\frac{1}{\Delta x}[-1 \; +1]$
	y''_m	$\frac{1}{(\Delta x)^2}[+1 \; -2 \; +1]$
	y'''_m	$\frac{1}{(\Delta x)^3}[-1 \; +3 \; -3 \; +1]$
	y^{IV}_m	$\frac{1}{(\Delta x)^4}[+1 \; -4 \; +6 \; -4 \; +1]$
Backward	y'_m	$[-1 \; +1]\frac{1}{\Delta x}$
	y''_m	$[+1 \; -2 \; +1]\frac{1}{(\Delta x)^2}$
	y'''_m	$[-1 \; +3 \; -3 \; +1]\frac{1}{(\Delta x)^3}$
	y^{IV}_m	$[+1 \; -4 \; +6 \; -4 \; +1]\frac{1}{(\Delta x)^4}$
Combined	y'_m	$[-1 \; +1]\frac{1}{\Delta x}$
	y''_m	$[+1 \; -2 \; +1]\frac{1}{(\Delta x)^2}$
	y'''_m	$[-1 \; +3 \; -3 \; +1]\frac{1}{(\Delta x)^3}$
	y^{IV}_m	$[+1 \; -4 \; +6 \; -4 \; +1]\frac{1}{(\Delta x)^4}$
point		$m-4 \; m-3 \; m-2 \; m-1 \; m \; m+1 \; m+2 \; m+3 \; m+4$

Table 3.1.b

Central difference	$y_m^{(k)}$	COEFFICIENTS
	y'_m	$[-1 \; +1]\frac{1}{2(\Delta x)}$
	y''_m	$[+1 \; -2 \; +1]\frac{1}{(\Delta x)^2}$
	y'''_m	$[-1 \; +2 \; -2 \; +1]\frac{1}{2(\Delta x)^3}$
	y^{IV}_m	$[+1 \; -4 \; +6 \; -4 \; +1]\frac{1}{(\Delta x)^4}$
	point	$m-2 \; m-1 \; m \; m+1 \; m+2$

Table 3.1: Schematic representation of various finite difference expressions (Reference 3).

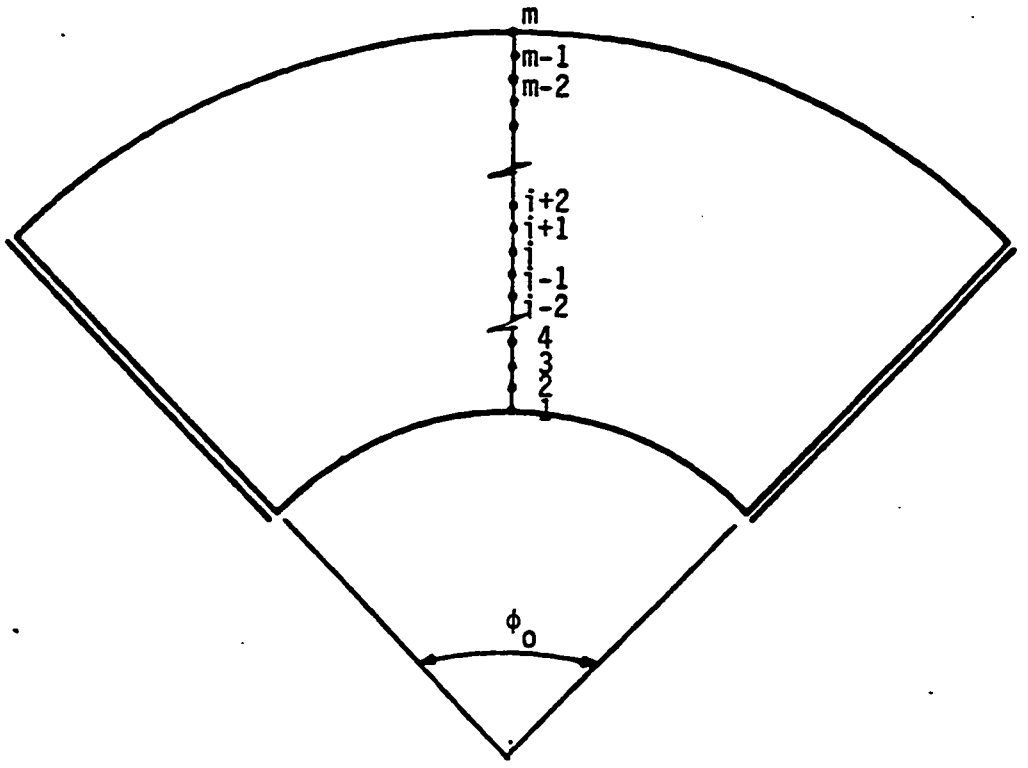

Fig. 3.2 Curved plate plan with nodal points at the radial center line

yields the following difference expressions:

$$\frac{d^4W}{dr^4} = \frac{1}{h^4}\left[W_{i+2} - 4W_{i+1} + 6W_i - 4W_{i-1} + W_{i-2} \right] \qquad (3.5)$$

$$\frac{d^3W}{dr^3} = \frac{1}{2h^3}\left[W_{i+2} - 2W_{i+1} + 2W_{i-1} - W_{i-2} \right] \qquad (3.6)$$

$$\frac{d^2W}{dr^2} = \frac{1}{h^2}\left[W_{i+1} - 2W_i + W_{i-1} \right] \qquad (3.7)$$

$$\frac{dW}{dr} = \frac{1}{2h}\left[W_{i+1} - W_{i-1} \right] \qquad (3.8)$$

Therefore, the typical central difference form for Eq. (2.20) at an interior node i (i = 3 to m - 2) is written as:

$$C_{i+2}\, W_{i+2} + C_{i+1}\, W_{i+1} + C_i W_i + C_{i-1}\, W_{i-1} + C_{i-2}\, W_{i-2} = P_i \qquad (3.9)$$

For clarity of presentation, expressions of coefficients C are shown in Appendix A.

P_i is the distributed load along the radial line at node i. (Eqs. 2.17 - 2.19).

The equations at the first two nodes 1, 2 and at the last two nodes m-1, m require implementation of the boundary conditions. This will be discussed in Section (3.2.2).

3.2.1.2 Force-Displacement Relationships: Applying the finite difference form of Eqs. (2.21 - 2.27), the internal forces at a typical

interior node i be expressed as follows:

$$M_r = -\frac{D_r}{h^2}\sum_{n=1}^{\infty}(A_{i+1}\,W_{i+1} + A_i\,W_i + A_{i-1}\,W_{i-1})\,\sin N\theta \qquad (3.10)$$

$$M_\theta = -\frac{D_\theta}{h^2}\sum_{n=1}^{\infty}(B_{i+1}\,W_{i+1} + B_i W_i + B_{i-1}\,W_{i-1})\,\sin N\theta \qquad (3.11)$$

$$M_{r\theta} = \frac{D_{r\theta}}{hr}\sum_{n=1}^{\infty}\left(-W_{i+1} + \frac{2h}{r}\,W_i + W_{i-1}\right) N.\cos N\theta \qquad (3.12)$$

$$Q_r = \sum_{n=1}^{\infty}\left[\,D_{i+2}\,W_{i+2} + D_{i+1}\,W_{i+1} + D_i\,W_i + D_{i\,1}\,W_{i-1} + D_{i-2}\,W_{i-2}\,\right]\sin N\theta \qquad (3.13)$$

$$Q_\theta = -\sum_{n=1}^{\infty}\left[\,E_{i+1}\,W_{i+1} + E_i\,W_i + E_{i-1}\,W_{i-1}\,\right] N.\cos N\theta \qquad (3.14)$$

$$V_r = \sum_{n=1}^{\infty}\left[\,G_{i+2}\,W_{i+2} + G_{i+1}\,W_{i+1} + G_i\,W_i + G_{i\,1}\,W_{i-1} + G_{i-2}\,W_{i-2}\,\right]\sin N\theta \qquad (3.15)$$

$$V_\theta = -\sum_{n=1}^{\infty}\left[\,H_{i+1}\,W_{i+1} + H_i\,W_i + H_{i-1}\,W_{i-1}\,\right] N.\cos N\theta \qquad (3.16)$$

The coefficients A, B, D, E, G and H are given in Appendix A.

3.2.2 Boundary Conditions

Solution of the governing plate equations (2.20 and 2.33) by finite difference method requires proper implementation of the boundary conditions at the two curved edges to obtain the difference equations at the first two nodes (i = 1, 2) and the last two nodes (i = m-1, m), Fig. 3.2.

For a typical bridge deck, the two opposite circumferenceal edges can be generally considered as free.

The boundary conditions at a free edge are:

$$M_r = 0 \tag{3.17}$$

$$V_r = 0 \tag{3.18}$$

Using the finite difference form of M_r (Eq. 3.10) we get the condition at the free edge nodes (i = 1 and i = m):

$$A_{i+1} W_{i+1} + A_i W_i + A_{i-1} W_{i-1} = 0 \tag{3.19}$$

Also, substituting the finite difference form of V_r (Eq. 3.15) into Eq. (3.18), yields:

$$G_{i+2} W_{i+2} + G_{i+1} W_{i+1} + G_i W_i + G_{i-1} W_{i-1} + G_{i\ 2} W_{i-2} = 0 \tag{3.20}$$

(A) Node 1

Application of the difference form of equation of equilibrium at node 1 (Fig. 3.2), involves two fictitious nodes lying outside the deck. These two nodes are eliminated by applying the conditions (3.17, 3.18). Using Eqns. (3.19, 3.20), we get:

$$W_{i-1} = - \frac{1}{A_{i-1}} [A_i W_i + A_{i+1} W_{i+1}] \tag{3.21}$$

$$W_{i-2} = - \frac{G_{i+2}}{G_{i-2}} W_{i+2} + [\frac{G_{i-1}}{G_{i-2}} \frac{A_{i+1}}{A_{i-1}} - \frac{G_{i+1}}{G_{i-2}}] W_{i-1}$$

$$+ [\frac{G_{i-1}}{G_{i-2}} \frac{A_i}{A_{i-1}} - \frac{G_i}{G_{i-2}}] W_i \tag{3.22}$$

substitution of Eqns. 3.21 and 3.22 in the load equation at node i = 1 leads to:

$$J_3 W_3 + J_2 W_2 + J_1 W_1 = 0 \tag{3.23}$$

where J_1, J_2 and J_3 are expressions shown in Appendix A.

(B) Node 2

Substituting Eqn. (3.21) for W_{i-1} into the load equation at node i + 1 = 2 leads to:

$$F_4 W_4 + F_3 W_3 + F_2 W_2 + F_1 W_1 = P_2 \tag{3.24}$$

where the coefficients F_1, F_2, F_3 and F_4 are as shown in Appendix A.

(C) Node m

The application of the load equation at node m (Fig. 3.2) requires two fictitious nodes. From Eqns. 3.19, 3.20, we get:

$$W_{i+1} = \frac{-1}{A_{i+1}} [\, A_i W_i + A_{i-1} W_{i-1} \,] \tag{3.25}$$

and

$$W_{i+2} = [\, \frac{G_{i+1}}{G_{i+2}} \frac{A_i}{A_{i+1}} - \frac{G_i}{G_{i+2}} \,] W_i + [\, \frac{G_{i+1}}{G_{i+2}} \frac{A_{i-1}}{A_{i-1}} - \frac{G_{i-1}}{G_{i+2}} \,] W_{i-1} - \frac{G_{i-2}}{G_{i+2}} W_{i-2} \tag{3.26}$$

where i = m

Substituting in the load equation we get:

$$M_m W_m + M_{m-1} W_{m-1} + M_{m-2} W_{m-2} = 0 \tag{3.27}$$

where M_m, M_{m-1} and M_{m-2} are shown in Appendix A.

D) Node m - 1

Applying Eq. 3.25 in the load equation for this node we eventually get:

$$R_m W_m + R_{m-1} W_{m-1} + R_{m-2} W_{m-2} + R_{m-3} W_{m\,3} = P_{m-1} \qquad (3.28)$$

where R_m, R_{m-1}, R_{m-2} and R_{m-3} are shown in Appendix A.

Furthermore, for general purposes, the case of simple and fixed angular edges has also been considered in the program

3.2.3 Curved Plate of Non-Uniform Thickness

3.2.3.1 Governing Differential Equation

Due to the variation of slab thickness, the rigidities (D_r, D_θ, $D_{r\theta}$) become functions of the radius r at each node. The effect of these functions appears in the governing differential equation (Eq. 2.33). Thus the finite difference expressions should be applied for both the deflection amplitude W and the rigidities. This leads to cumbersome and lengthy expressions. Algebraic manipulation and simplification leads to the typical finite difference equation at an interior node i as

$$C^*_{i+2} W_{i+2} + C^*_{i+1} W_{i+1} + C^*_i W_i + C^*_{i-1} W_{i-1} + C^*_{i\,2} W_{i-2} = P_i \qquad (3.29)$$

where the coefficients C^* are shown in Appendix A.

3.2.3.2 Force-Displacement Relationships

The finite difference formulations of moment-displacement relationships for a slab of non-uniform thickness are exactly the same as those of slab of uniform thickness. Only the shear-displacement relationships will be different and they are as follows:

$$Q_r = \sum_{n=1}^{\infty} [\, D^*_{i+2} W_{i+2} + D^*_{i+1} W_{i+1} + D^*_i W_i + D_{i\ 1} W_{i-1} + D^*_{i-2} W_{i-2} \,] \sin N\theta \tag{3.30}$$

$$Q_\theta = -\sum_{n=1}^{\infty} [\, E^*_{i+1} W_{i+1} + E^*_i W_i + E^*_{i-1} W_{i-1} \,] N.\cos N\theta \tag{3.31}$$

$$V_r = \sum_{n=1}^{\infty} [\, G^*_{i+2} W_{i+2} + G^*_{i+1} W_{i+1} + G^*_i W_i + G^*_{i\ 1} W_{i-1} + G^*_{i-2} W_{i-2} \,] \sin N\theta \tag{3.32}$$

$$V_\theta = -\sum_{n=1}^{\infty} [\, H^*_{i+1} W_{i+1} + H^*_i W_i + H^*_{i-1} W_{i-1} \,] N.\cos N\theta \tag{3.33}$$

where the coefficients D^*, E^*, G^* and H^* are shown in Appendix A.

Chapter 4

METHOD OF SOLUTION

4.1 Introduction

The proposed computerized solution technique can account for variable deck slab thickness, arbitrary loading and arbitrary locations of pier supports. Using Levy-type series formulation, equilibrium difference equations are written along the radial center line of the simply supported deck by removing the discrete redundant pier supports, if any. Using the method of consistent deformations, the pier support reactions are determined and hence the entire structure is solved. It is assumed that at each interior support, the slab is held against deflection but it is free to rotate.

4.2 Simply Supported Bridge Decks

4.2.1 Problem Formulation

Each applied loading on the deck $P(r,0)$ is transformed into Fourier sine series (Eq. 2.16). For each harmonic load cycle, the governing differential equation in difference form (Eq. 3.29) is written along the nodal points of the radial center line ($0 = \varphi_{o/2}$) For m number of nodes, the m number of nodal equations in terms of the amplitude of nodal displacements can be expressed as:

$$[K]\{W\} = \{P\} \tag{4.1}$$

where:

[K] is the coefficient matrix of the order m x m.

{W} is the vector of nodal displacement coefficients (m x 1).

{P} is the load vector (m x 1)

The coefficient matrix [K] and the load vector {P} are generated for each cycle then equation (4.1) is solved to yield the amplitude vector {W}. Once the displacement amplitudes are determined, the displacement w elsewhere and hence the internal forces can easily be computed. Eq. 4.1 must be solved repeatedly for a sufficient number of harmonic cycles to satisfactorily yield convergence. Final solutions of deflection and internal forces are the algebraic summation of results from each cycle.

4.3 Continuous Bridge Decks

The proposed method of analysis has been extended to solve bridge decks with intermediate pier supports using method of consistent deformations.

For a bridge deck simply supported at its radial edges and internally supported by pier supports, the number of redundants is determined by the number of these pier supports. The pier reaction is assumed to be uniformly distributed over the support area (bearing area). If this bearing area at the cross section of the pier

support is circular or rectangular, an equivalent curved area can be used as indicated in Fig. 4.1 for convenience of numerical computations.

4.3.1 Method of Consistent Deformation

For a continuous slab-type bridge deck, the slab is analyzed first as a simple plate (primary structure, Fig. 4.2b) by removing the redundants (interior pier supports). The analysis of the primary structure is mentioned in Section 4.2. A unit load is then applied at each pier location (one after the other) causing deflection at each of the pier supports. For k number of pier supports, k number of linear equations in terms of vertical deflections of the simple curved deck can be written as follows:

$$\Sigma\, X_j\, \delta_{ij} = \delta_{io} - \delta_{is} \quad , \qquad (i,j = 1,k) \tag{4.2}$$

where:

X_j = unknown support reactions at pier j

δ_{ij} = deflection of primary structure at pier i due to unit upward load at j only. (See Fig. 4.2.c).

δ_{io} = deflection of the primary structure at pier i due to the applied load on the deck.

δ_{is} = foundation settlement at Pier i relative to abutments (end supports), if any.

Denoting $(\delta_{io} - \delta_{is})$ as Δ_{io}, Eq. 4.2 can be expressed in matrix form, as

$$[\delta] \{X\} = \{\Delta_o\}. \tag{4.3}$$

The unknown pier reactions can be evaluated from Eq. 4.3 as:

$$\{X\} = [\delta]^{-1} \{\Delta_o\}. \tag{4.4}$$

4.3.2 Problem Formulation

The location of a pier j for a continuous deck can be prescribed by the angle $0 = \varphi_j$ from the reference end and the radial distance $r = r_j$ (Fig. 4.2.c). A unit upward load at pier j can be expressed into Fourier series as:

$$\sum_{n=1}^{\infty} \frac{4}{n\pi} \sin N\varphi_j \sin N\frac{\beta}{2} \sin N0 = 1 \tag{4.5}$$

where $N = \dfrac{n\pi}{\varphi_o}$

Applying each component of Fourier loading of Eq. 4.5 and summing up the results, the value of δ_{ij} can be evaluated hence the displacement matrix $[\delta]$ can be formed. Using Eq. 4.4, the unknown pier reactions $\{X\}$ then can be determined.

The simplicity of the proposed method of analysis lies in the

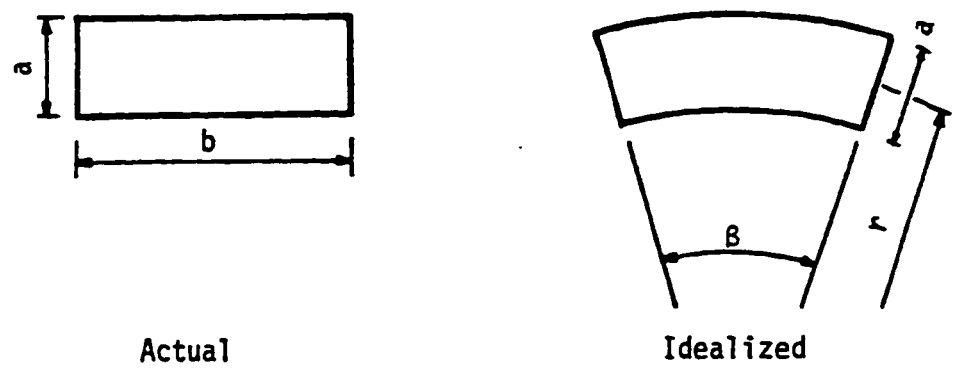

(a)

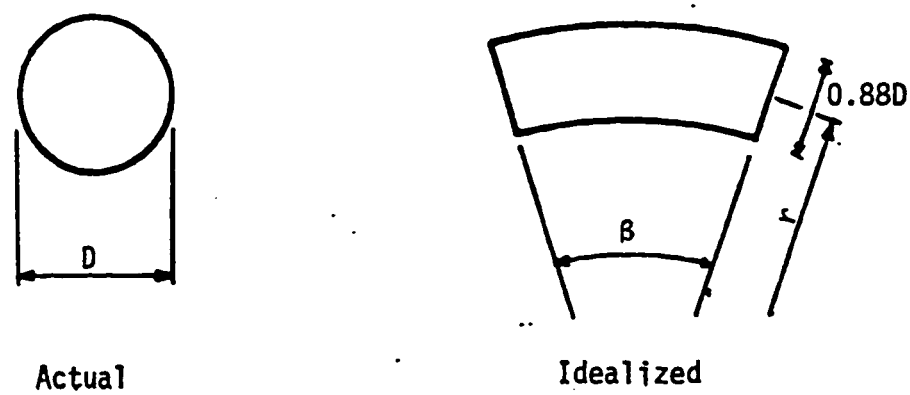

(b)

Fig. 4.1 Idealization of different shapes of cross-section of bearings (a)$\beta = b/r$, (b) $\beta = 0.88D/r$

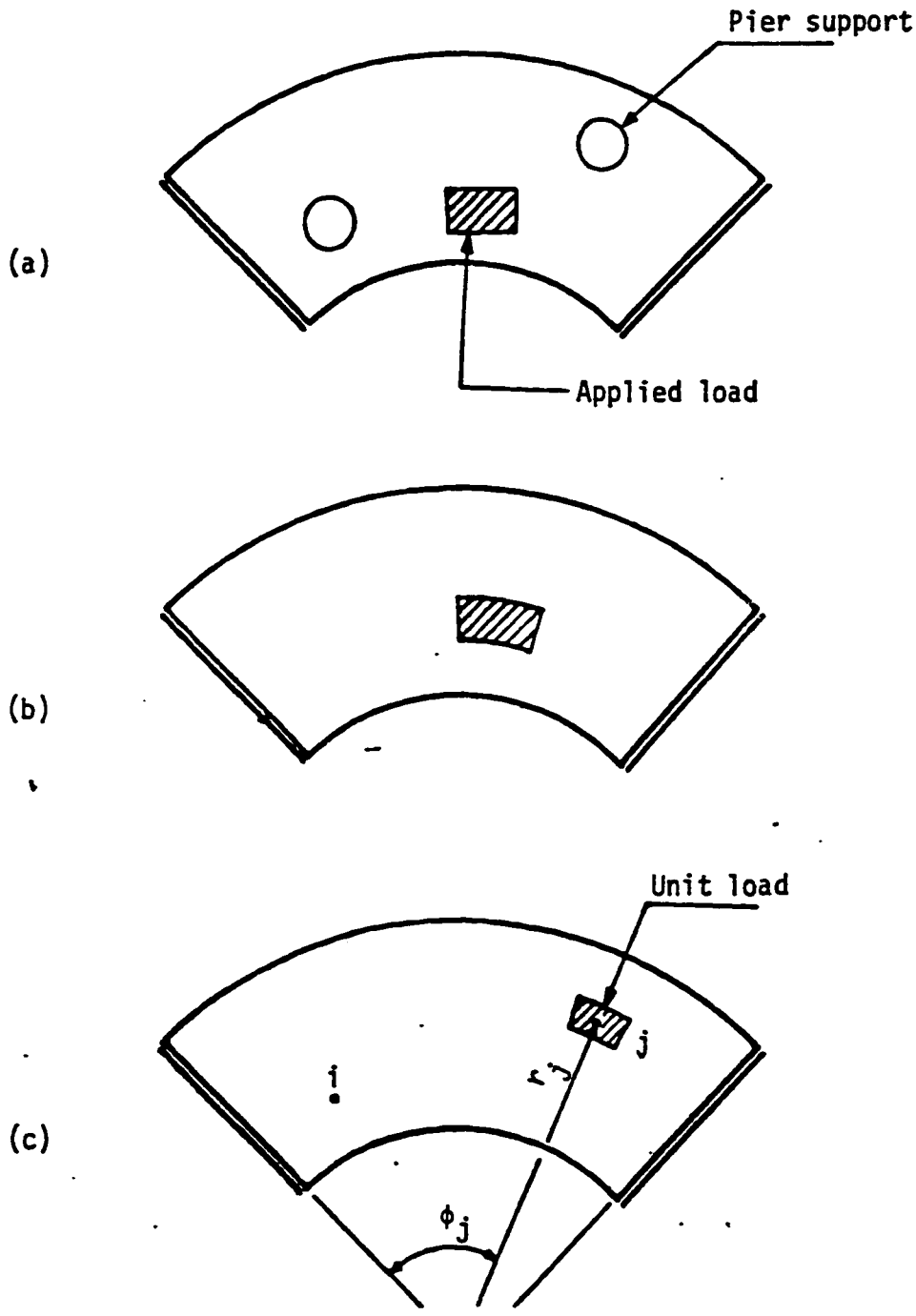

Fig. 4.2 Consistant deformation method (a) Actual structure, (b) primary structure with applied load (c) secondary structure with unit load applied at support j

fact that the primary structure is solved (k + 1) times with different loads, once with the actual load on the deck and k times with unit upward loads at k locations of pier supports. Each individual solution however comprises of a sufficient number of repetitive cycles for a satisfactory convergence. The expression for coefficient matrix [K] for the difference equations and all other equations for internal forces remains unchanged throughout. Thus the solution is essentially an algebraic manipulation of the solution of Eq. 4.1.

4.4 Method of Solution

The different steps of the procedure for solving a continuous bridge deck can be summarized as follows:

(1) The primary structure (after removing the interior supports) is solved with all applied loads as prescribed in Section 4.2. The coefficient matrix, the displacements and the internal forces at the desired locations are all computed.

(2) Then, the primary structure is solved with a unit load applied upward at each pier location (one after the other) and the resulting displacements at interior support locations are assembled properly to generate the flexibility matrix [δ] for the entire structure.

(3) Applying Eq. 4.4, the unknown pier reactions are

evaluated. Each reaction is divided by the area of the bearing to obtain the pier reaction in the form of a patch load.

(4) The primary structure is solved again due to pier reactions as prescribed in Section 4.2.

(5) The final solution of displacements and internal forces is obtained by adding the results of Step (1) and Step (4).

The procedure can be easily programmed for a computer application. The details of the computer program are given in Chapter 5.

Chapter 5

COMPUTER PROGRAM

5.1 Introduction

A computer program in FORTRAN-77 is developed incorporating the proposed method to readily analyze a horizontally curved slab type bridge-deck continuous over discrete pier supports. The program is named as FSTCBA (Fast Curved Bridge Analysis).

It is a general program which can be used for bridge decks with any number of loads and arbitrarily located pier supports. The accuracy of the results depends on the number of harmonic cycles NC. In general NC = 30-45 gives adequate accuracy for these results. The CPU-time is much smaller compared to that required by a program incorporating a different method of analysis. Also the storage required is considerably small (less than 300 KB).

5.2 Description of the Program

The program is written in FORTRAN-77 for IBM370 operating mainframe. It consists of different subroutines coordinated by a main part by which these subroutines are called in sequence. The main subroutines in this program are as follows:

5.2.1 Main Subroutines

Subroutine INPUT:

This subroutine reads the data required to define the geometry of the deck and the properties of the constituent materials.

Subroutine PATCH1:

It reads the location and intensity of the applied loads.

Subroutine SUPP1:

It reads the location and geometry of the pier supports.

Subroutine PROP:

It calculates the structural properties (e.g. Dr, D_0,D_{r0}, etc.).

Subroutine PATCH2:

It generates the load vector {P} for each harmonic cycle.

Subroutine COEFF:

It calculates the required coefficients at each node for the coefficient matrix [COEF] for each harmonic cycle.

Subroutine GELM1:

It solves any set of simultaneous equations.

Subroutine FORCES:

It calculates the deflection and internal forces at the specified location by using the deflection function W.

Subroutine FLEX:

It generates the flexibility matrix required to calculate the support reactions.

Subroutine OUT:

It prints the output of the program which is prepared for an 80-character printer.

5.2.2 Main Steps

The program can be divided into the following main steps:

1) Assemblage of structural data and calculations of relevant parameters.
2) Generation of Coefficient Matrix [COEF].
3) Assemblage of load data and generation of Load Vector {P}.
4) Solution of Equation 4.1 for Deflection Coefficient {W}.
5) Calculation of deflection and internal forces for the primary structure.
6) Generation of Flexibility Matrix [δ].
7) Solution of Equation 4.4 to get the pier reactions {X}.
8) Repetition of Steps 4 and 5 for pier reactions.
9) Addition of result obtained from applied loads to those obtained from pier reactions to get the final results.

The essential features of the program are shown in a flow chart in Fig. 5.1.

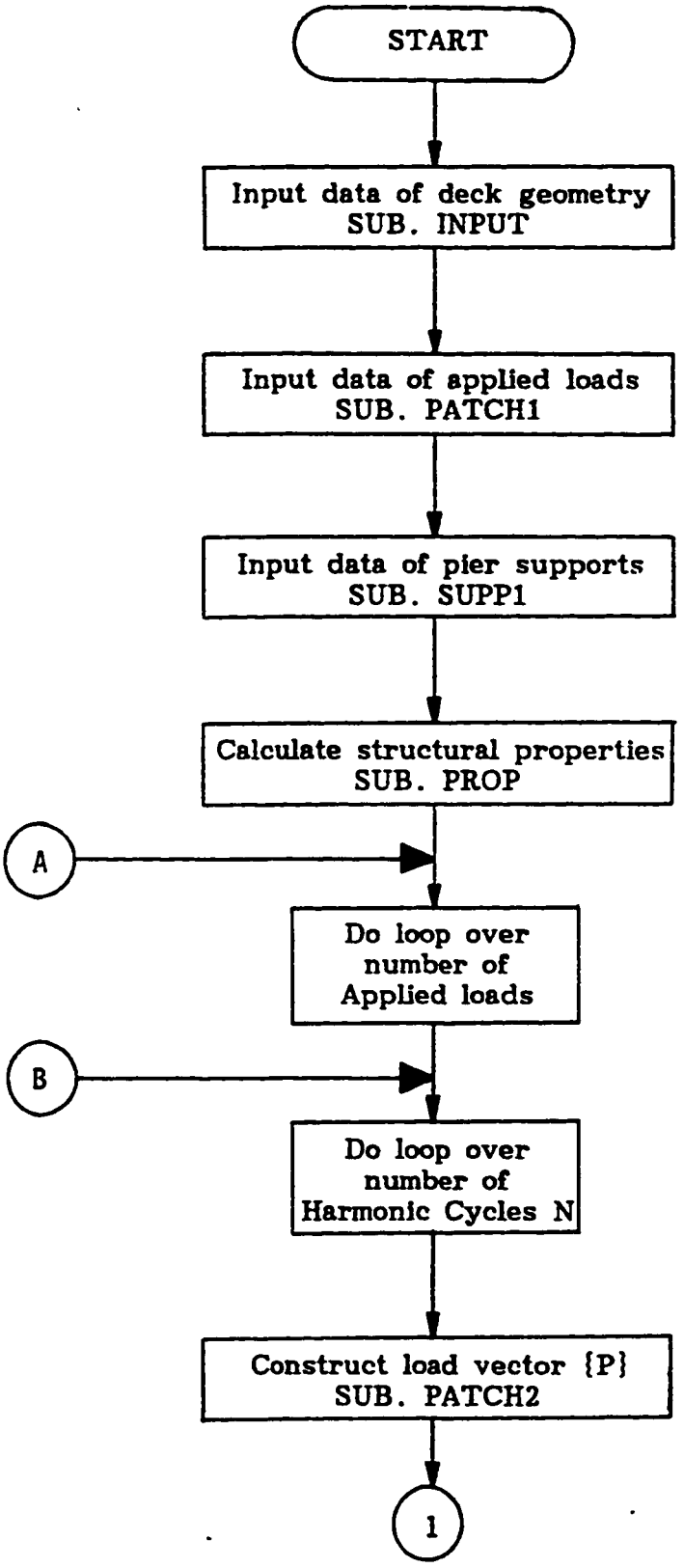

Fig. 5.1: Flow Chart

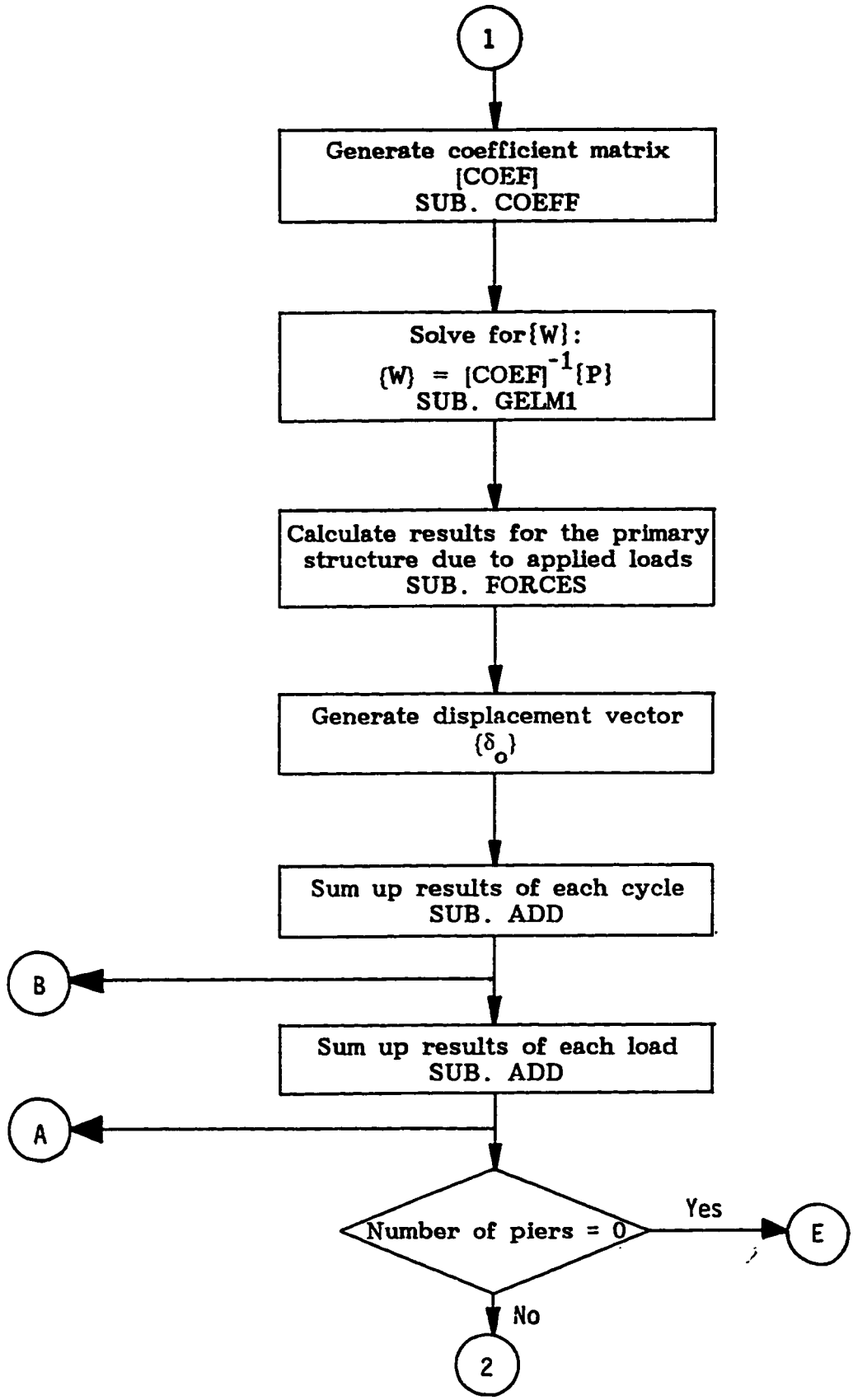
1
Generate coefficient matrix
[COEF]
SUB. COEFF
Solve for{W}:
{W} = [COEF]$^{-1}${P}
SUB. GELM1
Calculate results for the primary structure due to applied loads
SUB. FORCES
Generate displacement vector
{δ_o}
Sum up results of each cycle
SUB. ADD
B
Sum up results of each load
SUB. ADD
A
Number of piers = 0
Yes
E
No
2

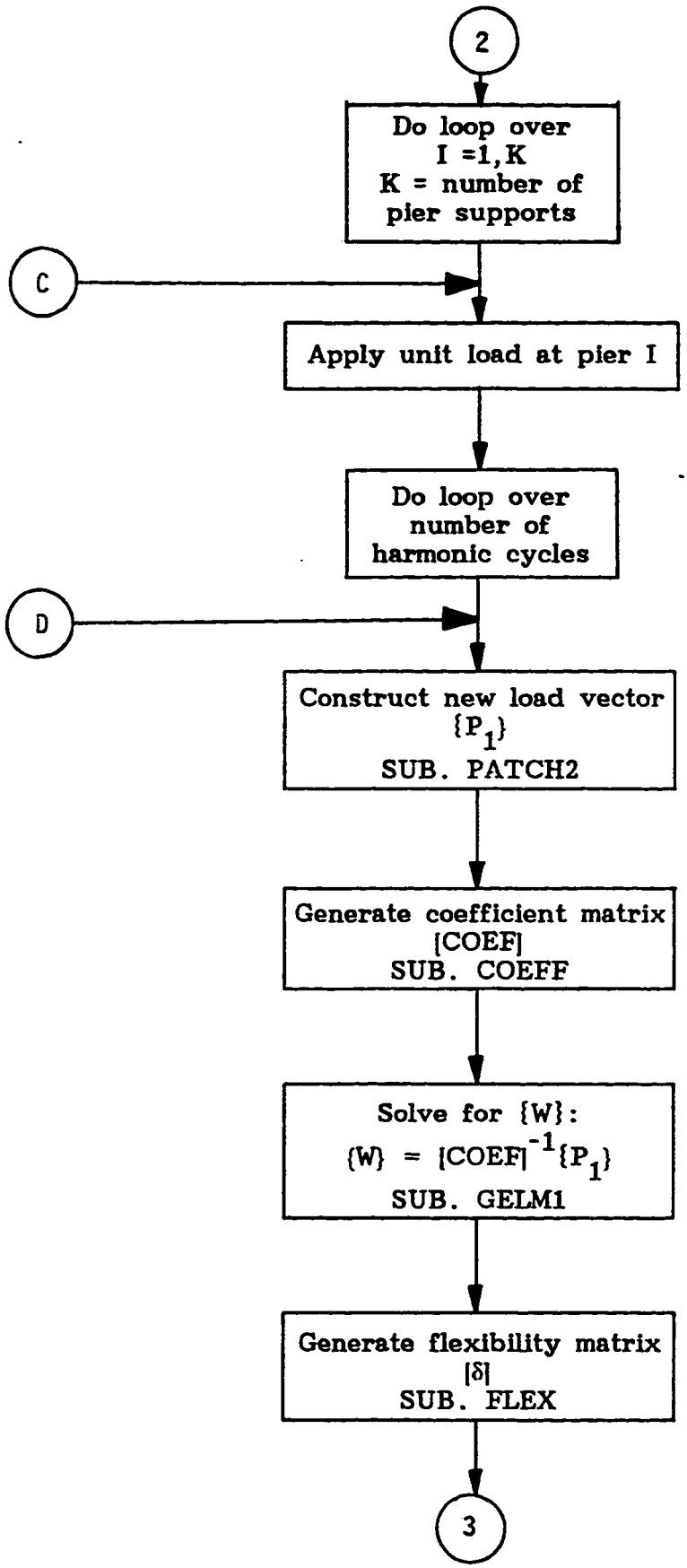
2
Do loop over
I =1,K
K = number of
pier supports
C
Apply unit load at pier I
Do loop over
number of
harmonic cycles
D
Construct new load vector
$\{P_1\}$
SUB. PATCH2
Generate coefficient matrix
[COEF]
SUB. COEFF
Solve for {W}:
$\{W\} = [COEF]^{-1}\{P_1\}$
SUB. GELM1
Generate flexibility matrix
[δ]
SUB. FLEX
3

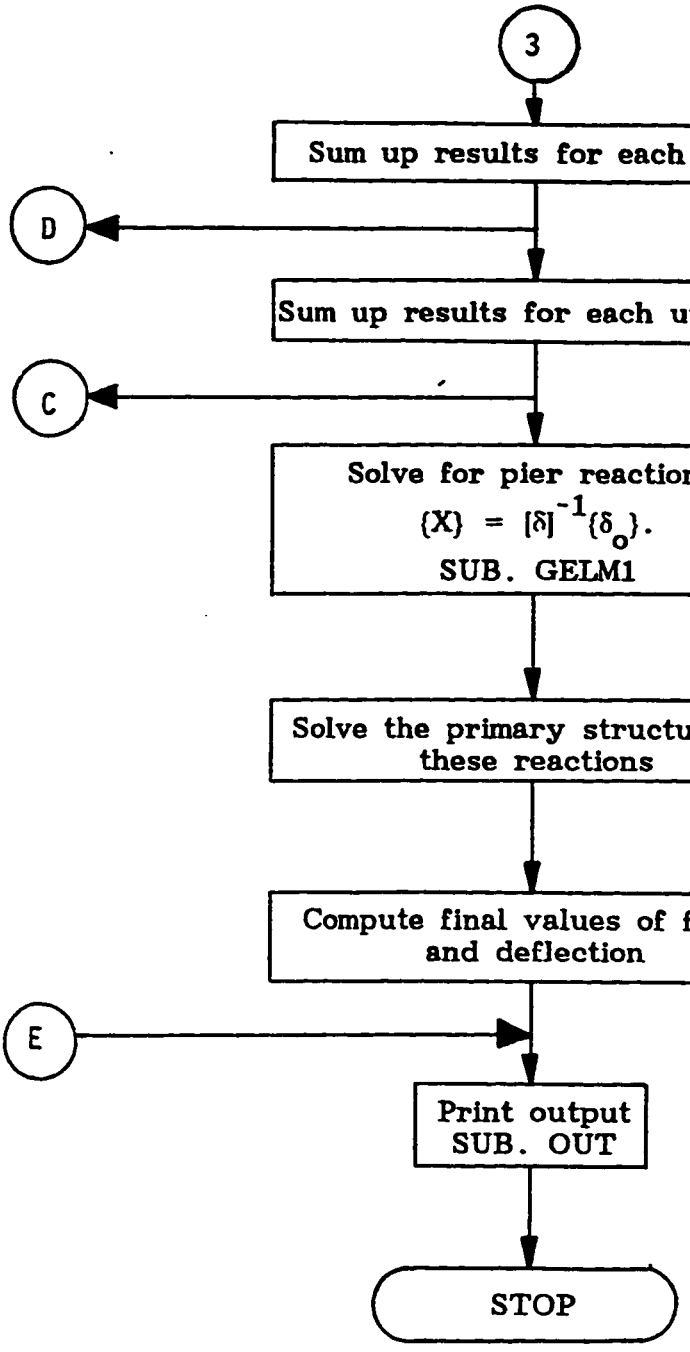
3
Sum up results for each cycle
D
Sum up results for each unit load
C
Solve for pier reactions:
$\{X\} = [\delta]^{-1}\{\delta_o\}$.
SUB. GELM1
Solve the primary structure for these reactions
Compute final values of forces and deflection
E
Print output
SUB. OUT
STOP

5.2.3 Input

Two important points should be observed:

(a) The PARAMETER statement (at the beginning of the program) should be adjusted according to the problem within hand to control the storage required.

(b) The units should be consistent.

The following data are required:

CARD No:

1.	TITLE	Title of the problem
2.a	RCL	Geometry of bridge deck (Fig. 5.2)
2.b	BBR	
2.c	PHI	
2.d	TBR	
3.a	NSP	Number of pier supports
3.b	NPCH	Number of patch loads
3.c	NLOCS	Number of radial lines at which deflection and internal forces are required.
4.a	NN	Number of nodes
4.b	NC	Number of harmonic cycles
5.a	ICOD1	= 1 for ISOTROPIC Plates = 2 for ORTHOTROPIC Plates
5.b	ICOD2	= 1 if it is required to calculate structural parameters (D_r, D_θ...,etc.) = 2 if these parameters will be read directly
5.c	ICOD3	= 1 for plates of UNIFORM THICKNESS

= 2 for plates of NON-UNIFORM THICKNESS

6.a IDG1 = 1 if the inner edge is FREE
= 2 if the inner edge is FIXED
= 3 if the inner edge is SIMPLE

6.b IDG2 = 1 if the outer edge is FREE
= 2 if the outer edge is FIXED
= 3 if the outer edge is SIMPLE

7. THTLC(I) Angle at location I at which deflection and internal forces are required (RAD).

Repeat line 7 for next location.

8.a RPCH(I)
8.b THTPCH(I)
8.c BETPCH(I)
8.d BPCH(I)
Location and geometry of patch load I, (see Fig. 5.3.a)

8.e WPCH(I) Intensity of patch load I (Force/Unit Area)

Repeat line 8 for next load.

9.a RSP(I)
9.b THTSP(I)
9.c BETSP(I)
9.d BSP(I)
Location and geometry of support I, (see Fig. 5.3.b)

9.e ASP(I) Cross-section area of pier I

9.f SETT(I) Foundation settlement at support I, (even if zero)

9.g ELST(I) Elastic shortening of support I (even if zero)

Repeat line 9 for next pier support.

10.a E Modulus of elasticity for the bridge deck (if

ICOD1 = 2, E should be replaced by E_r, E_θ)

10.b PR — Poisson's Ratio υ (if ICOD1 = 2, υ should be replaced by υ_r, υ_θ)

FOR ICOD2=2 only:

11.a DRB — Bending rigidity/unit length in radial direction

11.b DTHTB — Bending rigidity/unit length in angular direction

11.c DRTHTB — Torsional rigidity/unit length

FOR ICOD3=2 only:

12. NTHIK — Number of different thicknesses of the bridge deck

13.a XT(I) — Distance of the location of thickness I measured from the inner edge (Fig. 5.2).

13.b TT(I) — Value of thickness I

Repeat line 13 for next thickness.

5.2.4 Output

The output is formatted for an 80-character printer and it can be adjusted for other printers very easily.

All data are printed out then, the values of deflection, moments and shearing force (per unit length) along the nodes at each specified radial location are printed followed by the values of angular edge shearing force V_θ (per unit length) at the two simply supported radial edges and finally the pier reactions are printed.

For a clear idea about the input data and output, reference can

be made to the example shown in Chapter 6.

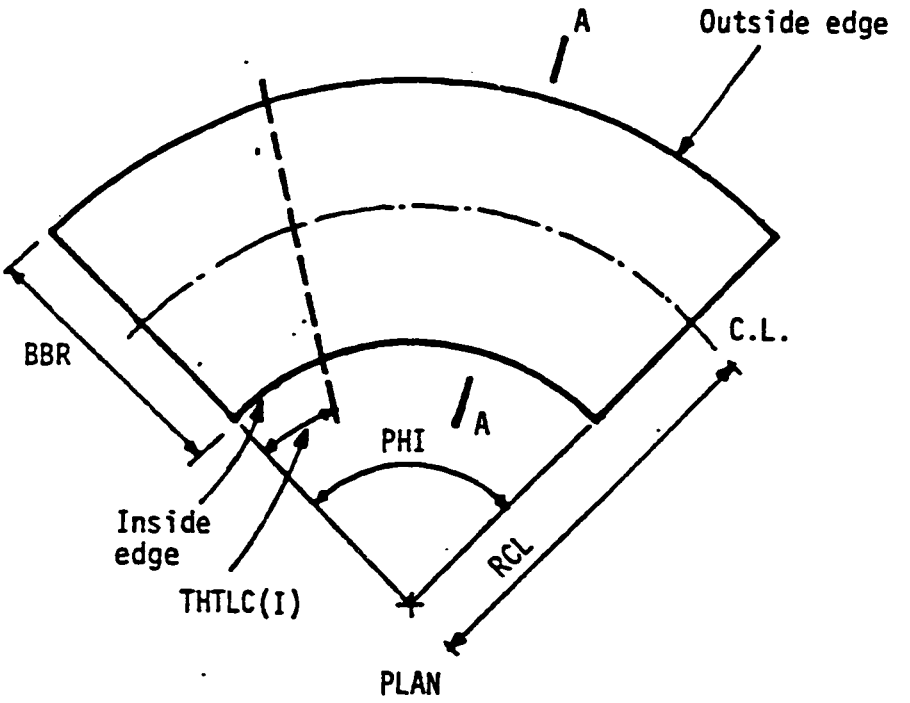

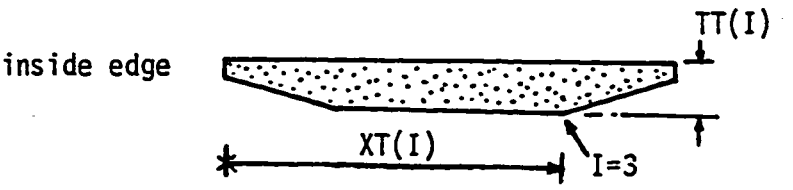

Cross Section A-A

Fig. 5.2 Geometry of bridge deck for input data

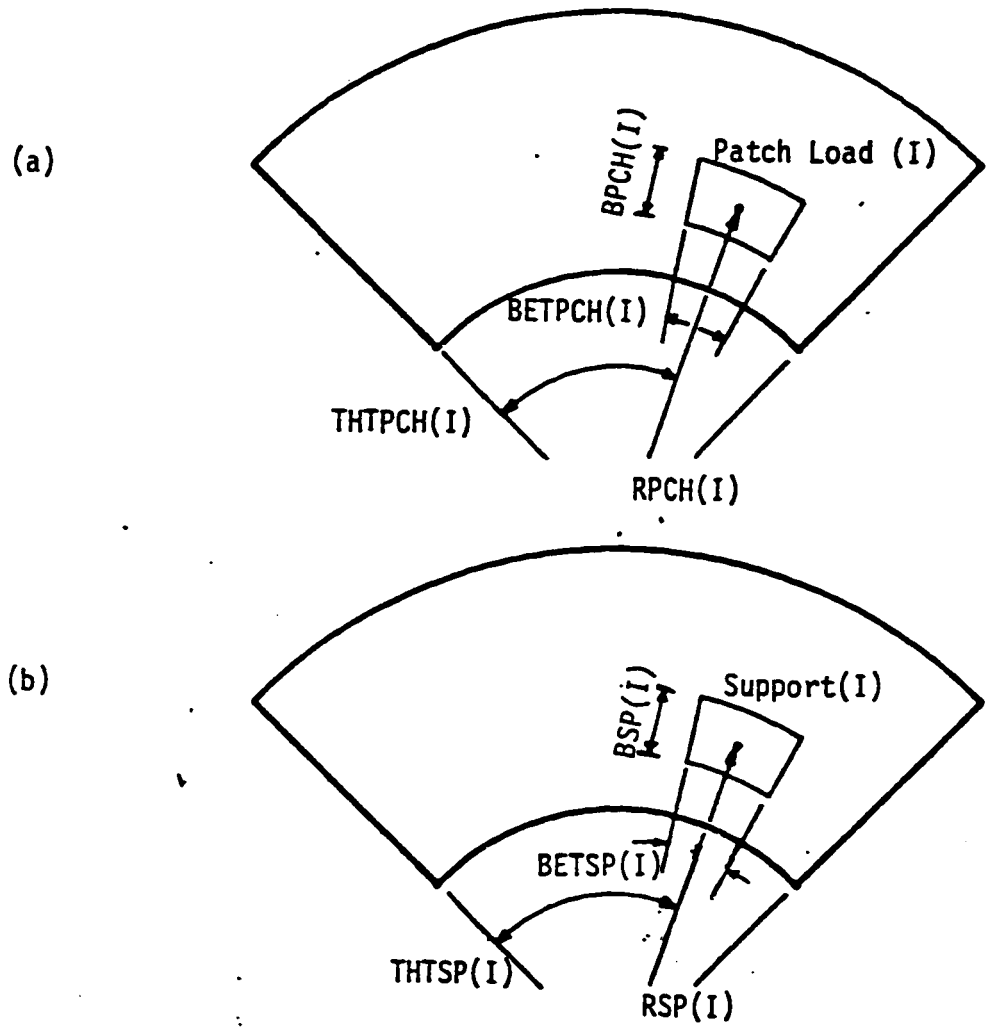

Fig. 5.3 Load and support geometry for input data, (a) location and geometry of patch loads, (b) location and geometry of pier supports

Chapter 6

RESULTS AND DISCUSSIONS

6.1 General

The accuracy of the proposed method is tested first to check its reliability using some known solved problems and some other test problems which are solved by using the STRUDL finite element program. Then, the influence of various parameters on the behavior of curved bridge decks is presented followed by a verification of the simplified method of analysis (22). An example is presented as an illustration at the end of this chapter.

6.2 Reliability of Proposed Method of Analysis

To test the accuracy of the proposed method and the developed program, the results of three test cases were compared with available data.

6.2.1 Simply Supported Curved Slab Bridge

Fig. 6.1 shows the details of a simply supported curved bridge model made of perspex for which the theoretical and experimental results were obtained by Coull and Das (5). The loading cases are a point load of 10 lbs applied separately along the radial center line at the outer edge, the inner edge and the center of the slab

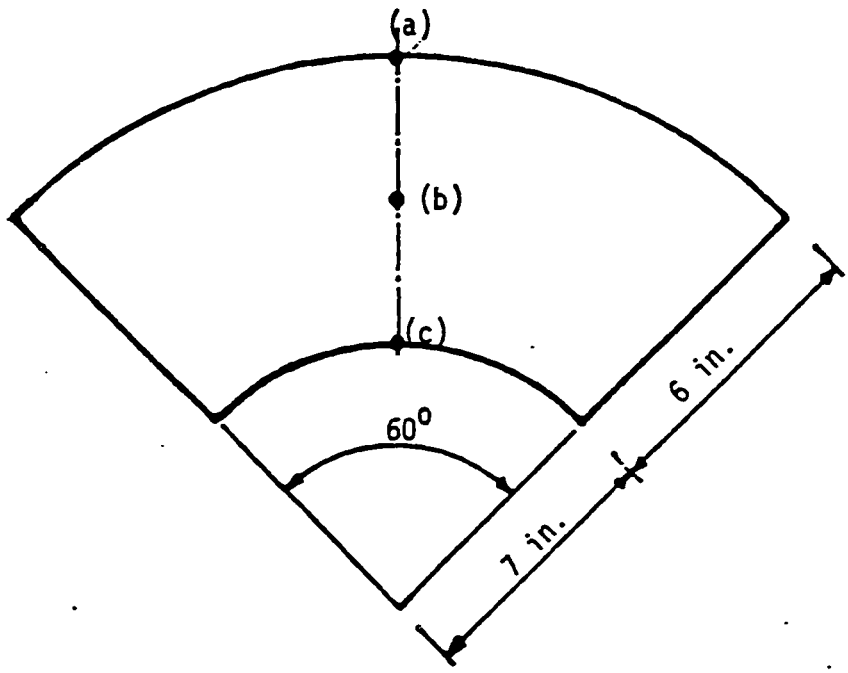

$E = 24 \times 10^5$ lb/in^2

$\nu = .35$

$t = .168$ in.

Fig. 6.1 Simply supported curved bridge model of Perspex

respectively.

This model was solved by Sawko et al (23) using 16 degrees of freedom conforming annular element. Cheung (10) solved this model using the finite strip method with 8 strips across the width of the deck. The same model was solved twice by Fam and Turkstra (24) using annular bending elements and two different mesh divisions. The first mesh has a total of 105 degrees of freedom and the second mesh has a total of 135 degrees of freedom.

Table 6.1 shows the center line deflections obtained by these different methods. Also shown in Table 6.1 are the results obtained from the proposed method of analysis using the computer program FSTCBA. Figs. 6.2, 6.3 and 6.4 show the distributions of experimental values of bending moment at mid span reported by Coull and Das (5). The analytical results obtained from Coull and Das and from FSTCBA are shown in these figures, by referring to them as C & D and FSTCBA, respectively. From Table 6.1 and Figs. 6.2 - 6.4, it is observed that the results from the proposed method correlate well with the experimental values and also agree with the theoretical solutions from other numerical methods.

6.2.2 Rectangular slabs with Different Boundary Conditions

Figs. 6.5-a and 6.5-b show the details of two rectangular slabs. The first one (Fig. 6.5-a) is simply supported at the two short edges and internally supported by a pier support. The loading

Table 6.1 A comparison between FSTCBA and other methods for deflections in inches across mid-span deck (Perspex Model)

Loading case	Radius (in)	Theoretical (5)		Finite Strip(10) 8 Harmonics	Finite Element Method			FSTCBA
		Experiment	Theory 3 Harmonics		Conforming Element(23) 140 Degrees of freedom	Non-Conforming (24) (Present) 105 Degrees of freedom	Non-Conforming (24) (Present) 135 Degrees of freedom	
(a)	13	0.876	0.750	0.995	0.851	0.880	0.881	0.831
	11	0.578	0.500	0.624	0.559	0.577	0.578	0.552
	9	0.353	0.300	0.388	0.344	0.353	0.354	0.339
	7	0.194	0.180	0.206	0.192	0.193	0.194	0.188
(b)	13	0.457	0.470	0.441	0.445	0.456	0.457	0.458
	11	0.342	0.370	0.329	0.333	0.342	0.343	0.343
	9	0.241	0.250	0.222	0.236	0.241	0.241	0.241
	7	0.155	0.170	0.147	0.154	0.154	0.158	0.155
(c)	13	0.195	0.150	0.180	0.192	0.193	0.194	0.216
	11	0.163	0.135	0.152	0.162	0.163	0.164	0.179
	9	0.157	0.125	0.149	0.151	0.151	0.151	0.161
	7	0.169	0.145	0.173	0.170	0.169	0.168	0.172

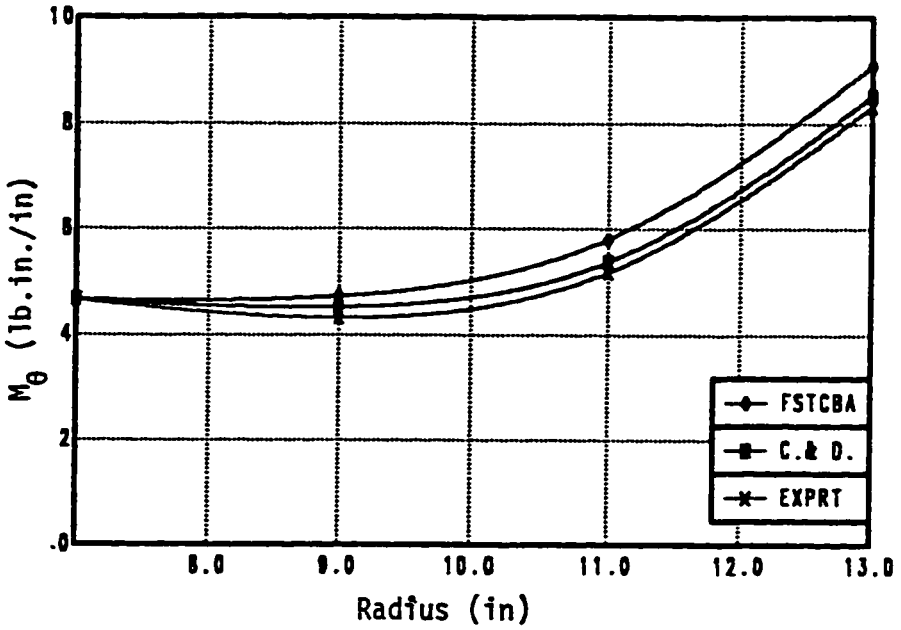

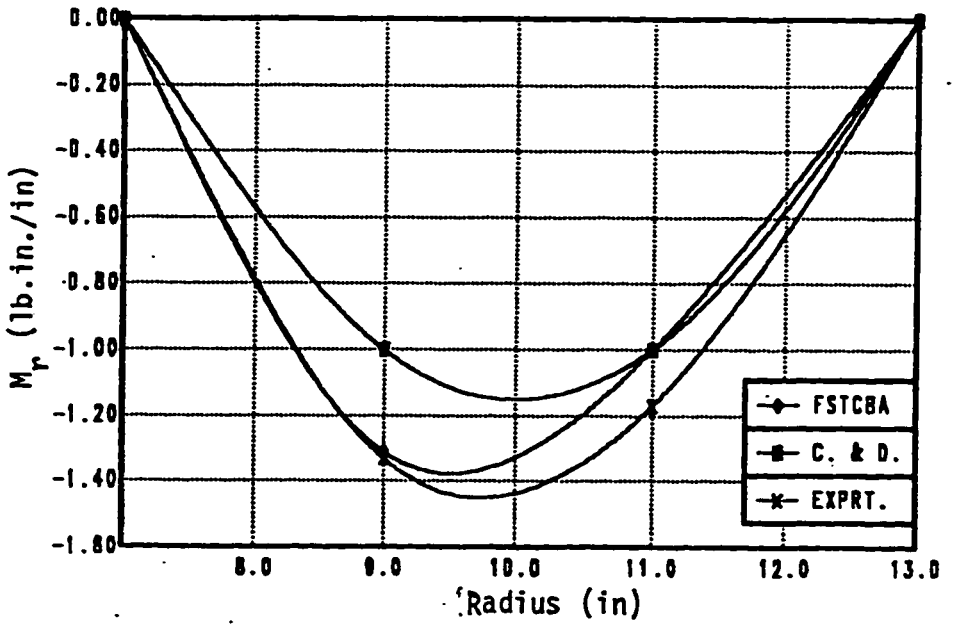

Fig. 6.2 M_θ and M_r obtained by FSTCBA, Coull and Das, and experimentally due to a point load at location a

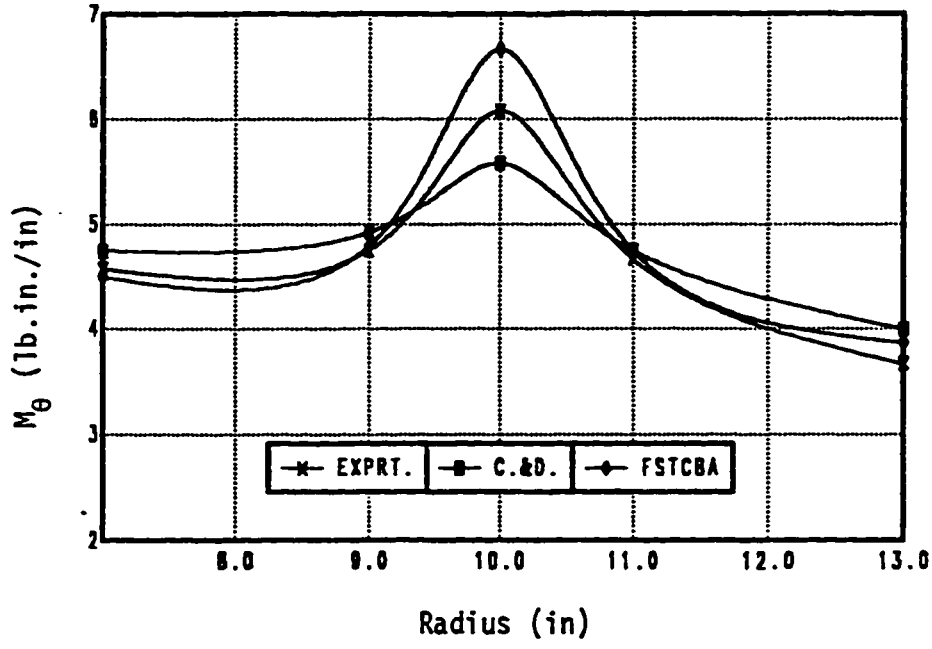

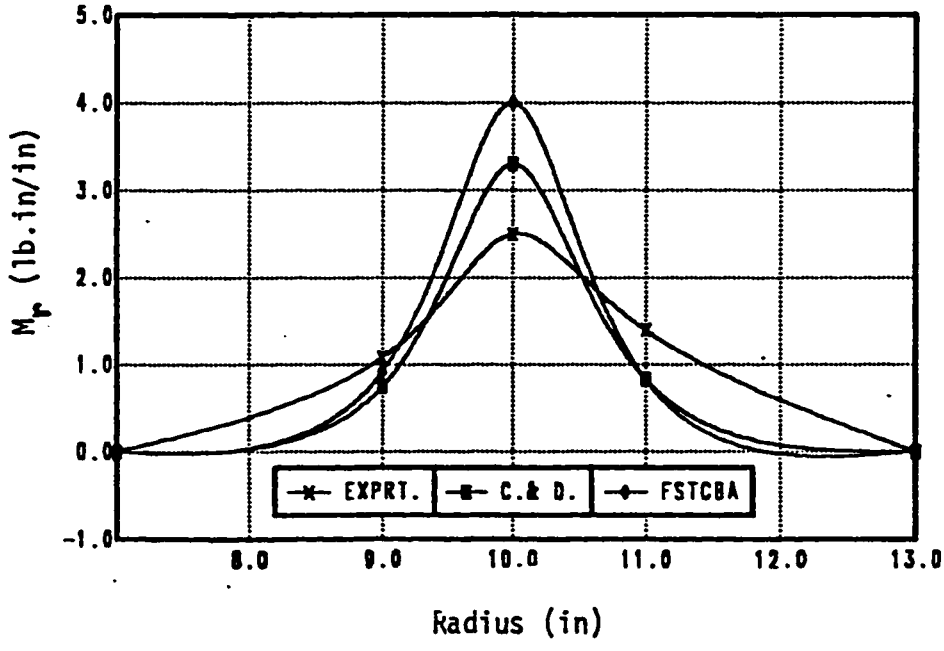

Fig. 6.3 M_θ and M_r obtained by FSTCBA, Coull and Das and experimentally due to a point load at location b

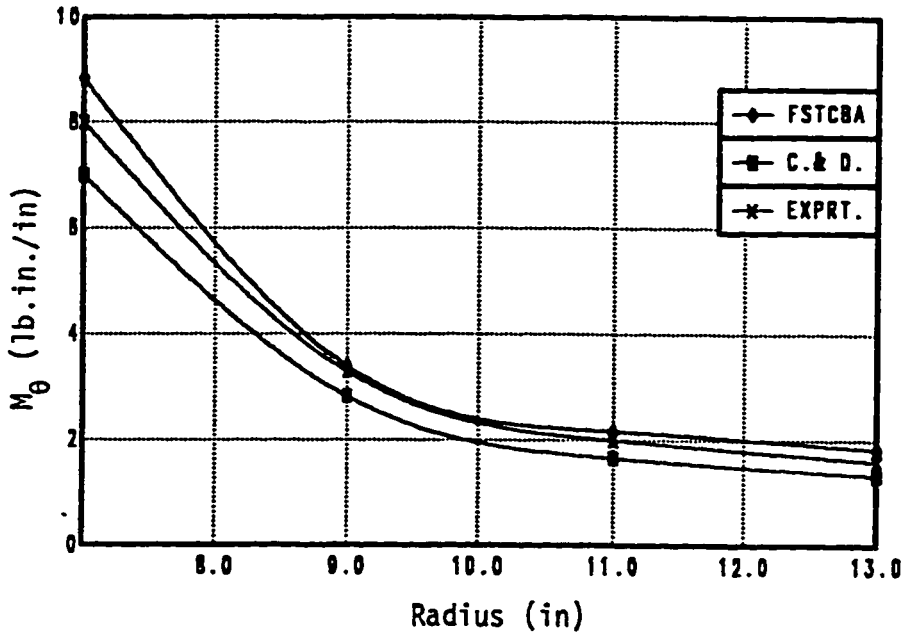

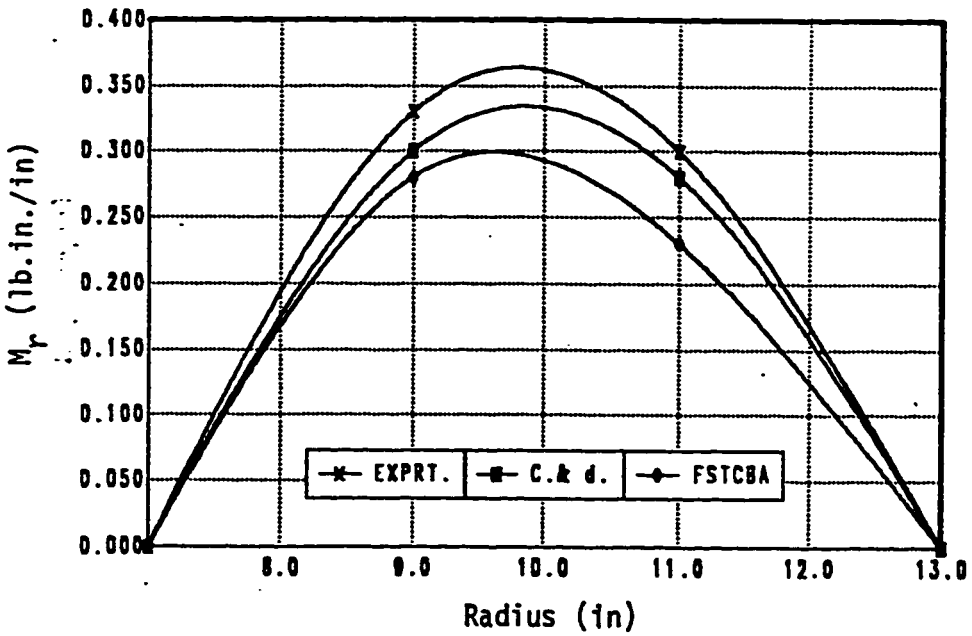

Fig. 6.4 M_θ and M_r obtained by FSTCBA, Coull and Das and experimentally due to a point load at location c

is a uniformly distributed load of $5t/m^2$ and an eccentric concentrated load of 50 tons. The second one (Fig. 6.5-b) is simply supported at three edges and the fourth edge is fixed and is supported additionally by an interior pier support. The loading is a uniformly distributed load of $5t/m^2$. The two decks were solved using FSTCBA and STRUDL to compare the efficiency and accuracy of the proposed method.

When using FSTCBA a large radius of 10^8 m. was assumed to account for the rectangularity of the slab. The concentrated force was transformed to a patch load distributed over a small square area (25 x 25 cm). Table 6.2.a shows the results obtained by both programs at some points on the deck shown in Fig. 6.5-a and Table 6.2.b shows the results for the deck in Fig. 6.5.b. The results of FSTCBA are identical to those obtained by STRUDL. It should be mentioned here that the number of cycles used in FSTCBA was 45 and the number of element used in STRUDL was 200, but the CPU-time consumed by FSTCBA and STRUDL (for the deck in Fig. 6.5-a as an example) was 4.9 and 111.6 seconds respectively which illustrates how much faster is the proposed method compared to the finite element method.

6.2.3 Rectangular Slab Bridge Deck of Non-Uniform Thickness

Fig. 6.6 shows a plan and a cross section for a rectangular

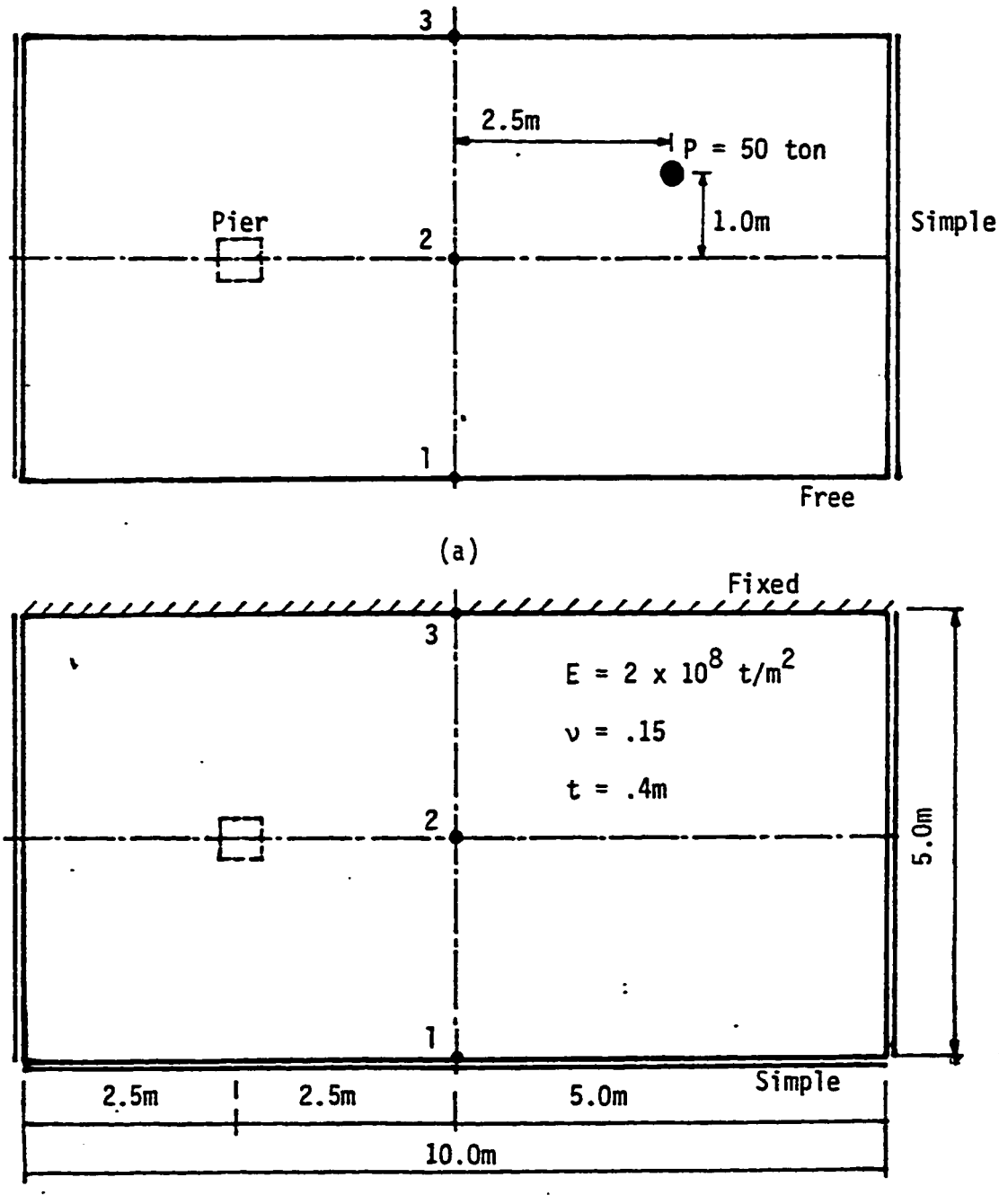

Fig. 6.5 Rectangular slab with different boundary conditions

Table 6.2a A comparison between FSTCBA and STRUDL for a rectangular slab with two simply supported edges, two free edges and one pier support

Point	DEF (m)	M_θ (t.m/m)	M_r (t.m/m)	$M_{r\theta}$ (t.m/m)	Q_θ (t/m)	Q_r (t/m)	
1	.122E-3	15.5	0	-1.9	12.37	0.3	*
	.122E-3	15.5	0	-1.96	11.96	0.223	•
2	.121E-3	18.06	-4.86	-1.21	18.03	0.97	*
	.121E-3	18.36	-4.6	-1.31	19.56	0.83	•
3	.153E-3	17.12	0	0.6	13.34	0.27	*
	.154E-3	17.11	0	0.692	13.25	0.121	•

* Results obtained by STRUDL

• Results obtained by FSTCBA

Table 6.2b A comparison between FSTCBA and STRUDL for a rectangular slab with three simply supported edges, one fixed edge and one interior support

POINT	DEF (m)	M_θ (t-m/m)	M_r (t-m/m)	$M_{r\theta}$ (t-m/m)	Q_θ (t/m)	Q_r (t/m)	
1	0.0	0.0062	0.086	-1.55	0.34	7.25	*
	0.0	0.0	0.0	-1.56	0.0	8.09	●
2	0.97E-5	2.62	5.09	0.29	2.05	-1.99	*
	0.98E-5	2.71	5.12	0.31	2.36	-2.03	●
3	0.0	-2.01	-11.42	0.17	-2.28	-14.3	*
	0.0	-1.72	-11.46	0.0	-2.66	-13.2	●

* Results obtained by STRUDL

● Results obtained by FSTCBA

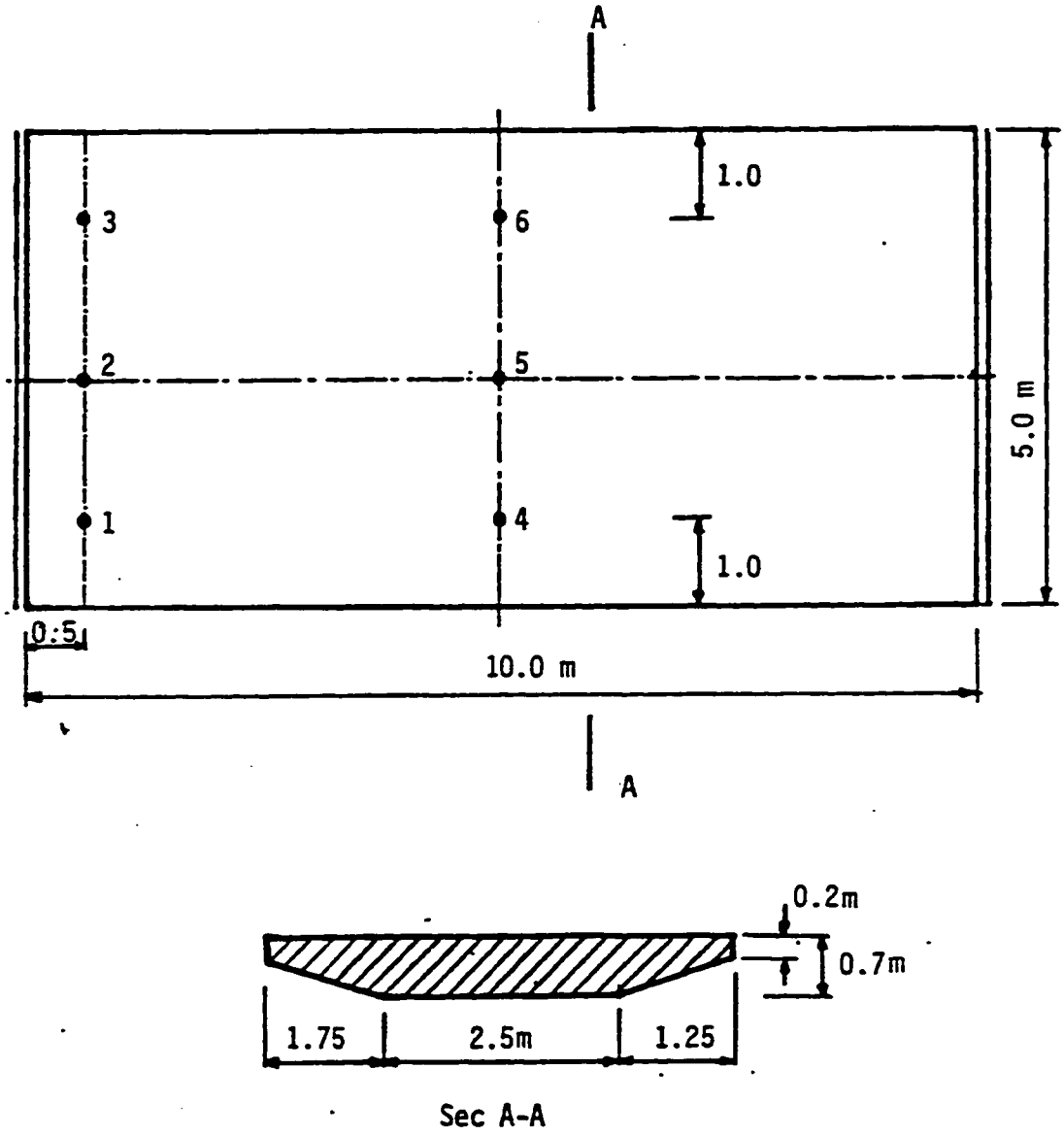

Fig. 6.6 Rectangular slab bridge deck of non-uniform thickness

Table 6.3 A comparison between FSTCBA and STRUDL for a bridge deck with non-uniform thickness

Node	DEF	M_θ	M_r	$M_{r\theta}$	Q_θ	Q_r	
1	0.28E-4	6.65	-0.37	5.07	25.1	-0.65	*
	0.27E-4	6.1	-0.3	4.98	29.64	-1.5	●
2	0.27E-4	17.2	-0.41	0.69	27.5	0	*
	0.26E-4	16.6	-0.25	0.0	27.17	0	●
3	0.28E-4	6.65	-0.73	-5.07	25.1	0.65	*
	0.27E-4	6.61	-0.63	-4.98	29.64	1.5	●
4	0.174E-4	70.0	-1.33	0	0	-1.57	*
	0.166E-3	65.5	-1.16	0	0	-2.23	●
5	0.172E-3	94.4	-1.9	0	0	0.0	*
	0.163E-3	89.25	-1.48	0	0	0.0	●
6	0.174E-3	70.0	-1.33	0	0	1.57	*
	0.166E-3	65.5	-1.15	0	0	2.23	●

* Results obtained by STRUDL

● Results obtained by FSTCBA

slab bridge deck with variable thickness and simply supported at the two short edges. The loading is a uniformly distributed load of $5t/m^2$. The problem was solved by STRUDL after idealizing the variable thickness as a stepped thickness.

Table 6.3 shows a comparison between the results obtained by the proposed method and STRUDL. The two results are almost identical and the proposed method is proved to be very accurate noting that the CPU-time consumed is 3.088 seconds and 253.8 seconds by FSTCBA and STRUDL respectively. This illustrates that the problems with variable thickness can be solved much faster with FSTCBA.

6.3 Parametric Variation Study

6.3.1 Radius of Curvature

Radius of curvature is the most significant geometric parameter which governs the behavior of a curved deck. To show the influence of radius of the curvature on internal forces, a hypothetical bridge deck of two spans is considered, Fig. 6.7. The slab is idealized as a plat of uniform thickness of 1.2 m. The slab width is 16.0 m and the span lengths along the curved central line of the deck, 20 m and 20 m, were kept unchanged but the radius of curvature R was varied. This way the angle φ_o was varied to introduce different degrees of curve. The deck was analyzed with a uniformly distributed load of

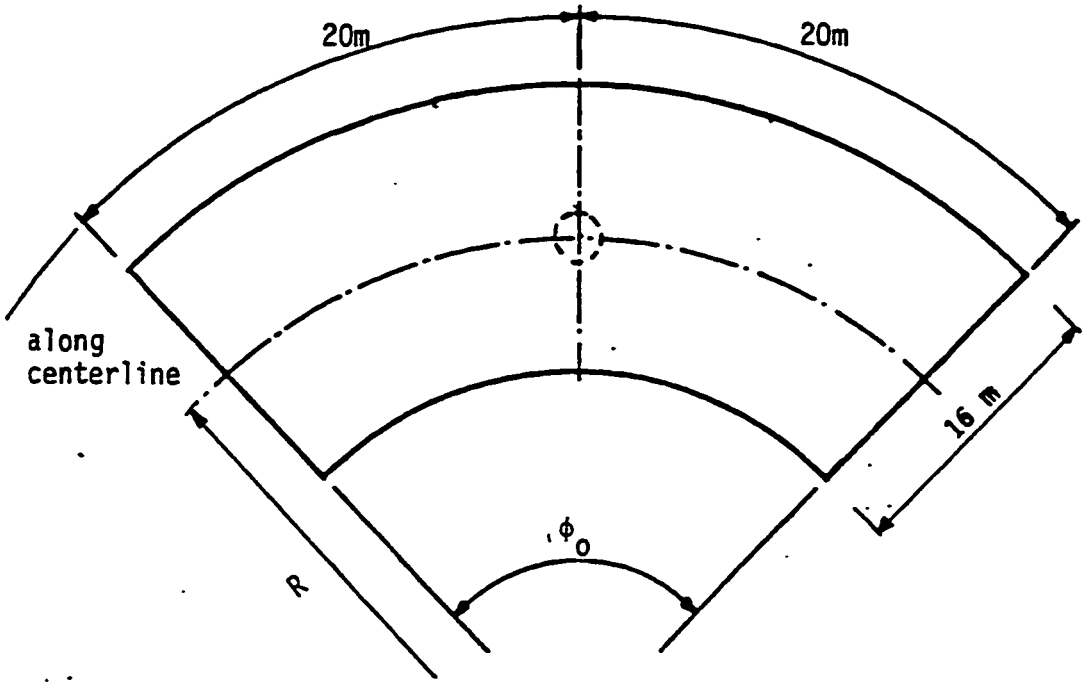

Fig. 6.7 Effect of radius of curvature

10.0 t/m^2.

To show the variation in deflection and internal forces due to varying R, the analysis was carried out for the deck with different degrees of curve, D, i.e. with different values of R.

Figs. 6.8 - 6.11 show the normalized plots of deflection at midspan, Q_0, at the face of pier support, support reaction, and M_0 respectively with D by expressing α as the ratio of the curved plate values to the straight plate values ($R = \infty$) and Fig. 6.12 shows the distribution of Q_r along the radial centerline for $D = 0^0$ and 20^0. As seen from these figures, the deflection, Q_0, support reaction, the angular moment M_0 and Q_r are relatively insensitive to the degree of curve. The deflection, Q_0, the pier reaction and the negative M_0 at the pier support are slowly increasing and the positive moment M_0 at midspan is gradually decreasing by decreasing the radius R, i.e. by increasing the degree of curvature, but these changes are marginally influenced by D. For example, when D is varied from 0 to 20^0, the variation of α being of order of 1.5%, 0.9%, 4% for the deflection, the pier reaction and M_0 respectively. This further confirms the generally accepted notion that the effect of curvature can be neglected to determine the bending moments and shearing forces and thus for practical purposes, a curved bridge can be analyzed as a straight bridge ($R = \infty$) for normal bridge geometry. The torsional moment

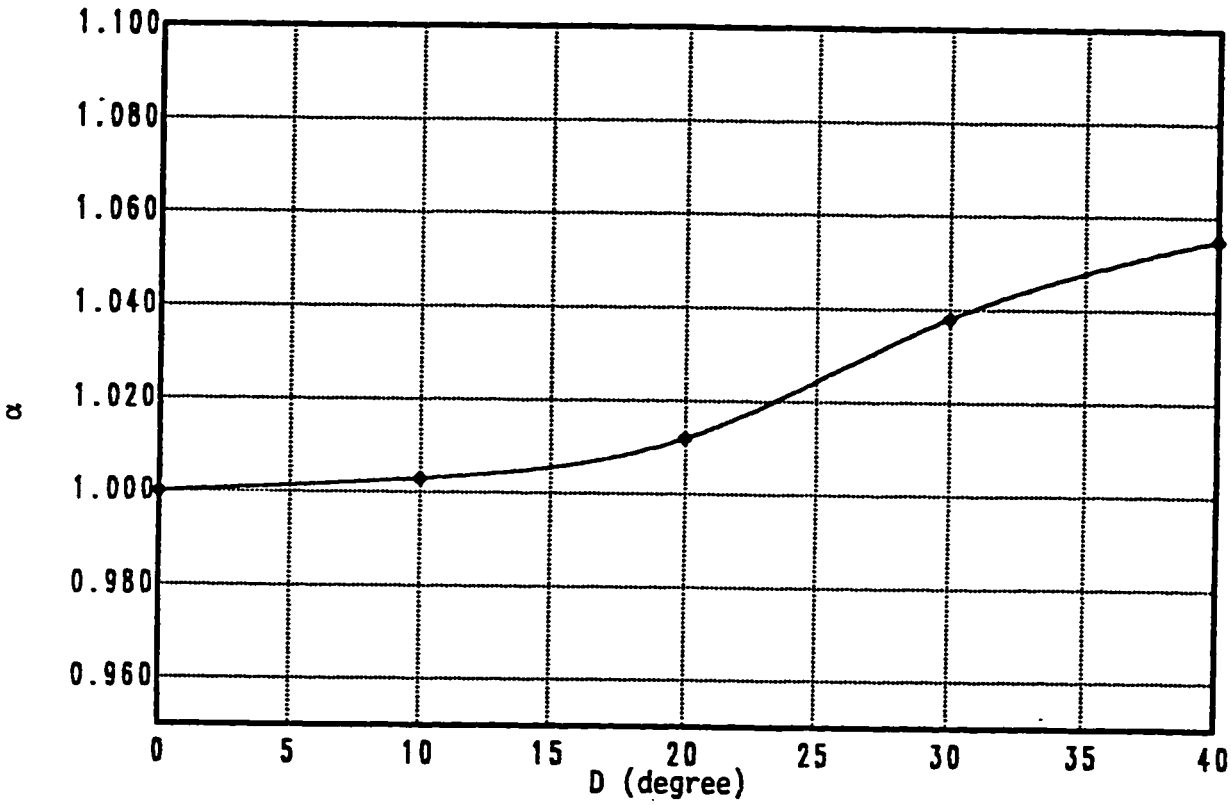

Fig. 6.8 Effect of radius of curvature on the mid-span deflection

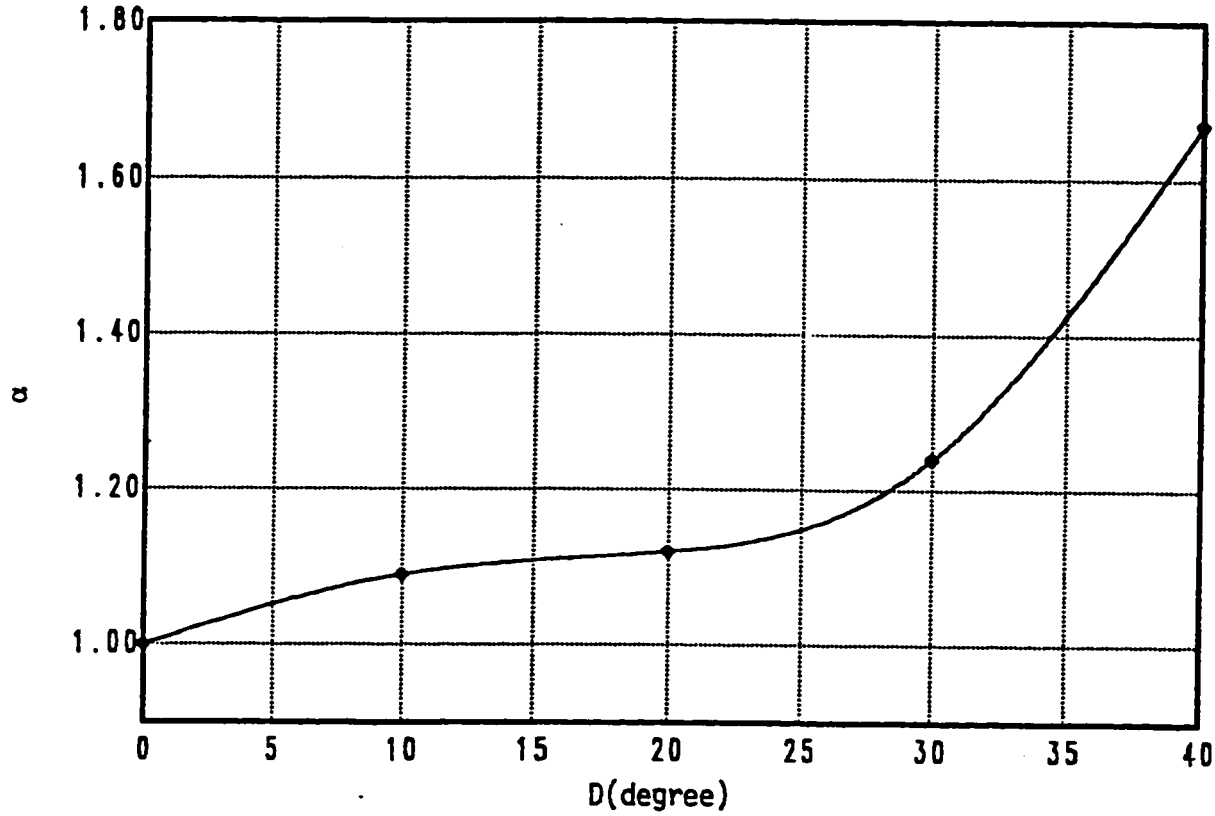

Fig. 6.9 Effect of radius of curvature on Q_0

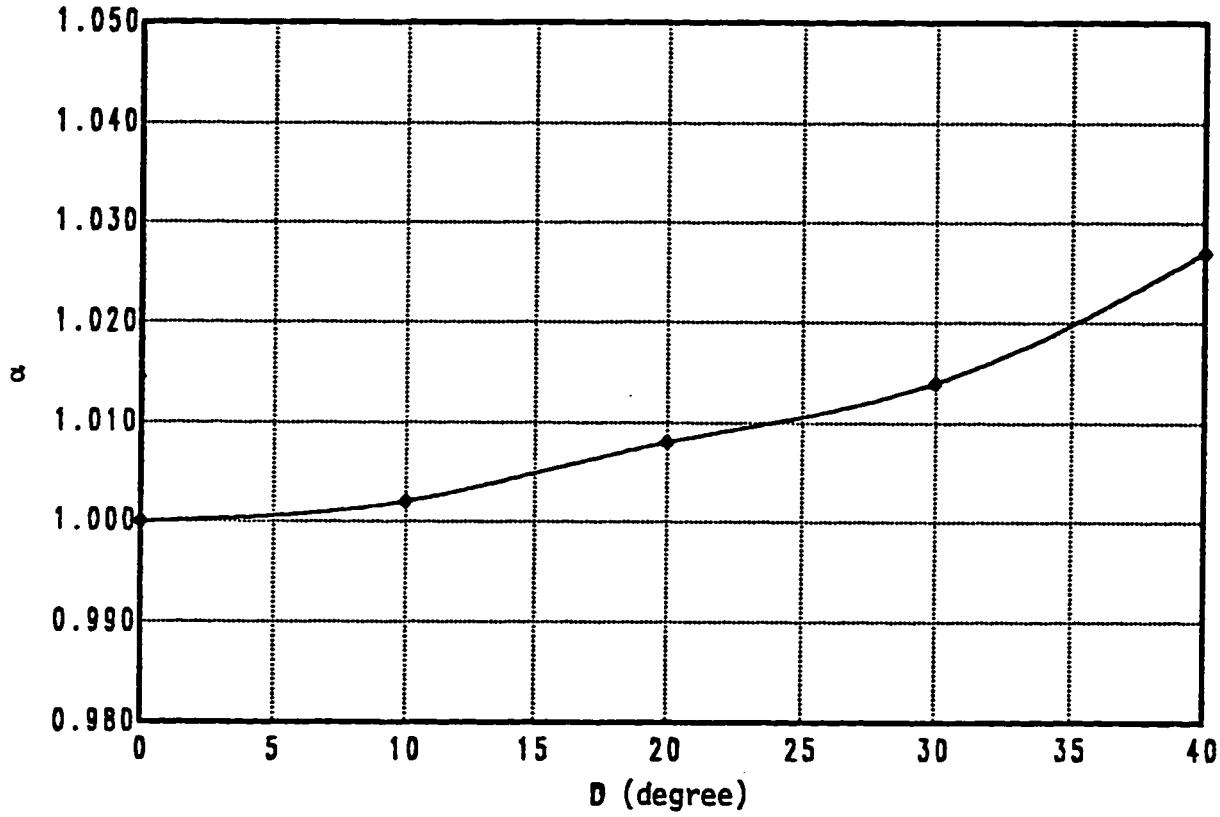

Fig. 6.10 Effect of radius of curvature on pier reaction

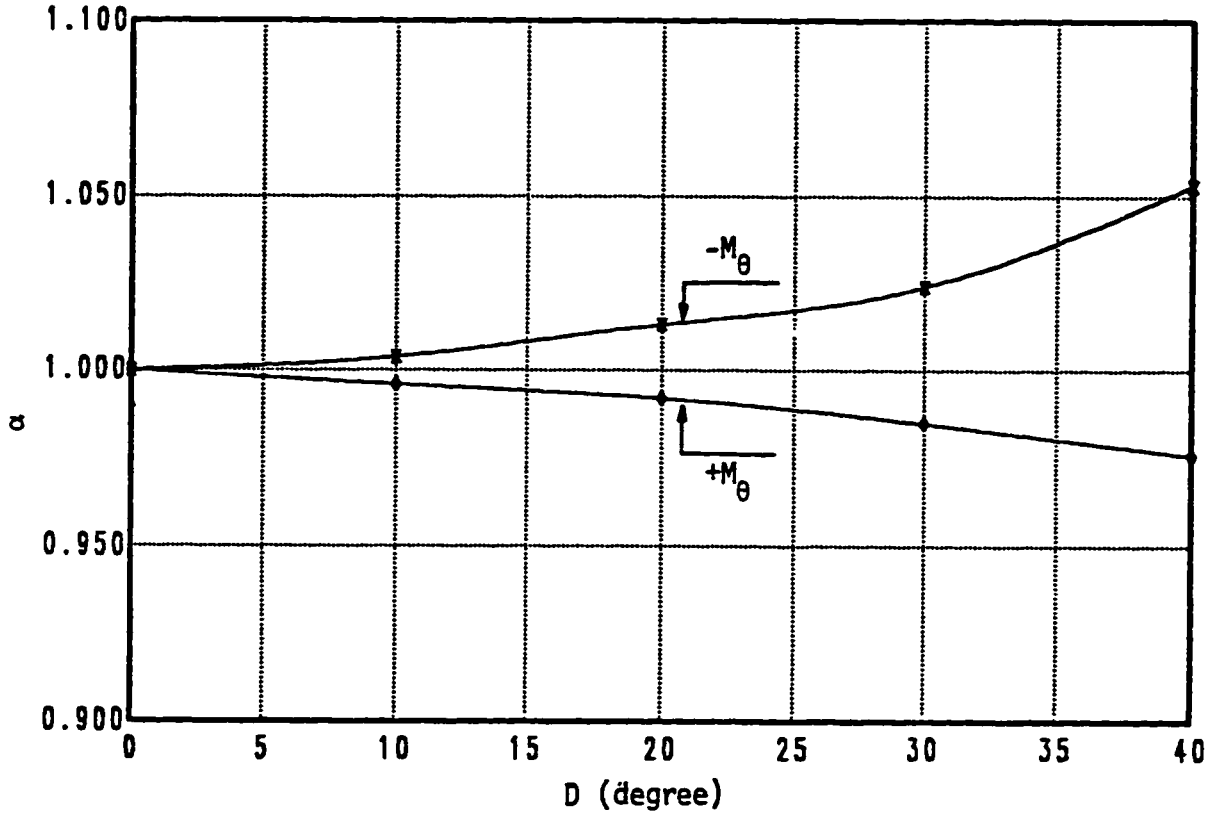

Fig. 6.11 Effect of radius of curvature on M_0

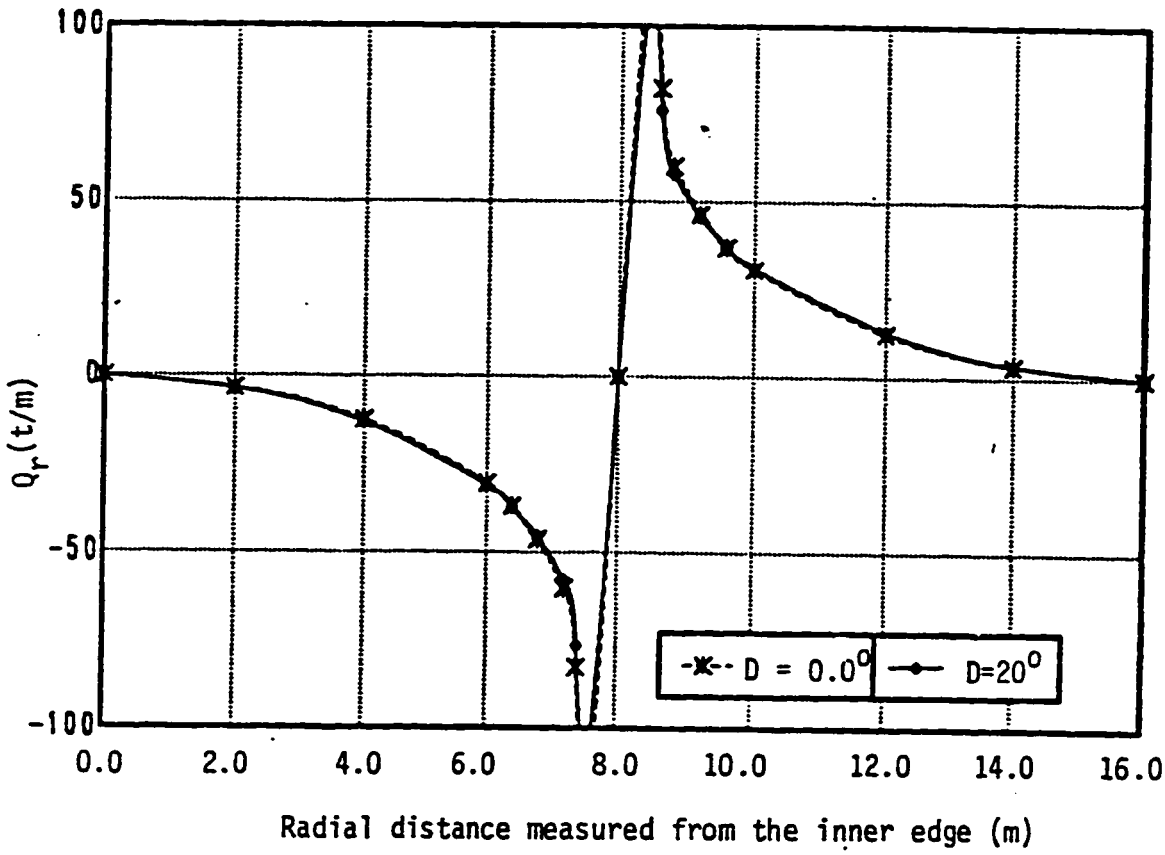

Fig. 6.12 Effect of radius of curvature on Q_r

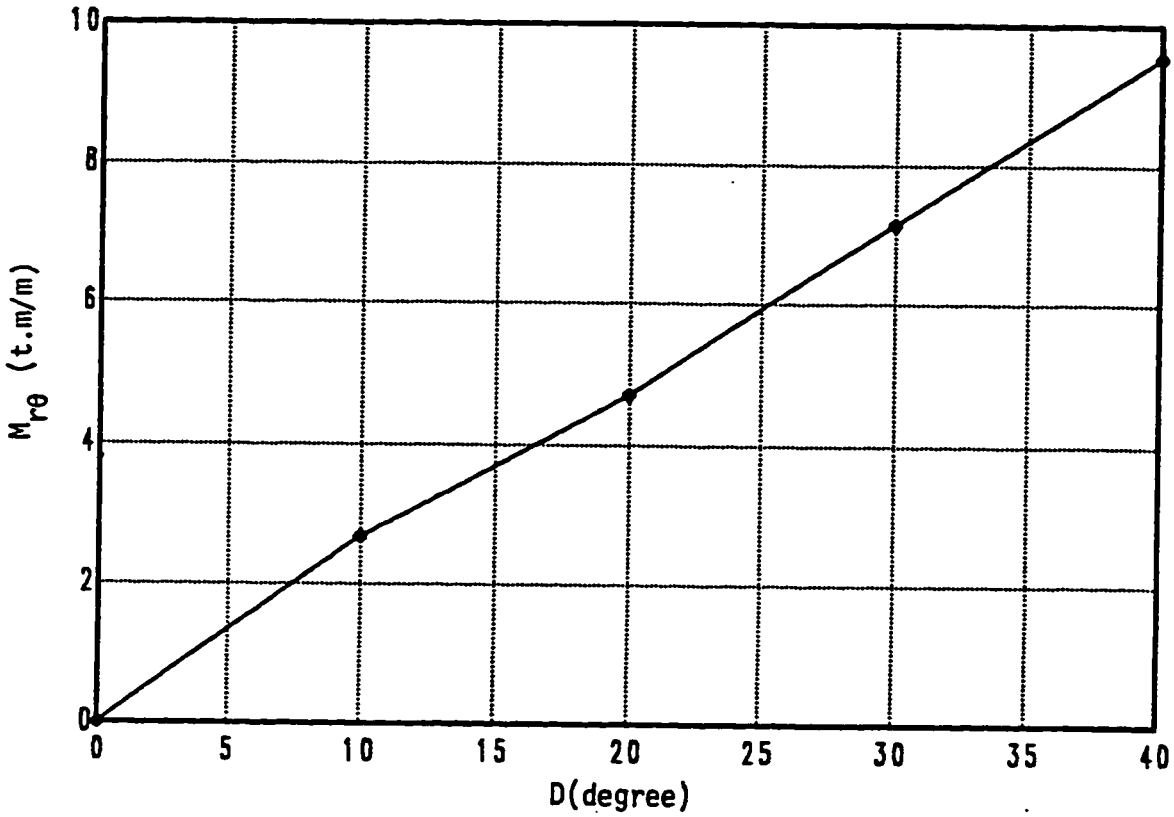

Fig. 6.13 Effect of radius of curvature on M_{r0}

M_{r0} at the abutment ends is plotted in Fig. 6.13 which shows that the torsional moment increases progressively with increasing D and the value is relatively sensitive to the radius of curvature. As for example M_{r0} increases from 0.0 to 43 m.t/m when D varies from 0.0° to 20°.

6.3.2 Width of Deck

The influence of the width of bridge decks on the angular moment M_0 was studied using the hypothetical bridge deck shown in Fig. 6.14. The slab is considered as a plate of uniform thickness of 45 mm. The width B is varied from 1.0 m to 6.0 m and the loading is a uniformly distributed load of $5t/m^2$. The problem was solved for two different radii of curvature 5 m and 25.0 m respectively. For each width, the angular moment M_0 for the first and last node located at the radial center line was plotted in Fig. 6.15.

It may be observed from Fig. 6.15 that for small values of B, M_0 for the first node is bigger than M_0 for last node. This is because the inner edge is stiffer than the outer edge due to the curvature of the bridge deck. But while B is increasing, M_0 for the inner edge is decreasing and M_0 for the outer edge is increasing and this is because the span of the inner edge decreases comparatively with the span for the outer edge which increases for increasing width B. For an intermediate width, the effect of the difference in spans

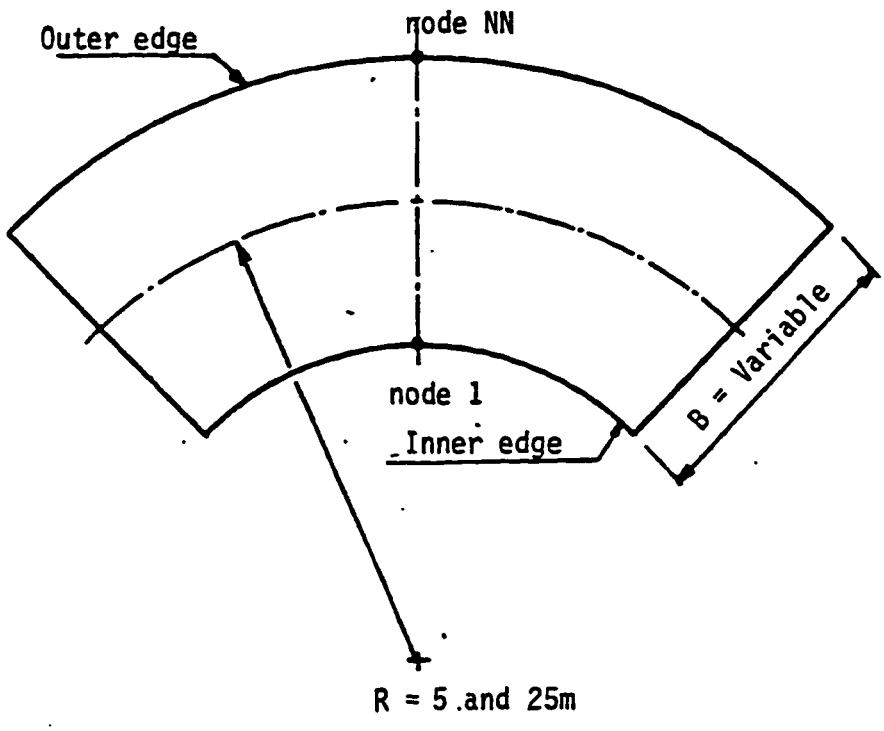

Fig 6.14 Bridge deck model with variable width B

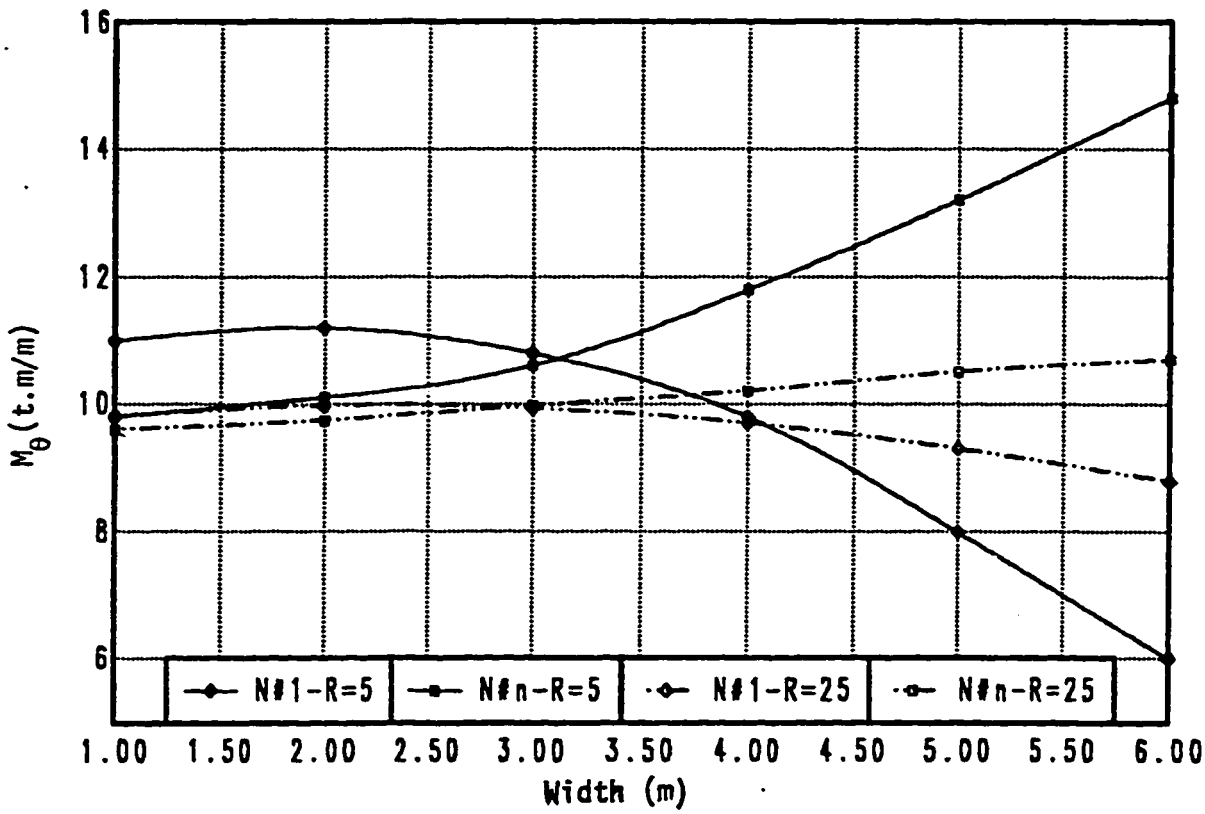

Fig. 6.15 Effect of width on M_θ

between the two edges matches the effect of the difference in their stiffness and M_0 becomes the same for both edges.

It is also observed when R = 25 m that the difference between the values of M_0 for both nodes is less than those values when R = 5 m and that these values (when R = 25) are approximately the same as those of a rectangular shape.

6.3.3 Various Load Positions

The variation of M_r distribution along the radial center line due to the variation of load position is studied using the same perspex model shown in Fig. 6.1 A single concentrated load of 10 lb is applied at stations 0, b/4, b/2, 3b/4 and b one at a time across the radial centerline line, b being the width of the deck. The radial centerline was divided into thirteen stations, Fig.6.15.a, for which the variation of M_r distribution is shown in Figs. 6.16 - 6.20. Also included in these figures are the results of analysis as a straight deck to show the differences.

From these figures it may be observed that the transverse moment M_r is highly localized under the load and the sign of the values across the width may be same or different for the same loading depending on the curvature of the bridge deck and the load position on deck. The peak value of M_r occurs directly under the load and its magnitude drops rapidly with distance away from the load position.

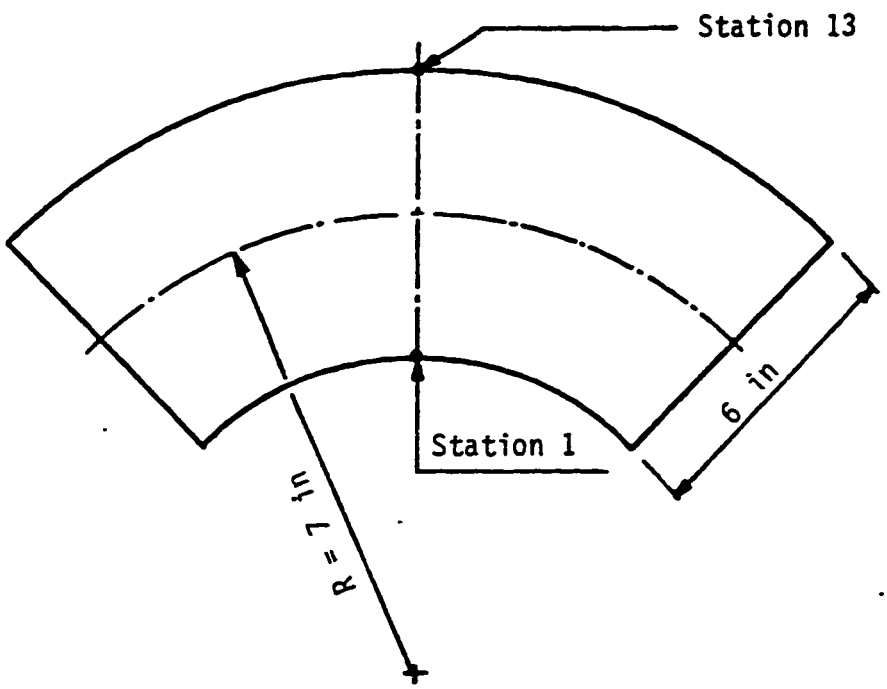

$t = 0.168$ in

$E = 24 \times 10^5$ lb/in^2

$\nu = 0.35$

$\phi_0 = 60$ Deg.

Fig. 6.15a The effect of varying load position on M_r

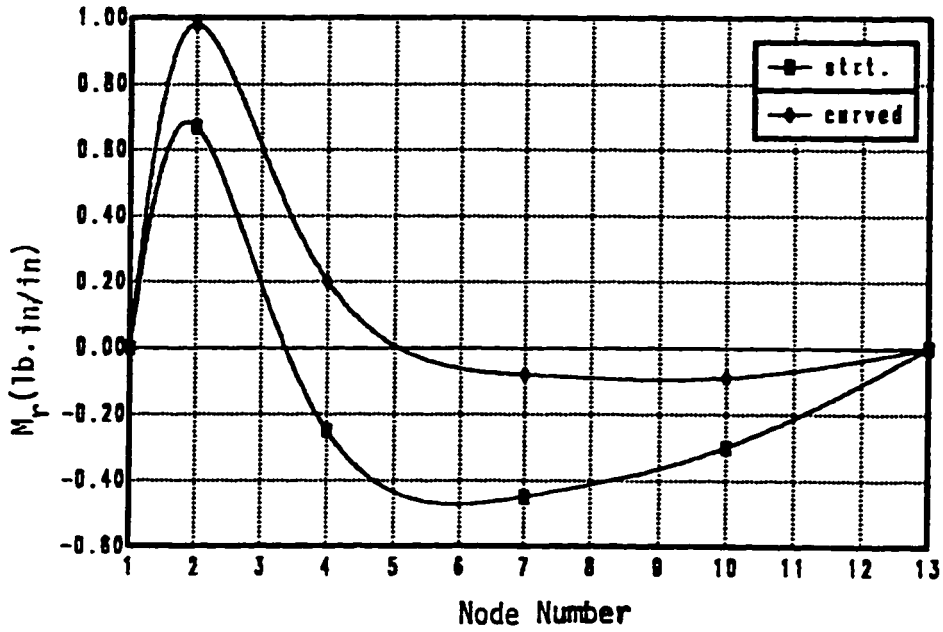

Fig. 6.16 M_r along the radial C.L. due to a point load at the inner edge

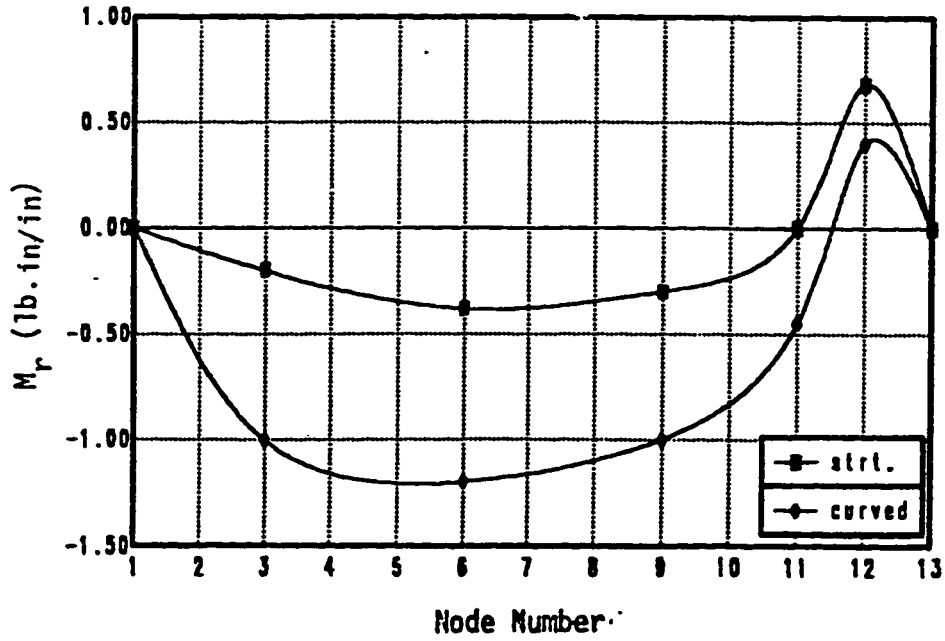

Fig. 6.17 M_r along the radial C.L. due to a point load at the outer edge

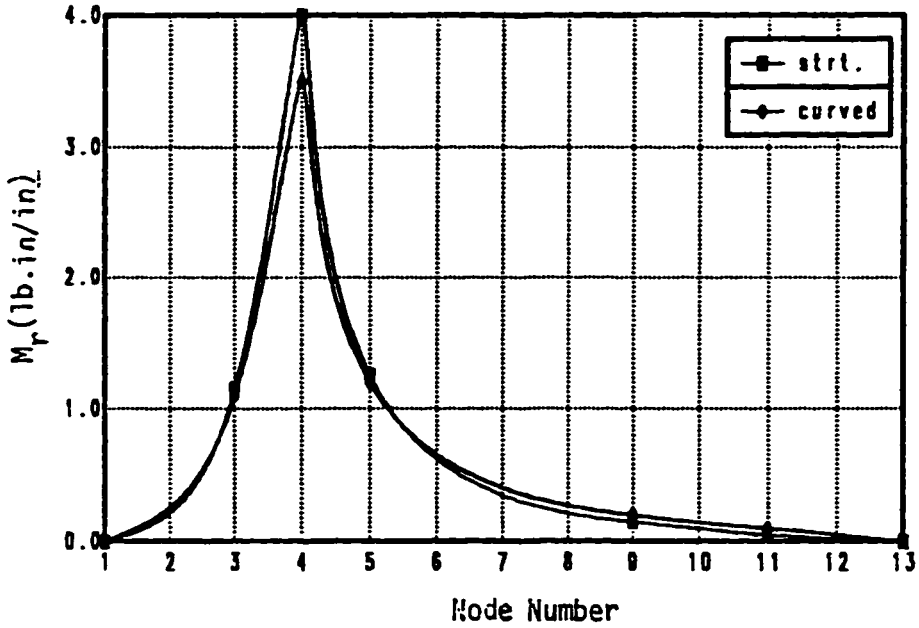

Fig. 6.18 M_r along the radial .C.L. due to a point load at a distance B/4 from the inner edge

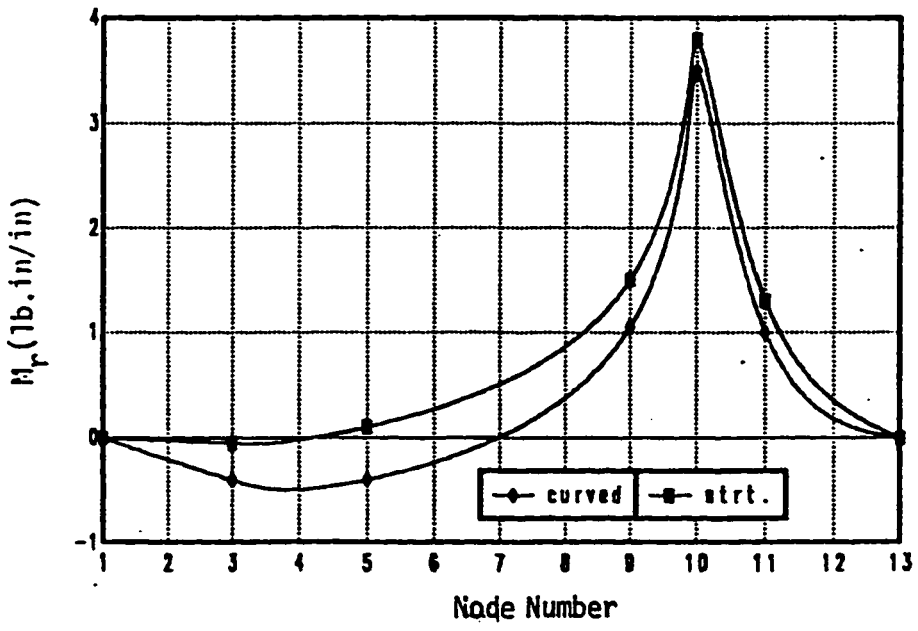

Fig. 6.19 M_r along the radial C.L. due to a point load at a distance 3B/4 from the outer edge

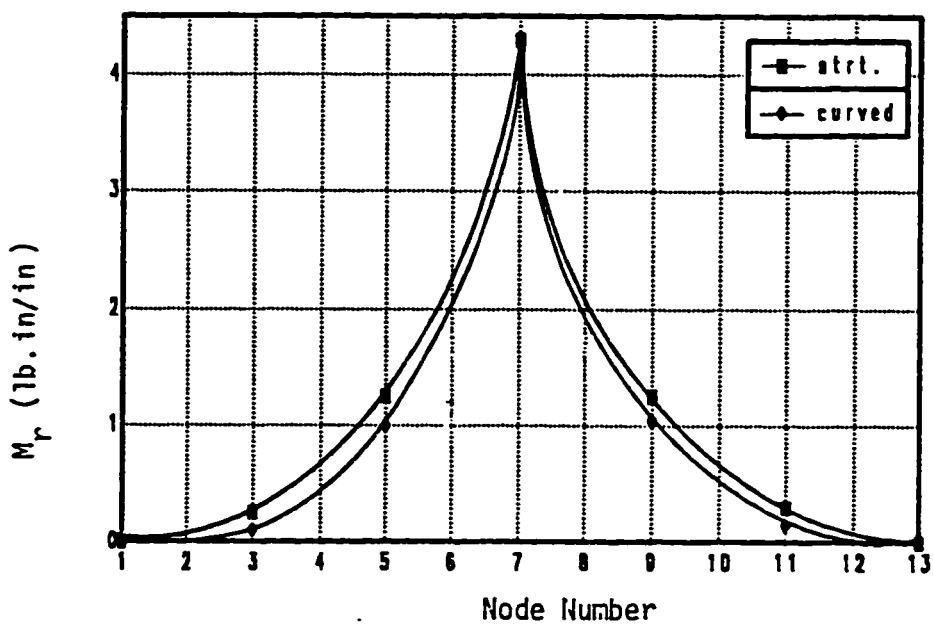

Fig. 6.20 M_r along the radial C.L. due to a point load at the center of the deck

6.3.4 *Effect of Thickness Variation on the Behavior of Curved Bridge Decks*

In most common design of slab type bridge decks, the two outer sides are tapered for economic reasons. The tapered cross section as shown in Fig. 6.21-b has a central zone of uniform thickness flanked by two outer zones of variable thickness. The effect of thickness variation in the behavior of curved decks was studied by analyzing the bridge deck shown in Fig. 6.21. The deck was analyzed first as a deck of a non-uniform thickness as shown in Fig. 6.21-b. The deck was analyzed again using two different idealizations as shown in Figs.6.21.c and 6.21.d.

In the first idealization, a cross section of a constant depth (0.635m) having the same width as the tapered one (5.0m) was analyzed. This constant depth was chosen such that the total angular rigidity of the tapered deck is maintained the same.

The second idealization was chosen as mentioned in Ref.(25) such that the tapered edges were replaced by slab portions of reduced width having the same per-unit-width angular rigidity as that in the middle portion. This transformation resulted in an equivalent deck having a constant depth of 0.7m and a reduced width of 3.85m. The loading is a uniformly distributed load of $5t/m^2$ for the cross sections having the same width (Figs. 6.21.b,c). For the cross section with a reduced width (Fig.6.21.d), the loading is a uniformly distributed load of $6.5t/m^2$. Thus, the total load for the three cases is

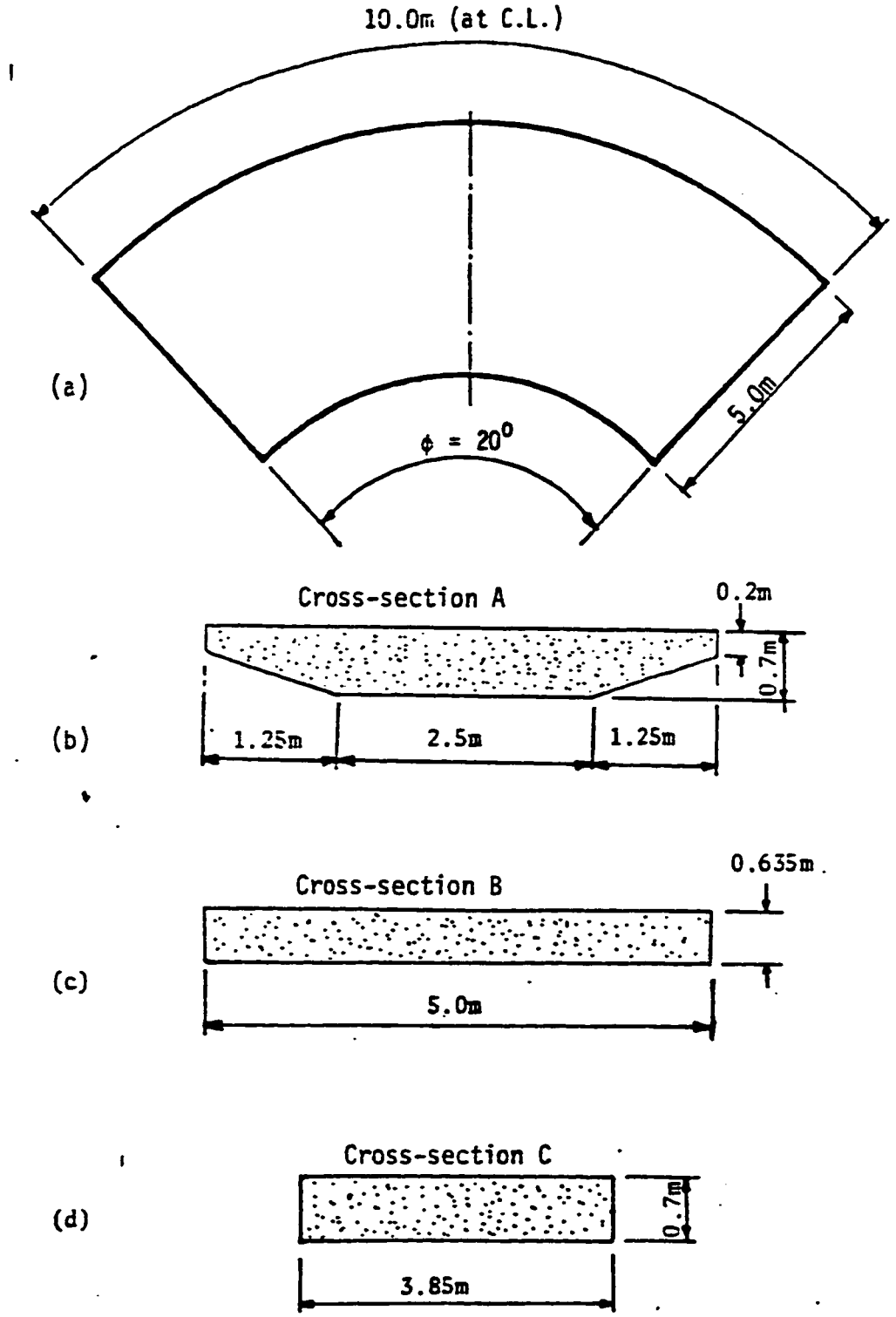

Fig. 6.21 Variable thickness vs. constant thickness

the same.

Figs. 6.22 - 6.24 show the variation of deflection, M_r and M_0 along the radial center line of the deck. Figs. 6.25 and 6.26 show the variation of M_{r0} and V_0 along the simply supported edge of the deck.

Due to the tapering of the edges, these thinner parts behave more like overhangs supported by the inner part of the deck which is stiffer. Thus, these overhangs transmit most of the load to the stiffer part by cantilever action, i.e. in the radial direction without carrying the load to the end supports. Thus, most of the load is taken in the angular direction by the inner part which is stiffer.

Fig.6.22 shows the plots of the deflection for the three cross-sections A, B, and C (Figs.6.21b,c, and d).The deflection for cross-sections B and C are almost identical with hardly any difference. However, that for A, which is the actual cross-section with tapered' overhangs, shows slight increase of the order of 12% . Thus for practical purposes, an idealized cross-section either of type B or C would produce reasonably accurate results.

The variation of M_r as shown in Fig. 6.23 is totally different for both the tapered cross section and its equivalents as the moment sign changes due to the cantilever action in the case of non-uniform thickness. This is expected, because the overhangs behave essen-

tially as cantilevers for example, taking the effective cantilever length approximately 0.675m, Following the method mentioned in Ref.(25), The cantilever moment is $5 \times 0.675^2 = 1.13$ T.m/m which is close to the value shown in fig.6.23 (1.3 T.m/m).

Also, the values of M_0 (Fig. 6.24) at the outer edge of the tapered cross-section is negligible compared with those of the uniform thickness because in this region most of the load is transferred in the radial direction as mentioned earlier.

Fig. 6.25 illustrates the distribution of M_{r0} along the width of the deck at the radial edge. For the cross-sections of a uniform thickness, the distribution of M_{r0} has the same slope-direction over the width but it is not the same for a cross-section of a non-uniform thickness where M_{r0} is almost zero at the thin edges and follows the pattern shown in the figure. This distribution of M_{r0} also affects the distribution of V_0 (Fig. 6.26), which is a function of M_{r0}.

As a point of interest, the total bending moments, torsional moment and edge shear, across the entire width, are shown in Table 6.4 for the three different types of cross-sections namely A, B, and C. It is noticed that these three sets of values are close to each other with small variation, except for the radial moment, which means that although the thickness variation affects significantly the distribution of internal forces, it has not too much influence on the total

values of these internal forces. This finding enables one to confirm that the total internal forces can be calculated by considering the tapered deck as an equivalent uniform deck following any one of the idealizations mentioned before .

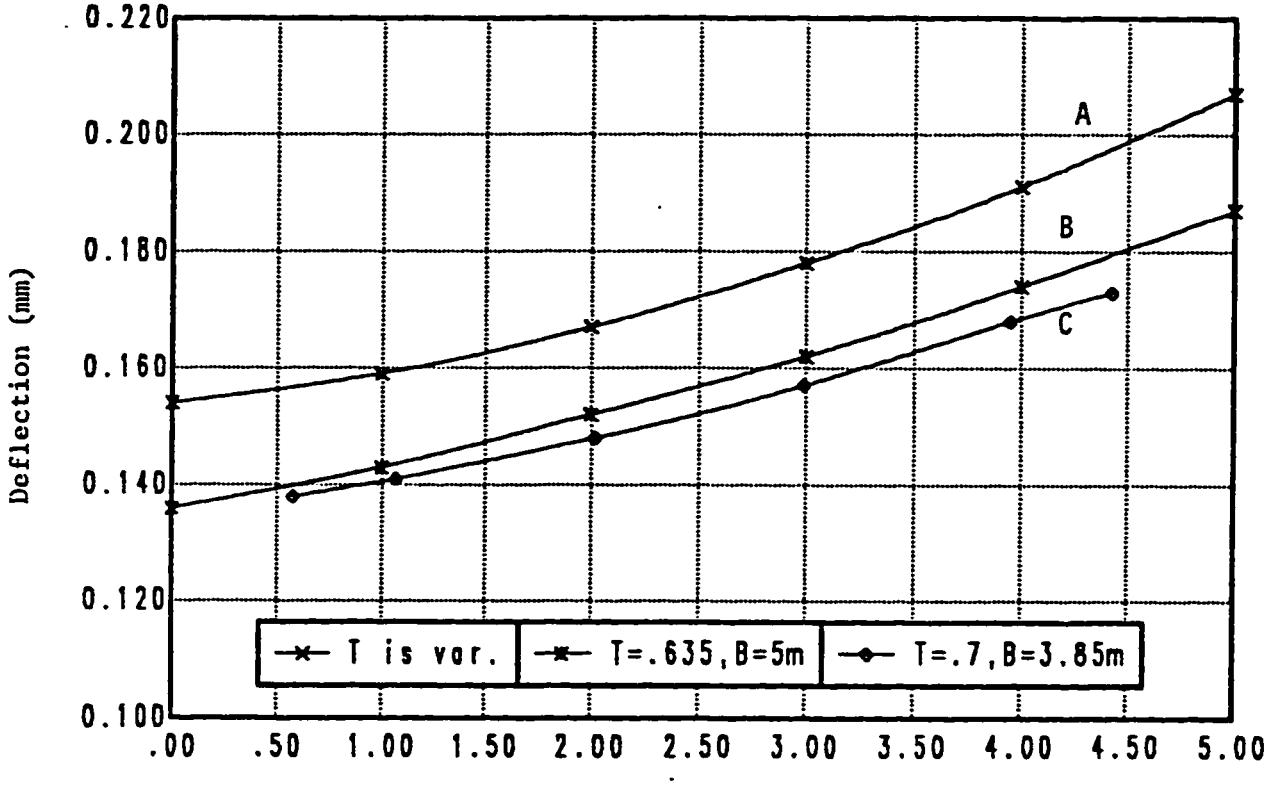

Fig. 6.22 Effect of thickness variation on the mid-span deflection

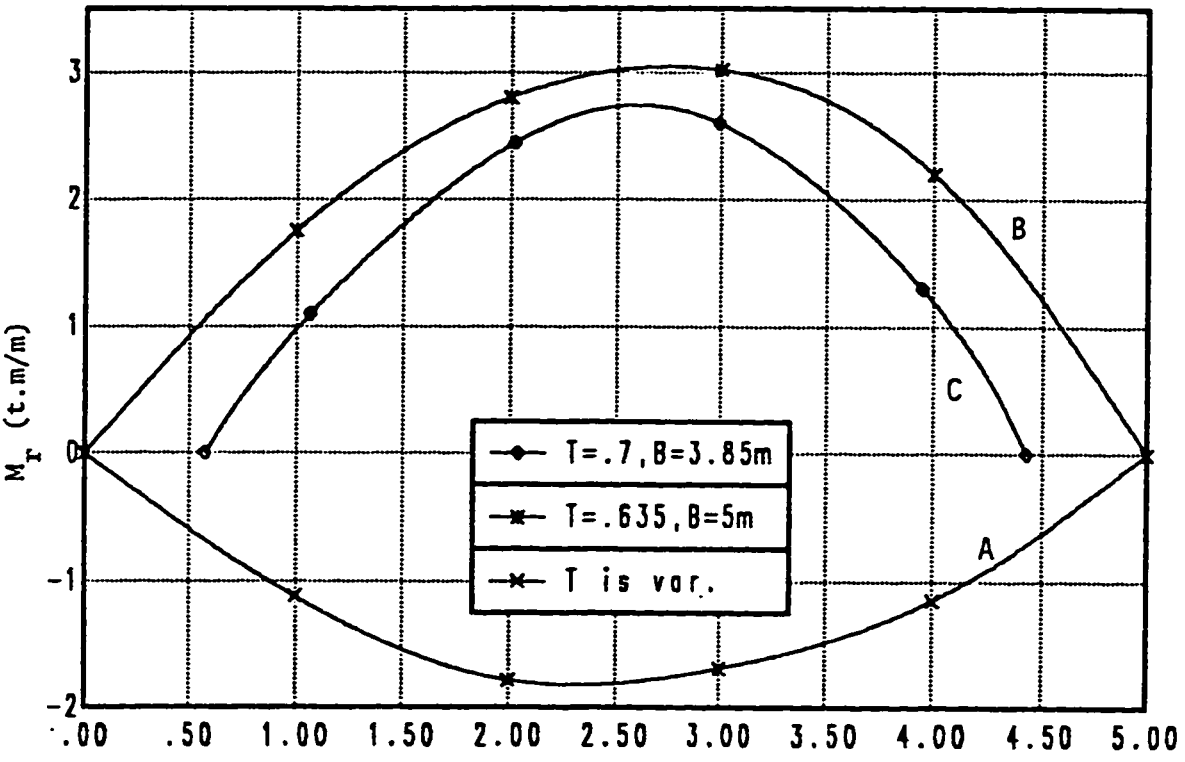

Fig. 6.23 Effect of thickness variation on M_r at mid-span

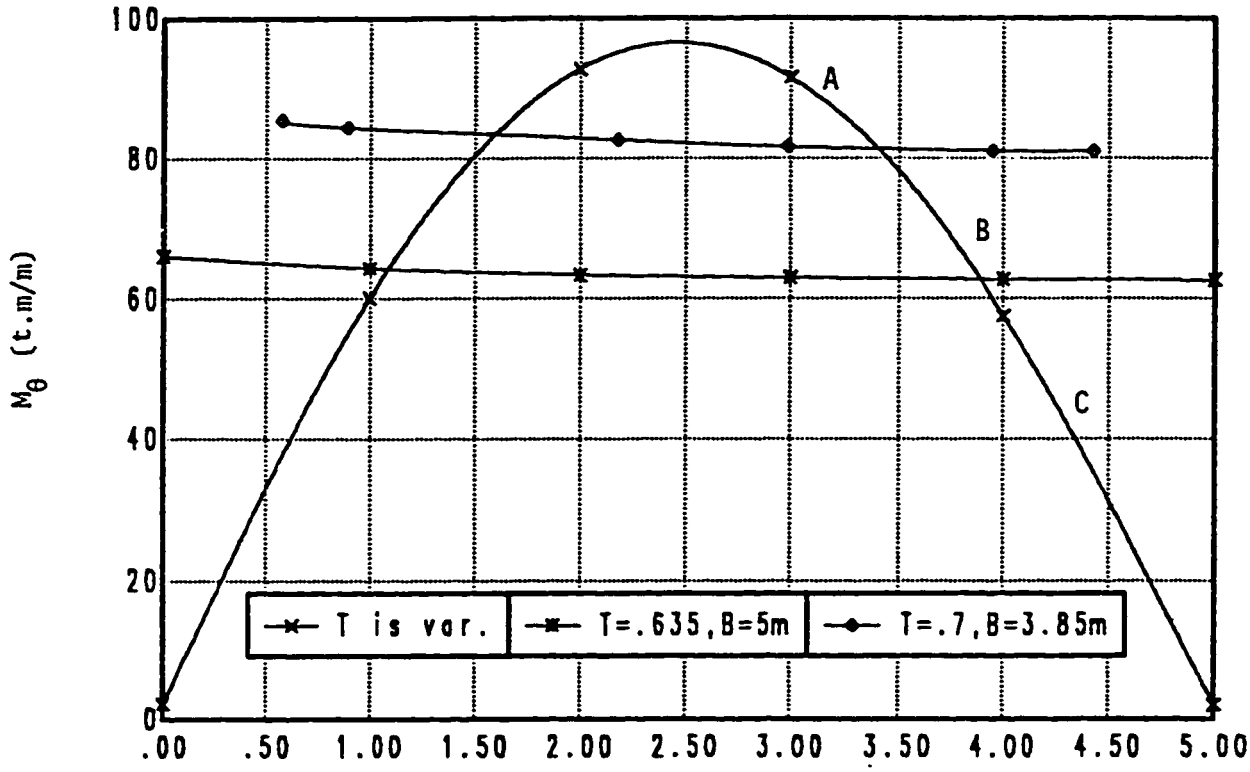

Fig. 6.24 Effect of thickness variation on M_0 at mid-span

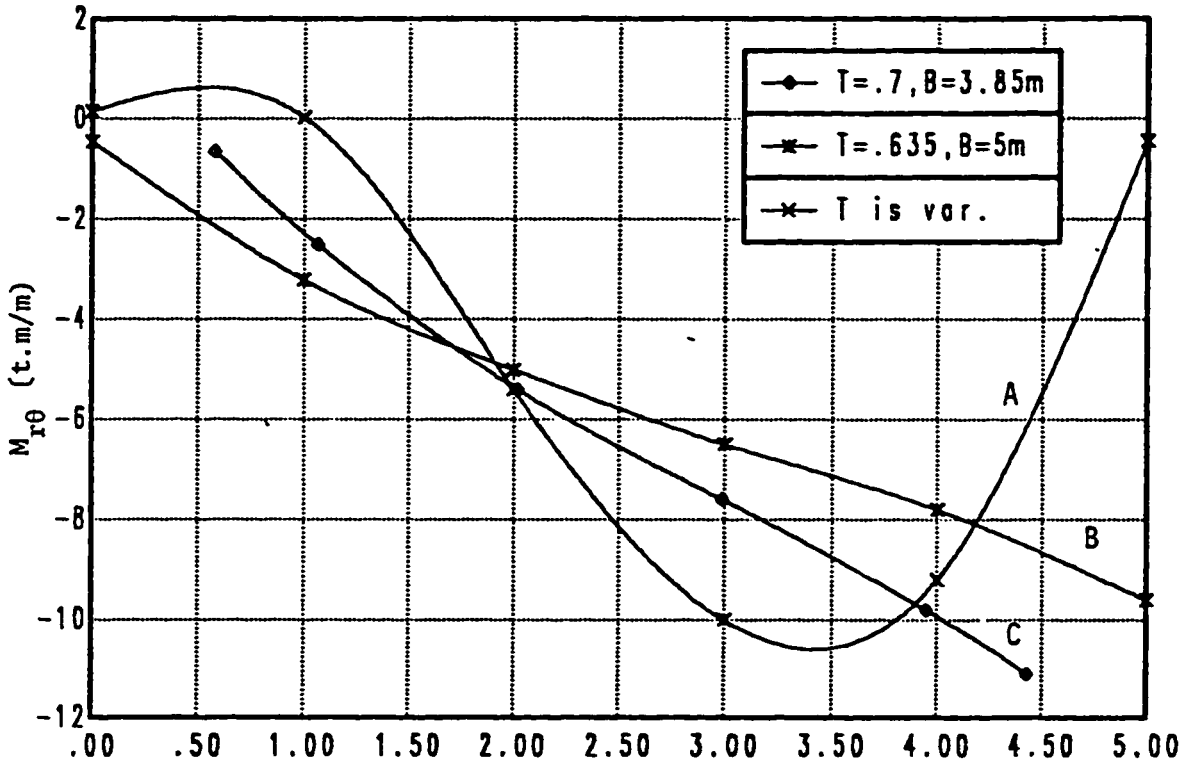

Fig. 6.25 Effect of thickness variation on M_{r0} at the end support

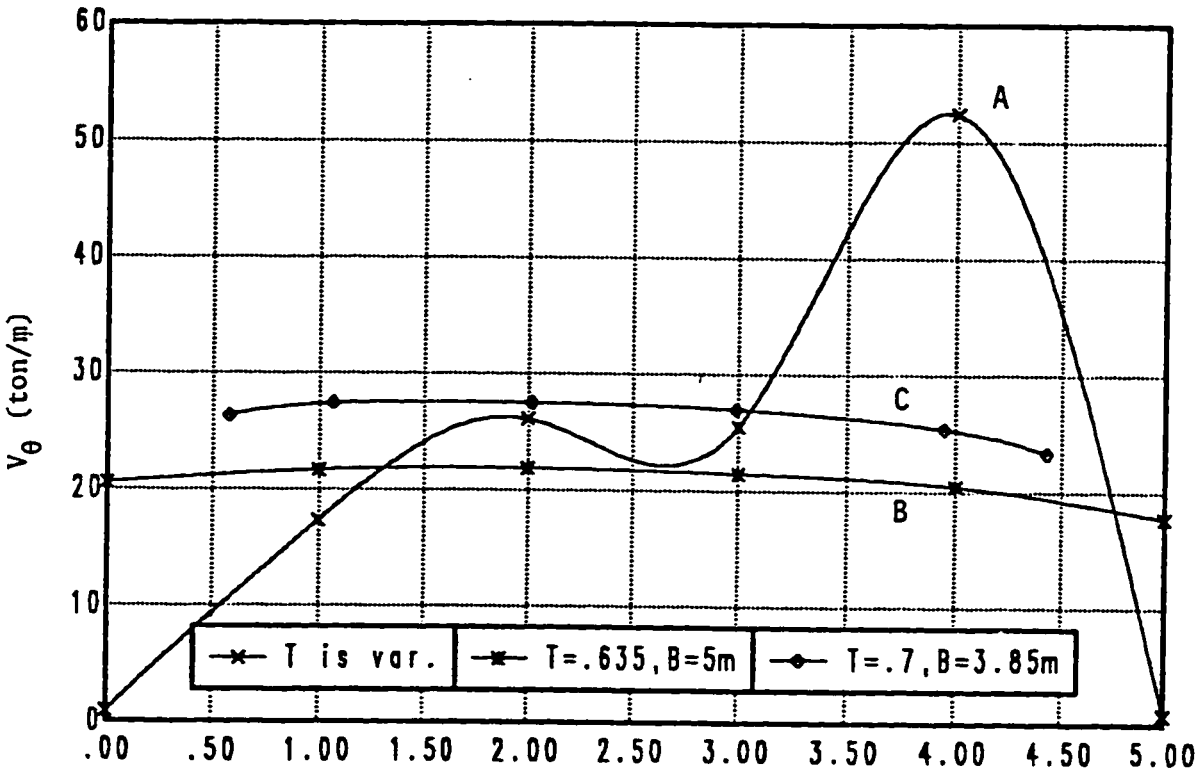

Fig. 6.26 Effect of thickness variation on V_0 at the end support

Table 6.4 Effect of the thickness variation on the total internal forces

Total Values	A	B	C
M_θ (T.m)	312.4	318.3	318.6
M_r (T.m)	- 5.6	8.14	4.8
$M_{r\theta}$ (T.m)	-20.7	-27.13	-28.5
V_θ (Ton)	102.6	103.3	100.7

- A is the tapered deck
- B is the deck with a depth of 0.635m and width of 5m.
- C is the deck with a depth of 0.7m and width of 3.85m.

6.4 Verification of the Simplified Method of Analysis

A. A. Witecki (22) introduced a simplified method of calculation for torsional moment in a horizontally curved multispan bridge. For a curved bridge with a degree of curve normally encountered in highway bridges, the longitudinal moment can be determined with sufficient accuracy by treating the curved deck as a straight deck. This allows to write the equation for torsional moment in a simple form as (22):

$$M_t = \int_0^S (\frac{M}{R} + T)\, dS \qquad (6.1)$$

where:

M_t = total torque on a cross-section

M = total longitudinal bending moment

R = radius to the center line of the deck

S = length of the deck on which the torque is being computed.

T = torque per unit length produced by eccentricity of the applied load.

(See Fig.6.27)

Thus, the procedure of the simplified method can be summarized in the following steps:

1) The longitudinal bending moment M is obtained from a straight beam.

2) The torque T due to the eccentricity of applied load is

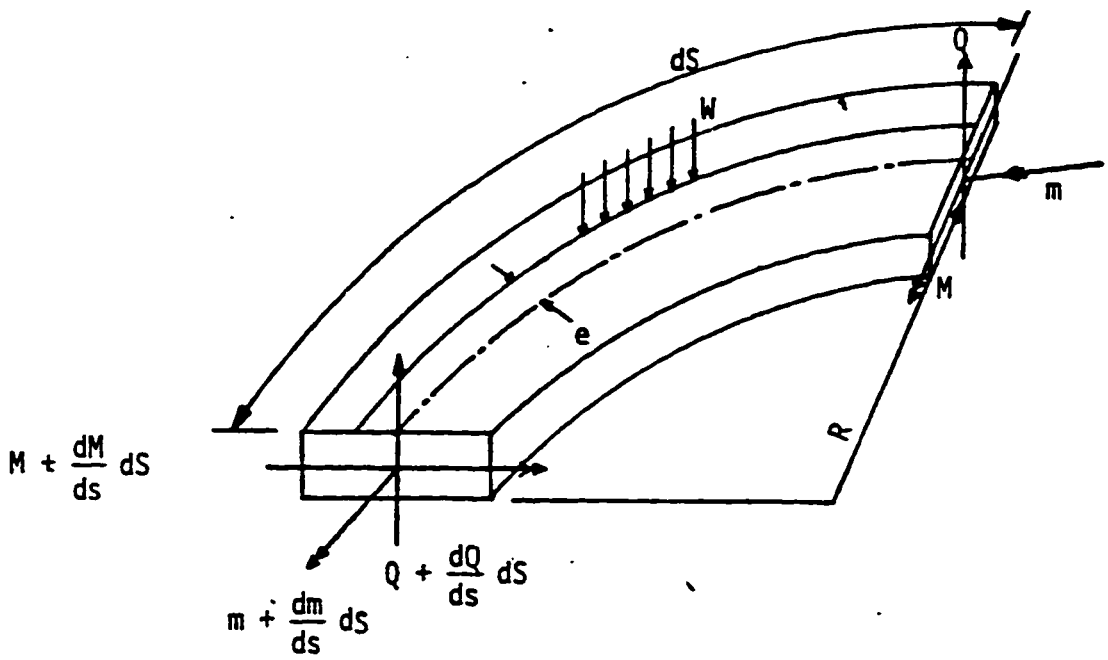

Fig. 6.27 Torque analysis element for curved bridge

obtained from the straight deck.

3) The total torsional moment M_t at any section is obtained from Eq. 6.1.

To study the accuracy of the simplified method, a curved bridge deck example was used. The geometry of the deck is illustrated in Fig. 6.28. The loading is a patch load of intensity $1t/m^2$ covering the outer four meters of the deck. The total torsional moment was calculated for sections A-A, B-B and C-C by both methods, FSTCBA and the simplified method. Table 6.5 shows a comparison between results obtained by the two methods.

It should be mentioned here that the total torsional moment M_t obtained by thin plate theory for sections at the edge (Section A-A) is the resultant of the torsional moment caused by the Kirchhoff's shear V_0 and the corner reactions 2R (Fig. 6.29-a). And the total torsional moment at internal sections (B-B and C-C) is the resultant of the distributed torsional moment M_{r0}. along with the width, the torsional moment caused by Q_0 and the torsional moment caused by concerted edge reaction R, (Fig. 6.29-b). Thus,

$$M_{t(\text{sec A-A})} = \sum_{i=1}^{n} (V_{0_i} \cdot S \cdot X_i) + 2R_1 \cdot \frac{B}{2} + 2R_2 \cdot \frac{B}{2}$$

and

$$M_{t(B\text{-}B\ \&\ C\text{-}C)} = \sum_{i=1}^{n} [M_{r\theta_i} \cdot S + Q_{0_i} \cdot S \cdot X_i] + R_1 \cdot \frac{B}{2} + R_2 \cdot \frac{B}{2}$$

where

n = Number of nodes

V_{0_i} = Kirchhoff's shear at node i

S = Spacing between nodes

X_i = Distance from node i to the center line

R = Corner reaction = M_{r0} at corner

B = Width of the bridge deck

From Table 6.5 one can make a conclusion that the simplified method can be considered as sufficiently accurate to calculate the total torsional moment which is hardly affected by the support dimensions but on the other hand, the distribution of the torsional moment along the width of the deck cannot be obtained by this method. The method also is not of the same accuracy regarding the longitudinal moment and support reaction due to the neglection of support dimensions and its eccentricity with respect to the angular center line which significantly affect these values However, the support dimensions are accounted for in the proposed method. As an example, if the support dimensions in Fig. 6.28 are changed from 1.0 x 1.0 to .25 x 10.0 m, the new values of M_0 at center of the support and the support reaction would be -47 t.m and 152 ton respectively, which are almost the same as those values obtained by the simplified

method (-45 t.m. and 150 ton).

It should also be mentioned that the computation of deflection using the simplified straight beam approach would result in considerable error, if the cross-section is not idealized properly for a bridge deck of variable thickness.

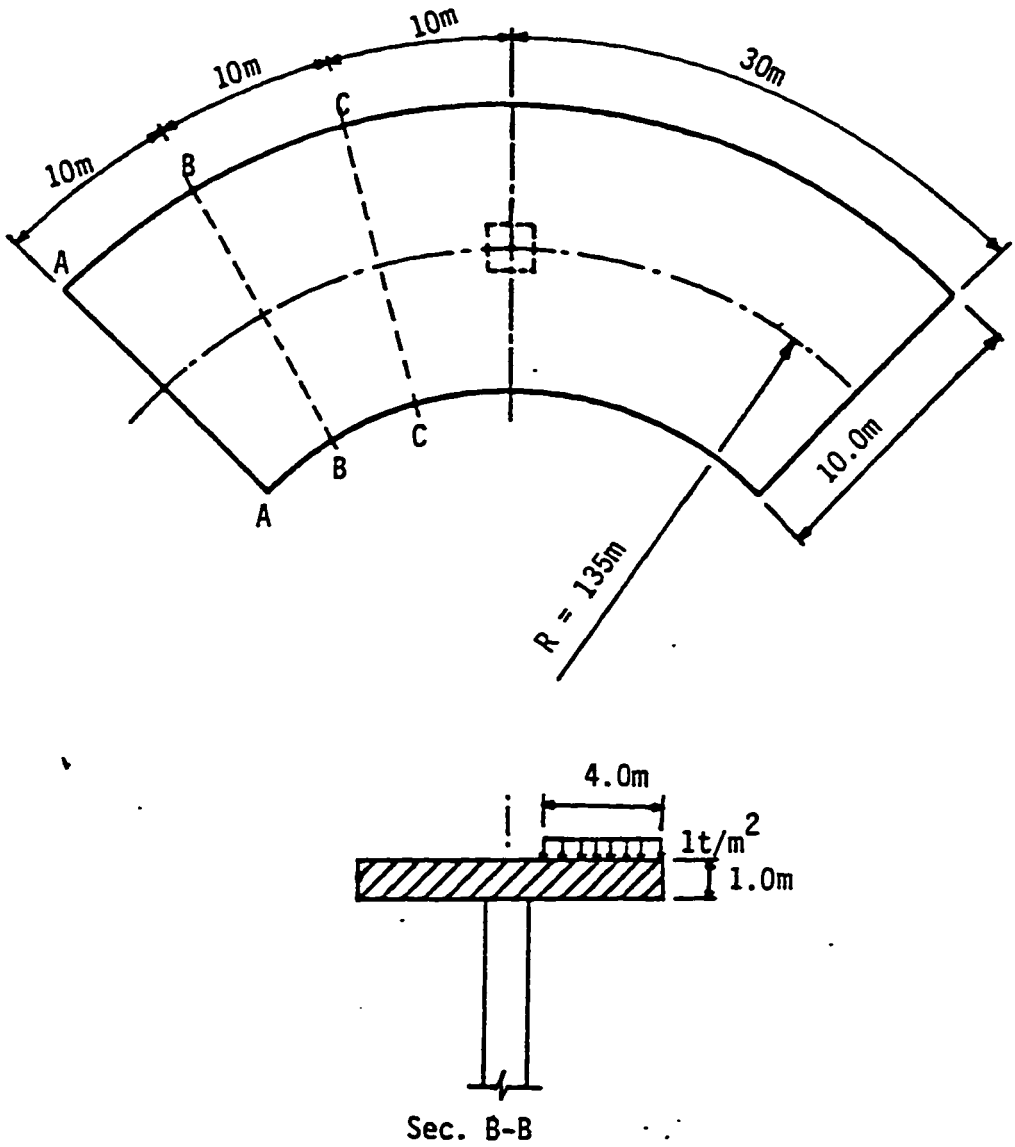

Fig. 6.28 Curved bridge deck example to verify the accuracy of the simplifie method of analysis

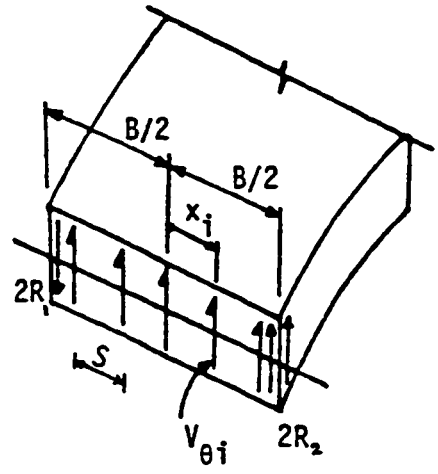

(a) Edge shear and corner reaction at the support edge.

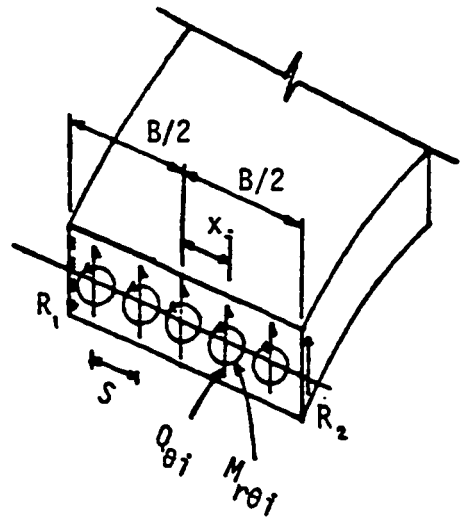

(b) Shear, torsional moment and corner reaction at an interior section.

Fig. 6.29 Total torsional moment-components in a curved deck

Table 6.5 A comparison between FSTCBA and the Simplified Method for a two-span curved bridge deck

RESULTS	FSTCBA	Simplified Method
Total $M_{r\theta}$ at Section A-A (t.m)	-378.21	-380.73
Total $M_{r\theta}$ at Section B-B (t.m)	-248.175	-249.21
Total $M_{r\theta}$ at Section C-C (t.m)	-105.49	-113.36
M_{θ} at center of the support(t.m/m)	- 59.2	- 45
Support reaction (ton)	-158	150

6.5 Solved Example

A three-span continuous bridge deck is solved to illustrate the application of the proposed method. The geometry of the deck is shown in Fig. 6.30. The example is solved for two types of live loads: (a) HS20-44 trucks (26) to obtain the maximum support reaction R, the maximum positive angular moment M_0 at the exterior span and the maximum negative angular moment M_0 at the interior support, Fig. 6.31 shows the location of truck loads to obtain these values. (b) A lane load of 950 kg/ m^2 located near the outer angular edge to obtain the maximum torsional moment M_{r0} at the radial edge. Table 6.6 shows a comparison of the two sets of results obtained by FSTCBA and the simplified method. In calculating the angular moment and support reaction by the simplified method, the bridge deck is treated as a straight three-span continuous bridge deck and the results are obtained using influence line tables.

Results in Table 6.6 show that the simplified method provides sufficiently accurate estimation of the total internal forces on a transverse section. The Input and Output for the case of maximum positive angular moments are shown in Appendix B.

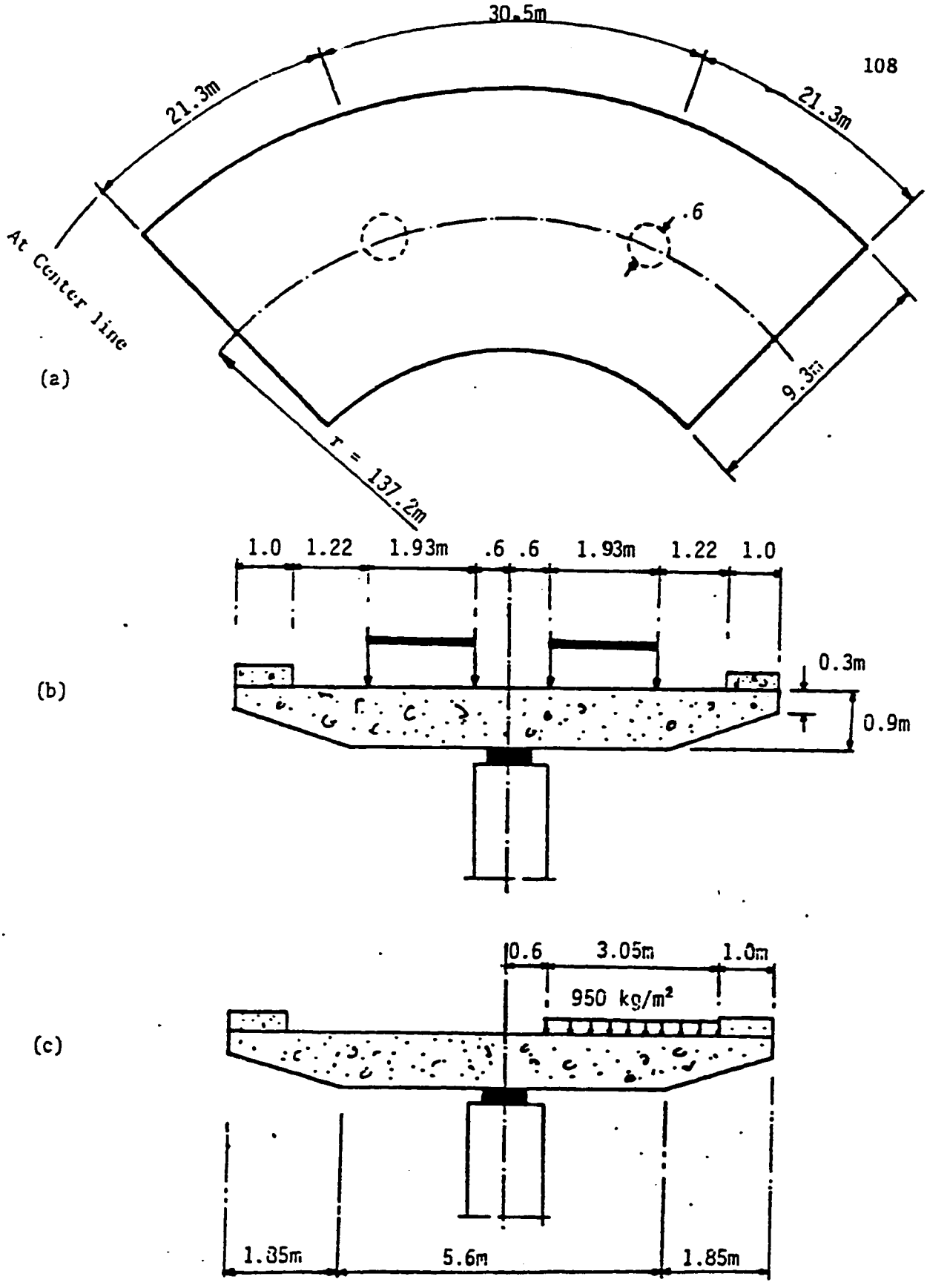

Fig. 6.30 Three-span bridge deck example, (a) plan of the bridge deck, (b) position of truck load, (c) position of lane loads

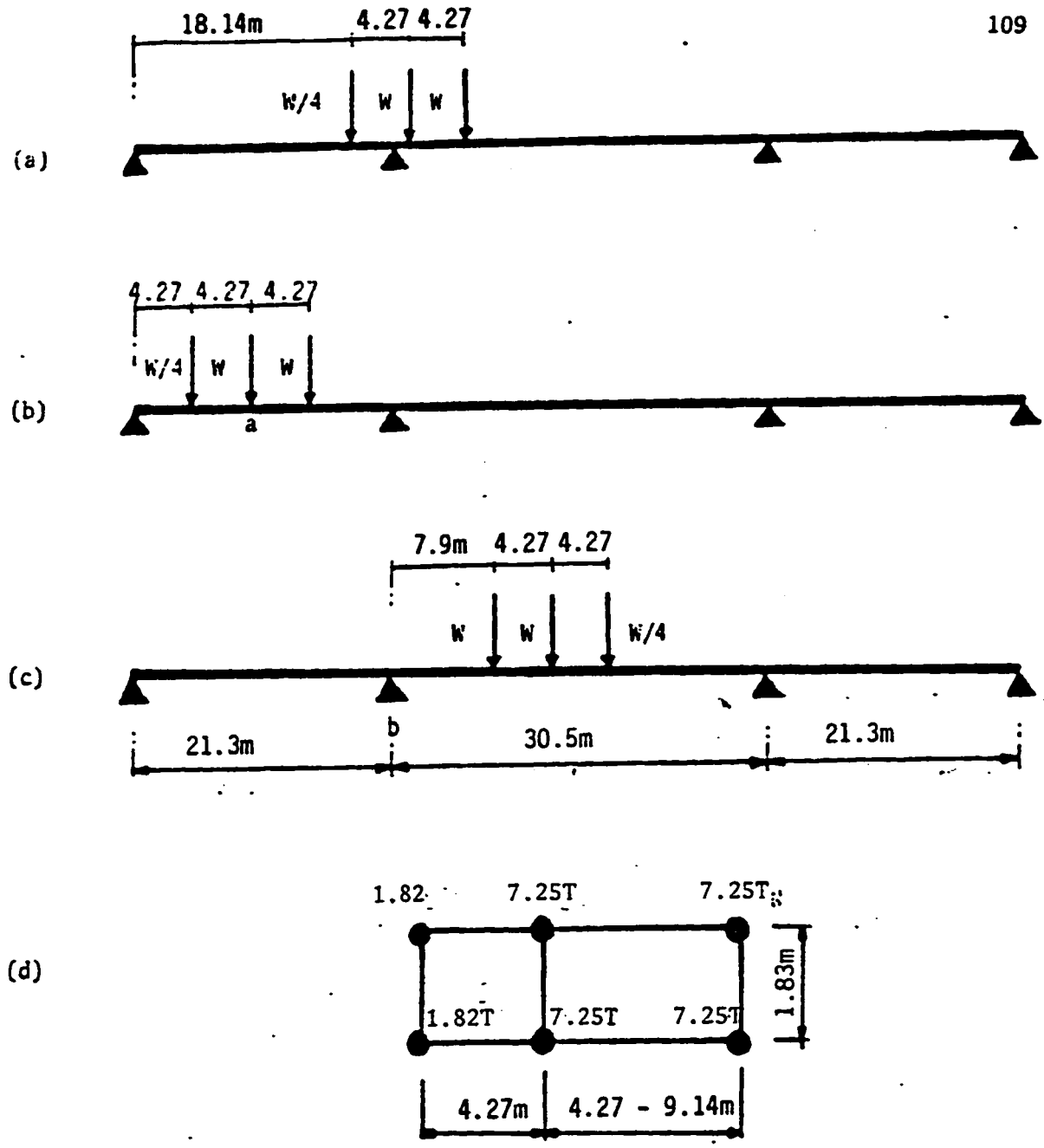

Fig. 6.31 Position of truck load, (a) maximum pier reaction, (b) maximum positive angular moment at a, (c) maximum negative angular moment at b, (d) AASHTO HS20-44 Truck

Table 6.6 A comparison between FSTCBA and the simplified method for a three-span curved bridge deck

Results	FSTCBA	Simplified Method
Maximum support reaction (ton)	78.5	64.1
Maximum positive M_θ (m.ton)	230.7	223.0
Maximum negative M_θ (m.ton)	164.7	167.9
Maximum $M_{r\theta}$ (m.ton)	514.6	527.5

Chapter 7

SUMMARY AND CONCLUSIONS

7.1 Summary

A computer aided method of analysis has been proposed for a curved slab type bridge deck with a variable thickness along the radial direction incorporating one dimensional finite difference method in conjunction with the method of consistent deformation. The deck is simply supported along the radial edges and may be continuous over arbitrarily located interior pier supports and is subjected to any arbitrary loading due to line load, patch load, uniformly distributed load and point load. A generalized computer program, FSTCBA, in FORTRAN-77 is developed to readily apply the proposed method. The accuracy of the proposed method has been verified using some available solutions. The method appears to be accurate and the computer program is shown to be very easy to use and economical with respect to C.P.U. time and storage required.

Several examples were analyzed using the proposed method to study the effect of various parameters on the internal forces. The proposed method was also used to verify the accuracy of the simplified method of analysis (22).

7.2 Conclusions

Based on this study, the following conclusions are drawn:

1) The proposed finite difference method of analysis of horizontally curved slab type bridge decks, both simply supported or continuous over a number of arbitrarily located pier supports, can be used to reliably predict the static response of the bridge deck subjected to an arbitrary loading. The method is relatively simple and straight forward for easy computer adoption.
2) The radius of curvature of the curved deck has minimal influence on the magnitude of internal forces (except for the torsional moment $M_{r\theta}$) within the range of commonly used radii for curved highway bridges. Thus, the angular moment M_{θ} can be calculated with sufficient accuracy by treating the curved deck as a straight deck. However, the torsional moment $M_{r\theta}$ is significantly affected by the radius of curvature.
3) The simplified method presented by Witteki (22) is sufficiently accurate to calculate the total torsional moment at any section. But, this method does not cater for the width of pier supports in the radial direction and their arbitrary location with respect to the angular center line which influences the values of the angular moment M_{θ} and the support

reactions.

4) The variation of deck thickness affects the distribution of internal forces along the deck width but, it hardly affects the magnitude of the total internal forces at any transverse section.

5) In calculating the total torsional moment across a section for the purpose of design, the summation of the distributed twisting moment should take into account the effect of both corner shear and internal shearing force Q_0.

6) For curved decks of identical radius of curvature to the center line and included angle φ_o, the distribution of the angular moment M_θ depends on the width of the deck.

References

1) S. S. Dey and A. T. Samuel, "Static Analysis of Orthotropic Curved Bridge Decks", Computers and Structures, Vol. 12, 1980, pp. 161-166.

2) S. G. Lekhnitskii, "Anisotropic Plates", Gordon and Breach, London, 1968.

3) R. Szilard, "Theory and Analysis of Plates - Classical and Numerical Methods", Prentice-Hall, New Jersey, 1974.

4) A. Coull and A. S. Ergin, "Analysis of Bridge Slabs Curved in Plane", Civil Engineering and Public Work Review, Dec., 1965, pp. 1745-1749.

5) A Coull and P. C. Das, "Analysis of Curved Bridge Deck", Proc. Instn. Civ. Engrs., Vol. 37, 1967, pp. 75-86.

6) Y. K. Cheung, I. P. King and O. C. Zienkiewics, "Slab Bridges with Arbitrary Shape and Support Conditions: A General Method of Analysis Based on Finite Element Method", Proc. Instn. Civ. Engrs., Vol. 40, May, 1968, pp. 9-36.

7) M. D. Olson and G. M. Lundberg, "Annular and Circular Sector Finite Element for Plate Bending", Int. Jour. of Mech. Science, Vol.12, 1970, pp. 17-33.

8) F. Sawko and P. A. Merriman, "An Annular Segment Finite Element for Plate Bending", Int. Jour. for Num. Methods Engg., Vol. 3, 1971, pp. 119-129.

9) S. Singh and G. S. Ramaswamy, "A Sector Element for Thin

Plate Flexure", Int. Jour. Num. Methods Engg. Vol. 4, 1972, pp. 133-142.

10) Y. K. Cheung, "The Analysis of Cylindrical Orthotropic Curved Bridge Decks", IABSE, Vol. 29, 1969, pp. 41-52.

11) E. H. Issam and P. Sasan, "Curved Bridge Decks: Analytical Strip Solution", Jour. Struc. Mech. ASCE, Vol.III, No.7, July, 1985, pp. 1517-1537.

12) E. Onate and B. Suarez, "A Unified Approach for the Analysis of Bridges, Plates and Axisymmetric Shells Using Linear Strip Element", Computers and Structures, Vol. 17, No.3, 1983, pp. 407-426.

13) S. S. Dey, "Finite Strip Method of Analysis for Orthotropic Curved Bridge Decks", Proc. Instn. Civ. Engrs. , Part 2, Vol. 69, June, 1980, pp. 511-519.

14) I. E. Harik and S. Pashanasangi, "Curved Bridge Decks: Analytical Strip Solution", Jour. of Struc. Engg., ASCE, Vol. III, July,1985, pp. 1517-1532.

15) C. P. Heins and R. L. Hails, "Behavior of Stiffened Curved Plate Model", Jour. of Struc. Division, ASCE, Vol. 95, No. ST11, Nov. 1969, pp. 2353-2370.

16) J.R. H. Otter, "Dynamic Relaxation Compared with Other Iterative Finite Difference Methods", NUCL. Eng. Des. Vol. 3, No.1, pp. 183-185.

17) J. Leray, "Calcul per Reflexions des Fonctions M-Harmoniques dens une Bande Plane Verifiant aux Bords M-Conditions Differ-

entielles, a Coefficients Constants", Arch. Mech. Strs., Vol. 16, 1964.

18) L. S. D. Morley, "The Analysis of Column Supported Plates with Special Application to Bridges", Publications, IABS, Vol. 27, 1967, pp.95-138.

19) A. I. Ali, "Static Analysis of Horizontally Curved Bridge Decks supported by Flexible Multi-Girders", M.S. Thesis, Department of Civil Engineering, University of Petroleum and Minerals, 1985.

20) A. K. Azad, A. Ali and M. H. Baluch, "Analysis by Finite Difference of a Horizontally Curved Multi-Girder Bridge Deck", Synopsis of paper 8982, Proc. Instn, Civ. Engrs., Part 2, Vol. 81, March 1986, pp. 133.

21) A. K. Azad, M. H. Baluch and A. Ali, "Influence of Torsional Stiffness of I-Girders in the Analysis of Curved Girder Bridges", Proc. 2nd Int. Conf. Civil and Struc. Eng. Computing, Civil-Comp 85, London, 1985.

22) A. A. Witecki, "Simplified Method for the Analysis of Torsional Moment as an Effect of a Horizontally Curved Multispan Continuous Bridge", ACI Publication, "Concrete Bridge Design", SP-23, 1969, pp. 193-204.

23) F. Sawko et al., "Finite Element Analysis of Bridges Curved in Plan", Conference of Development in Bridge Design and Construction, University College Cardiff, England, March 1971.

24) A. Fam and C. Turkstra, "A Finite Element Scheme for Box Bridge Analysis", Computer and Structures, Vol.5, 1975, pp.

179-186.

25) B. Bakht and L. G. Jager, "Bridge Analysis Simplified", McGraw-Hill, New York, 1985.

26) American Association of State Highway Transportation Officials (AASHTO), "Standard Specifications for Highway Bridges", Washington,D.C. Twelfth edition, 1977.

27) A. Ghali and A. M. Neville, "Structural Analysis, A unified classical and matrix approach", John Wiley and sons, New York, 1978.

APPENDIX - A

DIFFERENT COEFFICIENTS

$$C_{i+2} = \frac{D_r}{h^4}\left(1 + \frac{h}{r}\right)$$

$$C_{i+1} = \frac{-D_r}{h^4}\left(4 + 2\frac{h}{r}\right) - \frac{D_\theta}{r^2h^2}\left(1 - \frac{h}{2r}\right) - \frac{HN^2}{r^2h^2}\left(2 - \frac{h}{r}\right)$$

$$C_i = \frac{6D_r}{h^4} + \frac{D_\theta}{r^2}\left(\frac{2}{h^2} + \frac{N^4}{r^2} - \frac{2N^2}{r^2}\right) - \frac{2HN^2}{r^2}\left(\frac{1}{r^2} - \frac{2}{h^2}\right)$$

$$C_{i-1} = -\frac{D_r}{h^4}\left(4 - \frac{2h}{r}\right) - \frac{D_\theta}{r^2h^2}\left(1 + \frac{h}{2r}\right) - \frac{HN^2}{r^2h^2}\left(2 + \frac{h}{r}\right)$$

$$C_{i-2} = \frac{D_r}{h^4}\left(1 - \frac{h}{r}\right)$$

$$A_{i+1} = 1 + Uh/2r$$

$$A_i = -\left(2 + UN^2h^2/r^2\right)$$

$$A_{i-1} = 1 - Uh/2r$$

$$U = D_1/D_r$$

$$B_{i+1} = V + h/2r$$

$$B_i = -\left(2V + N^2h^2/r^2\right)$$

$$B_{i-1} = V - h/2r$$

$$V = D_1/D_\theta$$

$$D_{i+2} = -\frac{D_r}{2h^3}$$

$$D_{i+1} = D_r\left(\frac{1}{h^3} - \frac{1}{rh^2}\right) + \frac{D_\theta}{2r^2h} + \frac{N^2H}{2r^2h}$$

$$D_i = \frac{2D_r}{rh^2} - \frac{N^2}{r^3}(D_\theta + H)$$

$$D_{i-1} = -D_r\left(\frac{1}{h^3} + \frac{1}{rh^2}\right) - \frac{D_\theta}{2r^2h} - \frac{N^2H}{2r^2h}$$

$$D_{i-2} = \frac{D_r}{2h^3}$$

$$E_{i+1} = \frac{H}{rh^2} + \frac{D_\theta}{2r^2h}$$

$$E_i = -\frac{2H}{rh^2} - \frac{N^2D_0}{r^3}$$

$$E_{i-1} = \frac{H}{rh^2} - \frac{D_\theta}{2r^2h}$$

$$G_{i+2} = D_{i+2}$$

$$G_{i+1} = D_{i+1} + \frac{N^2 D_{r\theta}}{r^2 h}$$

$$G_i = D_i - \frac{2N^2 D_{r\theta}}{r^3}$$

$$G_{i-1} = D_{i-1} - \frac{N^2 D_{r\theta}}{r^2 h}$$

$$G_{i-2} = D_{i-2}$$

$$H_{i+1} = E_{i+1} + 2D_{r\theta} \left(\frac{1}{rh^2} - \frac{1}{r^2 h}\right)$$

$$H_i = E_i + 4D_{r\theta} \left(\frac{1}{r^3} - \frac{1}{rh^2}\right)$$

$$H_{i-1} = E_{i-1} + 2D_{r\theta} \left(\frac{1}{rh^2} + \frac{1}{r^2 h}\right)$$

$$J_1 = C_i - \frac{A_i}{A_{i-1}} C_{i-1} + \left(\frac{G_{i-1}}{G_{i-2}} \frac{A_i}{A_{i-1}} - \frac{G_i}{G_{i-2}}\right) C_{i-2}$$

$$J_2 = C_{i+1} - \frac{A_{i+1}}{A_{i-1}} C_{i-1} + \left(\frac{G_{i-1}}{G_{i-2}} \frac{A_{i+1}}{A_{i-1}} - \frac{G_{i+1}}{G_{i-2}}\right) C_{i-2}$$

$$J_3 = C_{i+2} - \frac{G_{i+2}}{G_{i-2}} C_{i-2}$$

$$F_1 = C_i - \frac{A_i}{A_{i-1}} C_{i-1}$$

$$F_2 = C_{i+1} - \frac{A_{i+1}}{A_{i-1}} C_{i-1}$$

$$F_3 = C_{i+2}$$

$$F_4 = C_{i+3}$$

$$M_{m-2} = C_{i-2} - \frac{G_{i-2}}{G_{i+2}} C_{i+2}$$

$$M_{m-1} = C_{i-1} - \frac{A_{i-1}}{A_{i+1}} C_{i+1} + C_{i+2} \left(\frac{G_{i+1}}{G_{i+2}} \frac{A_{i-1}}{A_{i+1}} - \frac{G_{i-1}}{G_{i+2}}\right)$$

$$M_m = C_i - \frac{A_i}{A_{i+1}} C_{i+1} + C_{i+2} \left(\frac{G_{i+1}}{G_{i+2}} \frac{A_i}{A_{i+1}} - \frac{G_i}{G_{i+2}}\right)$$

$$R_{m-3} = C_{i-3}$$

$$R_{m-2} = C_{i-2}$$

$$R_{m-1} = C_{i-1} - \frac{A_{i-1}}{A_{i+1}} C_{i+1}$$

$$R_m = C_i - \frac{A_i}{A_{i+1}} C_{i+1}$$

$$C^*_{i+2} = D_{ri}\left(\frac{1}{h^4} + \frac{1}{rh^3}\right) + \Delta D_r\left(\frac{1}{2h^4}\right)$$

$$C^*_{i+1} = -D_r\left(\frac{6}{h^4} + \frac{2}{rh^3}\right) + D_{ri+1}\left(\frac{1}{rh^3}\right) + D_{ri-1}\left(\frac{2}{h^4} - \frac{1}{rh^3}\right)$$

$$- D_{0i}\left(\frac{1}{r^2h^2} - \frac{1}{2hr^3}\right) - \Delta D_\theta\left(\frac{1}{4r^2h^2}\right)$$

$$- D_{1i}\left(\frac{1}{rh^3}\right) + D_{1i+1}\left(\frac{1}{rh^3}\right)$$

$$- H_i\left(\frac{2N^2}{r^2h^2} - \frac{N^2}{hr^3}\right) - \Delta H\left(\frac{N^2}{2r^2h^2}\right)$$

$$C^*_i = D_r\left(\frac{10}{h^4}\right) - D_{ri+1}\left(\frac{2}{rh^3} + \frac{2}{h^4}\right) - D_{ri-1}\left(\frac{2}{h^4} - \frac{2}{rh^3}\right)$$

$$- D_{0i}\left(\frac{2N^2}{r^4} - \frac{2}{r^2h^2} - \frac{N^4}{r^4}\right) + \Delta D_0\left(\frac{N^2}{2hr^3}\right)$$

$$+ D_{1i}\left(\frac{2N^2}{r^2h^2}\right) - D_{1_{i+1}}\left(\frac{1}{rh^3} + \frac{N^2}{r^2h^2}\right) - D_{1_{i-1}}\left(\frac{N^2}{r^2h^2} - \frac{1}{rh^3}\right)$$

$$- H_i\left(\frac{2N^2}{r^4} - \frac{4N^2}{r^2h^2}\right) + \Delta H\left(\frac{N^2}{hr^3}\right)$$

$$C^*_{i-1} = -D_{ri}\left(\frac{6}{h^4} - \frac{2}{rh^3}\right) + D_{ri+1}\left(\frac{2}{h^4} + \frac{1}{rh^3}\right) - D_{ri-1}\left(\frac{1}{rh^3}\right)$$

$$- D_{0i}\left(\frac{1}{h^2r^2} + \frac{1}{2hr^3}\right) + \Delta D_0\left(\frac{1}{4r^2h^2}\right)$$

$$+ D_{1i}\left(\frac{1}{rh^3}\right) - D_{1i-1}\left(\frac{1}{rh^3}\right)$$

$$- H_i N^2 \left(\frac{2}{r^2h^2} - \frac{1}{r^3h}\right) + \Delta H \left(\frac{N^2}{2r^2h^2}\right)$$

$$C^*_{i-2} = D_{ri} \left(\frac{1}{h^4} - \frac{1}{rh^3}\right) - \Delta D_r \left(\frac{1}{2h^4}\right)$$

$$D^*_{i+2} = D_{i+2}$$

$$D^*_{i+1} = D_{i+1} - \frac{\Delta D_r}{2h^3} - \frac{\Delta D_1}{4rh^2}$$

$$D^*_i = D_i + \frac{\Delta D_r}{h^3} + \frac{N^2 \Delta D_1}{2r^2h}$$

$$D^*_{i-1} = D_{i-1} - \frac{\Delta D_r}{2h^3} + \frac{\Delta D_1}{4rh^2}$$

$$D^*_{i-2} = D_{i-2}$$

$$E^*_{i+1} = E_{i+1} + \frac{\Delta D_{r\theta}}{2rh^2}$$

$$E^*_i = E_i - \frac{\Delta D_{r\theta}}{r^2h}$$

$$E^*_{i-1} = E_{i-1} - \frac{\Delta D_{r\theta}}{2rh^2}$$

$$G^*_{i+2} = G_{i+2}$$

$$G^*_{i+1} = G_{i+1} - \frac{\Delta D_r}{2h^3} - \frac{\Delta D_i}{4rh^2}$$

$$G^*_i = G_i + \frac{\Delta D_r}{h^3} + \frac{N^2 \Delta D_i}{2r^2 h}$$

$$G^*_{i-1} = G_{i-1} - \frac{\Delta D_r}{2h^3} + \frac{\Delta D_i}{4rh^2}$$

$$G^*_{i-2} = G_{i-2}$$

$$H^*_{i+1} = H_{i+1} + \frac{\Delta D_{r\theta}}{rh^2}$$

$$H^*_i = H_i - \frac{2\Delta D_{r\theta}}{r^2 h}$$

$$H^*_{i-1} = H_{i-1} - \frac{\Delta D_{r\theta}}{rh^2}$$

WHERE:

r is the radial coordinate at node i

h is the spacing between the nodes

n is the harmonic cycle

φ_o is the included angle

$$N = \frac{n\pi}{\varphi_o}$$

$$\Delta D_r = D_{r_{i+1}} - D_{r_{i-1}}$$

$$\Delta D_\theta = D_{\theta_{i+1}} - D_{\theta_{i-1}}$$

$$\Delta D_{r\theta} = D_{r\theta_{i+1}} - D_{r\theta_{i-1}}$$

$$\Delta D_1 = D_{1_{i+1}} - D_{1_{i-1}}$$

$$\Delta H = H_{i+1} - H_{i-1}$$

APPENDIX - B

Sample Input and Output for A Three-Span Bridge Deck Example

(Sec 6.5)

(The case of maximum positive angular moment)

```
*** SOLVED EXAMPLE ( TRUCK LOAD FOR MAX POS.M )***
137.2    9.3     .533    .9
2   12  1
21     45
1  1  2
1  1
.062222
134.98    .031    7.41E-04  .1    182
136.91    .031    7.30E-04  .1    182
138.11    .031    7.24E-04  .1    182
140.04    .031    7.14E-04  .1    182
134.98    .062    7.41E-04  .1    728
136.91    .062    7.30E-04  .1    728
138.11    .062    7.24E-04  .1    728
140.04    .062    7.14E-04  .1    728
134.98    .093    7.41E-04  .1    728
136.91    .093    7.30E-04  .1    728
138.11    .093    7.24E-04  .1    728
140.04    .093    7.14E-04  .1    728
137.2     .155556     3.85E-03   .53   .2827     0   0
137.2     .377778     3.85E-03   .53   .2827     0   0
2E06      .15
4
0.0   .3
1.85  .9
7.45  .9
9.3   .3
```

1

TITLE :*** SOLVED EXAMPLE (TRUCK LOAD FOR MAX POS.M)***

**** INPUT DATA.****

RADIUS AT CENTER LINE OF BRIDGE.....= 0.137200E+03

WIDTH OF BRIDGE.....= 0.930000E+01

INCLUDED ANGLE OF BRIDGE (RAD).....= 0.533000E+00

REFERENCE THICKNESS OF BRIDGE.....= 0.900000E+00

OUTSIDE RADIUS.....= 0.141850E+03

INSIDE RADIUS.....= 0.132550E+03

NUMBER OF PIER SUPPORTS.....= 2

NUMBER OF PATCH LOADS.....= 12

NUMBER OF LOCATIONS REQUIRED.....= 1

NUMBER OF HARMONIC CYCLES.....= 45

NUMBER OF NODES.....= 21

ICOD1.....= 1

ICOD2.....= 1

ICOD3.....= 2

IDG1(INNER EDGE).....= 1

IDG2(OUTER EDGE).....= 1

SPACING BETWEEN NODES.....= 0.465000E+00

**** POSITION OF RADIAL LINES FOR MOMENT,DEFLECTION ANDSHEAR.(RAD)****

THETA(1).....= 0.622220E-01

1

***** LOAD DATA.*****

*** LOAD NUMBER(1).***

R.....= 0.1350E+03
THETA.....= 0.3100E-01
BETA.....= 0.7410E-03
B.....= 0.1000E+00
DIST.LOAD.....= 0.1820E+03

*** LOAD NUMBER(2).***

R.....= 0.1369E+03
THETA.....= 0.3100E-01
BETA.....= 0.7300E-03
B.....= 0.1000E+00
DIST.LOAD.....= 0.1820E+03

*** LOAD NUMBER(3).***

R.....= 0.1381E+03
THETA.....= 0.3100E-01
BETA.....= 0.7240E-03
B.....= 0.1000E+00
DIST.LOAD.....= 0.1820E+03

*** LOAD NUMBER(4).***

R.....= 0.1400E+03
THETA.....= 0.3100E-01
BETA.....= 0.7140E-03
B.....= 0.1000E+00
DIST.LOAD.....= 0.1820E+03

*** LOAD NUMBER(5).***

R.....= 0.1350E+03
THETA.....= 0.6200E-01
BETA.....= 0.7410E-03
B.....= 0.1000E+00
DIST.LOAD.....= 0.7280E+03

*** LOAD NUMBER(6).***

R.....= 0.1369E+03
THETA.....= 0.6200E-01
BETA.....= 0.7300E-03
B.....= 0.1000E+00
DIST.LOAD.....= 0.7280E+03

*** LOAD NUMBER(7).***

R.....= 0.1381E+03

THETA.....= 0.6200E-01
BETA.....= 0.7240E-03
B.....= 0.1000E+00
DIST.LOAD.....= 0.7280E+03

*** LOAD NUMBER(8).***

R.....= 0.1400E+03
THETA.....= 0.6200E-01
BETA.....= 0.7140E-03
B.....= 0.1000E+00
DIST.LOAD.....= 0.7280E+03

*** LOAD NUMBER(9).***

R.....= 0.1350E+03
THETA.....= 0.9300E-01
BETA.....= 0.7410E-03
B.....= 0.1000E+00
DIST.LOAD.....= 0.7280E+03

*** LOAD NUMBER(10).***

R.....= 0.1369E+03
THETA.....= 0.9300E-01
BETA.....= 0.7300E-03
B.....= 0.1000E+00
DIST.LOAD.....= 0.7280E+03

*** LOAD NUMBER(11).***

R.....= 0.1381E+03
THETA.....= 0.9300E-01
BETA.....= 0.7240E-03
B.....= 0.1000E+00
DIST.LOAD.....= 0.7280E+03

*** LOAD NUMBER(12).***

R.....= 0.1400E+03
THETA.....= 0.9300E-01
BETA.....= 0.7140E-03
B.....= 0.1000E+00
DIST.LOAD.....= 0.7280E+03

1

***** DATA FOR SUPPORTING PIERS.*****

*** PIER NUMBER(1).***

R .....= 0.1372E+03
THETA .....= 0.1556E+00

BETA .....= 0.3850E-02
B .....= 0.5300E+00
AREA OF PIER .....= 0.2827E+00
SETTLEMENT OF FOUNDATION.....= 0.0000E+00
ELASTIC SHORTENING.....= 0.0000E+00

*** PIER NUMBER(2).***

R .....= 0.1372E+03
THETA .....= 0.3778E+00
BETA .....= 0.3850E-02
B .....= 0.5300E+00
AREA OF PIER .....= 0.2827E+00
SETTLEMENT OF FOUNDATION.....= 0.0000E+00
ELASTIC SHORTENING.....= 0.0000E+00

1

**** REFERENCE PLATE PROPERTIES.****

RADIAL BENDING RIGIDITY/UNIT LENGTH..... DR = 124296.6751918

TANGENTIAL BENDING RIGIDITY/UNIT LENGTH.. DTHT = 124296.6751918

TORSIONALL RIGIDITY/UNIT LENGTH ..... DRTHT = 52826.0869565

BENDING RIGIDITY DUE TO COUPLING..... D1 = 18644.5012788

D1+2DRTHT ..... H1 = 124296.6751918

D1/DR..... U = 0.1500000

D1/DTHT..... V = 0.1500000

H1/DTHT..... ALPHA = 1.0000000

DTHT/DR..... BETA = 1.0000000

(H1+2DRTHT)/DR .....DELTA = 1.8500000

1

**** DEFLECTION AND INTERNAL ACTIONS AT THETA= 0.6222E-01 (RAD.) ****

NOD	X	DEF	M.THETA	M.R	M.RTHET	Q.THETA	Q.R
1	0.000E+00	0.977E-02	0.118E+01	-0.132E-12	-0.187E-03	0.391E-01	0.674E-02
2	0.465E+00	0.978E-02	0.400E+01	0.546E-01	-0.919E-02	0.113E+00	0.156E+00
3	0.930E+00	0.980E-02	0.947E+01	0.158E+00	-0.403E-01	0.246E+00	0.280E+00
4	0.140E+01	0.983E-02	0.185E+02	0.387E+00	-0.114E+00	0.460E+00	0.665E+00
5	0.186E+01	0.987E-02	0.317E+02	0.863E+00	-0.255E+00	0.926E+00	0.153E+01

6	0.232E+01	0.991E-02	0.318E+02	0.173E+01	-0.309E+00	0.108E+01	0.174E+00
7	0.279E+01	0.996E-02	0.316E+02	0.114E+01	-0.358E+00	0.105E+01	-0.931E+00
8	0.326E+01	0.100E-01	0.315E+02	0.107E+01	-0.410E+00	0.106E+01	0.222E+00
9	0.372E+01	0.101E-01	0.315E+02	0.139E+01	-0.460E+00	0.111E+01	0.140E+01
10	0.419E+01	0.101E-01	0.318E+02	0.224E+01	-0.497E+00	0.124E+01	0.394E+00
11	0.465E+01	0.102E-01	0.317E+02	0.169E+01	-0.500E+00	0.139E+01	-0.720E+00
12	0.512E+01	0.103E-01	0.316E+02	0.162E+01	-0.508E+00	0.120E+01	0.494E+00
13	0.558E+01	0.104E-01	0.317E+02	0.214E+01	-0.544E+00	0.113E+01	-0.452E+00
14	0.605E+01	0.105E-01	0.315E+02	0.125E+01	-0.588E+00	0.105E+01	-0.148E+01
15	0.651E+01	0.106E-01	0.314E+02	0.865E+00	-0.637E+00	0.102E+01	-0.357E+00
16	0.698E+01	0.107E-01	0.315E+02	0.861E+00	-0.687E+00	0.101E+01	0.732E+00
17	0.744E+01	0.108E-01	0.318E+02	0.133E+01	-0.736E+00	0.136E+01	-0.306E+00
18	0.791E+01	0.109E-01	0.186E+02	0.554E+00	-0.459E+00	0.118E+01	-0.105E+01
19	0.837E+01	0.110E-01	0.948E+01	0.213E+00	-0.251E+00	0.710E+00	-0.444E+00
20	0.884E+01	0.111E-01	0.400E+01	0.702E-01	-0.112E+00	0.376E+00	-0.230E+00
21	0.930E+01	0.113E-01	0.118E+01	-0.390E-13	-0.353E-01	0.360E-01	-0.192E-01

1

*** ANGULAR EDGE SHEAR FORCE.-V.THETA-(F/L) ***

THETA.(RAD)---->		0.000000E+00	0.533000E+00
NODE 1	X= 0.0000E+00	0.126574E+00	0.000000E+00
NODE 2	X= 0.4650E+00	0.845582E+00	0.000000E+00
NODE 3	X= 0.9300E+00	0.148621E+01	0.000000E+00
NODE 4	X= 0.1395E+01	0.231296E+01	0.000000E+00
NODE 5	X= 0.1860E+01	0.337739E+01	0.000000E+00
NODE 6	X= 0.2325E+01	0.347556E+01	0.000000E+00
NODE 7	X= 0.2790E+01	0.344820E+01	0.000000E+00
NODE 8	X= 0.3255E+01	0.343942E+01	0.000000E+00
NODE 9	X= 0.3720E+01	0.341596E+01	0.000000E+00
NODE 10	X= 0.4185E+01	0.333362E+01	0.000000E+00
NODE 11	X= 0.4650E+01	0.300777E+01	0.000000E+00
NODE 12	X= 0.5115E+01	0.327202E+01	0.000000E+00
NODE 13	X= 0.5580E+01	0.340439E+01	0.000000E+00
NODE 14	X= 0.6045E+01	0.337101E+01	0.000000E+00
NODE 15	X= 0.6510E+01	0.333533E+01	0.000000E+00
NODE 16	X= 0.6975E+01	0.330437E+01	0.000000E+00
NODE 17	X= 0.7440E+01	0.558635E+01	0.000000E+00
NODE 18	X= 0.7905E+01	0.609483E+01	0.000000E+00
NODE 19	X= 0.8370E+01	0.392400E+01	0.000000E+00
NODE 20	X= 0.8835E+01	0.221613E+01	0.000000E+00
NODE 21	X= 0.9300E+01	0.117123E+00	0.000000E+00

1

*** PIER-SUPPORT REACTIONS.***

SUPPORT#	REACTION.(F)
1	38.8779
2	-5.9646

الحمد لله رب العالمين